

TECHNISCHE UNIVERSITÄT MÜNCHEN

Fachbereich Protein Modelling

MHC multimer purification of rare antigen specific T cells and direct T cell
receptor isolation by single cell PCR

Georg Dössinger

Vollständiger Abdruck der von der Fakultät Wissenschaftszentrum Weihenstephan für
Ernährung, Landnutzung und Umwelt der Technischen Universität zur Erlangung des
akademischen Grades eines

Doktors der Naturwissenschaften

genehmigten Dissertation.

Vorsitzender: Univ.-Prof. Dr. Martin Klingenspor

Prüfer der Dissertation: 1. Univ.-Prof. Dr. I. Antes
2. Univ.-Prof. Dr. D. Busch
3. Univ.-Prof. Dr. D. Haller

Die Dissertation wurde am 30.4.2013 bei der Technischen Universität München eingereicht
und durch die Fakultät Wissenschaftszentrum Weihenstephan für Ernährung, Landnutzung
und Umwelt am 13.3.2014 angenommen.

1. TABLE OF CONTENTS

1.	Table of Contents	1
2.	Index of Figures	3
3.	Index of Tables	4
4.	Abbreviations	5
5.	Introduction	9
5.1.	Basic Concepts of the Immune System	9
5.2.	Typical Course of an Immune Response	10
5.3.	The immunological Role of T cells	11
5.4.	Immune Escape by Mutation	11
5.5.	Induction of Immune Exhaustion	12
5.6.	Immune Escape by Prevention of Antigen Presentation	14
5.7.	Adoptive Cell therapy	15
5.7.1.	Stem Cell Transplantation and Donor Lymphocyte Infusion	16
5.7.2.	Tumor Infiltrating Lymphocytes	17
5.7.3.	Tumor-specific T cell-Clones	21
5.7.4.	Adoptive Transfer of virus-specific T cells	24
5.7.5.	Genetic Redirection of T cells	27
5.8.	TCR Isolation Strategies	33
6.	Aim of this Work	34
7.	Materials and Methods	36
7.1.	Materials	36
7.1.1.	Chemicals and Reagents	36
7.1.2.	Buffers and Media	38
7.1.3.	MHC Multimers	39
7.1.4.	Antibodies	40
7.1.5.	Enzymes	41
7.1.6.	Primers	42
7.1.7.	Equipment	43
7.1.8.	Kits	44
7.1.9.	Cells and Cell-Lines	44
7.1.10.	Software	45
7.2.	Methods	46

7.2.1.	Flow Cytometric Data Acquisition and Cell sorting	46
7.2.2.	Solid Phase cDNA Amplification	46
7.2.3.	Reverse Transcription and PCR of the TCR from single Cells	47
7.2.4.	Cloning and Sequencing.....	48
7.2.5.	Retroviral Transduction.....	48
7.2.6.	Magnetic Cell Separation.....	49
7.2.7.	<i>In vitro</i> T cell-Expansion.....	50
7.2.8.	Functional Analysis of T cells.....	50
8.	Results	51
8.1.	Establishment of a PCR Method for V-Segment independent Amplification of TCR α - and β - chain from single T cells.....	51
8.1.1.	Solid-phase Coupled cDNA-Amplification	53
8.1.2.	Gene-specific cDNA amplification without washing steps by volume upscaling	56
8.1.3.	Priming	58
8.1.4.	Optimization of Sensitivity by three Rounds of exponential Template Amplification	59
8.1.5.	RT-Temperature	60
8.1.6.	Precautions for Prevention of Cross-Contamination.....	62
8.2.	TCR-sequence Analysis of CMV-specific T cell Populations.....	63
8.3.	Repertoire analysis and demonstration of single cell -derived TCR-specificity by gene transfer.....	65
8.4.	Enrichment of Tumor-specific T cells from the naïve Repertoire of healthy Donors.....	72
8.5.	Functional Characterization of a Tumor Antigen-specific TCR.....	87
9.	Discussion	90
9.1.	Choice of TCR source	91
9.1.1.	Allo-MHC-restriction.....	91
9.1.2.	Autologous Antigen-specific T cells.....	92
9.1.3.	Auto-reactive Regulatory T cells	93
9.2.	Choice of Target Antigen	94
9.3.	Role of TCR Avidity	95
9.4.	TCR Analysis of Antigen-specific Repertoires.....	96
9.5.	Alternative Methods to detect Antigen-specific TCRs.....	97
9.6.	Extension of TCR isolation for ACT to other HLA- restrictions.....	98
10.	Summary	100
11.	Bibliography.....	103
12.	Acknowledgements.....	119

2. INDEX OF FIGURES

Figure 5.1:	Assessment of Response Rates to TIL therapy.	18
Figure 5.2:	Correlation of structural avidity and clinical response	29
Figure 8.1:	TCR, genomic locus.....	52
Figure 8.2:	Schematic overview of the single cell PCR strategy using solid phase coupled cDNA amplification	54
Figure 8.3:	Results from solid phase coupled cDNA amplification protocol.	55
Figure 8.4:	Sketch of the basic principle of the novel single-TCR sequencing strategy.....	57
Figure 8.5:	Evaluation of priming strategies for Reverse Transcription.....	58
Figure 8.6:	Test of third round of PCR amplification.	59
Figure 8.7:	Optimization of RT-temperature.	60
Figure 8.8:	Efficiency of Single cell PCR protocol.....	61
Figure 8.9:	Single cell PCR analysis of CMV Donor 1.....	64
Figure 8.10:	Single cell PCR analysis of CMV Donor 2.....	66
Figure 8.11:	Single cell PCR analysis of CMV Donor 3.....	68
Figure 8.12:	Repertoire analysis of CMV-specific T cells from Donor 3	70
Figure 8.13:	Avidity measurement of transduced TCRs.	71
Figure 8.14:	Schematic overview of MHC multimer based isolation of rare antigen-specific T cells.....	72
Figure 8.15:	Identification of fluorophores for MHC multimer staining.....	74
Figure 8.16:	Sequential labeling with two MHC multimers does not prevent labeling.	75
Figure 8.17:	Test of reagents for enrichment.....	76
Figure 8.18:	Sensitivity of MACS enrichment.	77
Figure 8.19:	Isolation of rare antigen-specific T cells from MHC-matched and MHC-mismatched repertoires	78
Figure 8.20:	FACS isolation of rare antigen-specific T cells.	80
Figure 8.21:	Differentiation state of isolated T cells	81

Figure 8.22:	Comparison of specificity and binding strength of auto and allo-repertoire.....	82
Figure 8.23:	Isolation of rare antigen-specific T cells from MHC-matched and MHC-mismatched repertoires	83
Figure 8.24:	Differentiation state of isolated T cells.	85
Figure 8.25:	Evaluation of MFI as an indicator of avidity	86
Figure 8.26:	Transgenic expression of WT1 specific TCRs.....	87
Figure 8.27:	Functional characterization of a single cell-derived TCR.	89

3. INDEX OF TABLES

Table 5.1	Overall survival after TIL therapy.....	20
Table 5.2	Response Rates after infusion of cancer-specific T cell-clones.	22
Table 5.3	Treatment settings of adoptive therapy with virus-specific T cells.	25
Table 5.4	Application of ex vivo isolated virus-specific T cells.	26
Table 5.5	Reported clinical application of genetically redirected patient T cells.	28
Table 5.6	Overview of characterized TCRs for clinical applications.....	30
Table 5.7	Overview of currently ongoing clinical trials of adoptive therapy with TCR-redirectioned T cells	32

4. ABBREVIATIONS

ACT	Adoptive cell therapy
Adj	Adjuvant
AdV	Adenovirus
AML	Acute Myeloid Leukemia
AP-1	clathrin adaptor protein complex 1
APC	Antigen Presenting Cell
β 2m	β 2-microglobuline
BCR	B cell receptor
B-LCL	B-lymphoblastoid cell line
BSA	Bovine serum albumin
CD	Cluster of differentiation
cDNA	complementary DNA
CDR	Complementarity Determining Region
CMV	Cytomegalovirus
cpm	counts per minute
CR	Complete Response
CTL	Cytotoxic T lymphocyte
CTLA-4	Cytotoxic T-Lymphocyte Antigen 4
CyP	Cyclophosphamid
DAC	Dacarbazin
DC	Dendritic cell
DFS	Disease free survival
DLI	Donor Lymphocyte Infusion
DTT	Dithiothreitol
DNA	Deoxyribonucleic acid
EAE	Experimental autoimmune encephalomyelitis
EBV	Epstein-Barr virus

EBNA-1	Epstein-Barr virus nucleic antigen 1
E. coli	Escherichia coli
EDTA	Ethylen-diamine-tetra-acetate
FACS	Fluorescence activated cell sorting
Fc-Domain	Fragment crystallizable Domain
FCS	Fetal calf serum
FITC	Fluorescein-isothiocyanat
Flud	Fludarabin
FoxP3	Forkhead box P3
FPLC	Fast performance liquid chromatography
FS	Forward Scatter
G-CSF	Granulocyte colony stimulating factor
GvHD	Graft versus Host Disease
GvL	Graft versus Leukemia
GvT	Graft versus Tumor
HD	High dose
HIV	Human immunodeficiency virus
HCV	Hepatitis C Virus
HLA	Human leukocyte antigen
IFA	Incomplete Freund's Adjuvant
IFN	Interferon
IL	Interleukin
LAG-3	Lymphocyte-activation gene 3
LAK	Lymphokine activated Killer
LCMV	Lymphocytic choriomeningitis Virus
LD	Low Dose
LMP	Latent Membrane Protein
MACS	Magnetically activated cell sorting
MM	Metastatic Melanoma

MHC-I/II	Major histocompatibility complex class I/II
mRNA	Messenger RNA
NK cell	Natural killer cell
Nef	Negative regulatory factor
NPC	Nasopharyngeal Carcinoma
dNTP	Deoxynucleoside-triphosphate
OR	Objective Response
OS	Overall Survival
PBS	Phosphate buffered saline
PCR	Polymerase chain reaction
PD	Programmed death
PE	Phycoerythrin
PECy7	Phycoerythrin-Cy7
PI	Propidium iodide
pMHC	peptide MHC
PNA	Peptide Nucleic Acid
PR	Partial Response
RACE	Rapid Amplification of cDNA ends
RECIST	Response Evaluation Criteria in Solid Tumors
RNA	Ribonucleic acid
RT	Reverse Transcription
SCD	Stem Cell Donor
SCID	Severe Combined Immune Deficiency
SCT	Stem Cell Transplantation
SS	Side Scatter
TAP	Transporter associated with antigen processing
TCR	T cell receptor
TdT	Terminal deoxyribonucleotidyl Transferase
Th	T helper

TIL	Tumor infiltrating Lymphocyte
Tim-3	T-cell immunoglobulin domain and mucin domain 3
TLR	Toll-like receptor
Treg	regulatory T cell
WT	Wildtype

5. INTRODUCTION

5.1. BASIC CONCEPTS OF THE IMMUNE SYSTEM

General models divide the mammalian immune system into an innate and an adaptive branch. The innate immune system involves a set of inherited, conserved mechanisms, whereas the adaptive immune system is characterized by the progressive development of highly specific responses to defined molecular structures. Generally the innate and adaptive immune systems interact to initiate or suppress the elimination of a target structure. In other words, both branches of the immune system form a complex network of mechanisms to balance tolerance and immunity. Interactions between immune cells function by direct contact formation of surface molecules or by secretion and binding of cytokines.

The rearrangement of antigen-specific binding-molecules, i.e. B cell receptors (BCR) and T cell receptors (TCRs) is one of two main mechanisms of adaptive immunity. The process of rearrangement, which modifies the genomic receptor locus during the differentiation of single cells to T or B cells, is termed somatic recombination. This creates a large pool of T and B cells with diverse specificity. After rearrangement BCRs undergo a second phase of affinity maturation by random mutagenesis in highly variable domains. This process is initiated by successful antigen recognition combined with further activating signals and leads to selection of BCR variants with improved antigen binding quality. Thereupon, further rearrangements of the BCR locus set off the secretion of their soluble form, termed antibodies. In addition, one out of several possible conserved domains, also termed Fc-domains (derived from fragment crystallizable domain), is rearranged to the mature antibody. Each different Fc-domain binds to a specific set of receptors, which shapes the type of immune reaction by selective activation of other cell types (Murphy *et al.* 2011).

TCRs are not further modified after somatic recombination. Their general binding partners are peptide loaded major histocompatibility complex (MHC) molecules. T cells are positively selected for low affinity binding to MHC class I or II complexes, presenting self-derived peptides during their maturation in the thymus. In contrast, if they display high affinity to MHC-I/II and auto-antigen-derived peptides, they are eliminated by negative selection. Alternatively, high affine and potentially auto-reactive T cells differentiate to become regulatory T cells (Treg), which suppress immune responses by antigen-specific and non-specific mechanisms (Jenkins *et al.* 2010).

The other main mechanism of adaptive immunity is the conservation of successful immune adaptation in the form of long-lived memory cells that can react to previously encountered threats. Besides B and T cells that express protective antibodies and TCRs, natural killer cells (NK) also produce memory (Paust *et al.* 2011; Weng *et al.* 2012).

T cells leave the thymus in a state termed naïve and need to be activated by several signals together with MHC-restricted TCR binding to their cognate target antigen. Different subtypes of T cells can be distinguished. After initial activation, mature CD8⁺ T cells commonly display cytotoxic function, which leads to induction of target cell death. CD4⁺ T cells primarily function as immune regulators and are further divided into functionally distinct subtypes Th1, Th2, Th17 and Treg cells (Yamane *et al.* 2012).

5.2. TYPICAL COURSE OF AN IMMUNE RESPONSE

In most cases an immune response targets a pathogen, which is first recognized by mechanisms of the innate immune system. The first line of activation is the direct interaction of pattern recognition receptors, e.g. Toll like receptors (TLRs), with a pathogen-derived molecule. The cell in turn secretes activating cytokines and chemokines to initiate an inflammation (Murphy *et al.* 2011). Activated antigen presenting cells (APCs) promote activation of naïve antigen-specific T cells by MHC-dependent contact and several co-stimulatory signals. T helper cells activate B cells to produce antibodies by direct cell interactions. Antigen-experienced T cells undergo a phase of rapid expansion and differentiation to short-lived effector T cells in response to repetitive antigen encounter. After complete pathogen clearance more than 95% of the pathogen-specific T cells undergo apoptosis, while memory T cells survive long-term (Kaech *et al.* 2002).

In some cases the immune system fails to completely eliminate a pathogen, which leads to persistent antigen stimulation. This also happens during tumor development (Hanahan *et al.* 2011).

5.3. THE IMMUNOLOGICAL ROLE OF T CELLS

T cells are a basic component of immune function. Different genetic defects cause T cell-deficiency, which result in severe recurrent infections in early childhood. Severe combined immune deficiency (SCID) causes complete absence of T cells and even goes along with major physiologic deficiency of lymphatic tissue. Similarly, less comprehensive conditions, which specifically affect T cell-function result in massive viral and fungal infections (Cole *et al.* 2010). T cells additionally can prevent tumor outgrowth. In a model of chemical mutagenesis T cell-deficient mice were significantly more prone to tumor outgrowth of detectable size than wild type (WT) mice. Late depletion of T cells from WT mice permitted outgrowth of tumors that had been chemically induced 200 days before. This underlines the role of T cells in tumor control (Koebel *et al.* 2007).

Immune deficiencies frequently undermine control over infections or tumors. Complete depletion of the host immune system and temporary immune suppression after hematopoietic stem cell transplantation cause chronic viral infections like CMV, EBV or Adenovirus to become relevant causes of mortality (Boeckh *et al.* 2003; Myers *et al.* 2005; Brunstein *et al.* 2006). Correspondingly, long-term immune suppression to avoid rejection of transplanted organs involves an increased incidence of cancers (Marcen *et al.* 2003).

5.4. IMMUNE ESCAPE BY MUTATION

Apart from immune deficiencies, immune escape can cause loss of disease control. Mutation of an antigenic peptide can reduce the selective pressure on a defined target structure. Immune escape was observed in various viruses that confer a high mutation rate e.g. HIV or HCV (Phillips *et al.* 1991; Erickson *et al.* 2001). In the same way, tumor growth is frequently accompanied by acquisition of mutations in highly immunogenic T cell-epitopes. Chemically induced tumors from T cell-deficient mice grew upon transfer to other T cell-deficient mice but were largely rejected in WT mice. In these mice, tumor suppression was correlated with a measurable T cell-response against a defined tumor-associated antigen. The exome – the entity of all transcribed genes - of transferred tumors that underwent progression in WT mice was analyzed by deep sequencing and revealed the emergence of escape mutants in formerly protective T cell-epitopes (Matsushita *et al.* 2012).

5.5. INDUCTION OF IMMUNE EXHAUSTION

Various chronic infections or general persistence of antigen can cause advancing T cell-dysfunction termed T cell-exhaustion. In chronically stimulated T cells different molecular pathways were frequently found to indicate and cause loss of immunologic activity.

Expression and signaling of the inducible cell surface protein PD-1 via B7-H1, a.k.a. PD-L1, was first shown to suppress T cell-activation *in vitro* (Freeman *et al.* 2000). Equally the presence of PD-1 on antigen-specific T cells could impair cell activity in chronically infected HIV patients, with the grade of expression correlating with disease progression. *In vitro* antibody blockade of the PD-1 signaling pathway led to restored T cell function (Day *et al.* 2006). Previously a similar finding was made in an *in vivo* mouse model with transferred B7-H1 positive and negative tumors (Dong *et al.* 2002). In two recent clinical trials cancer patients were treated with PD-L1 or PD-1 blocking antibodies respectively. The therapeutic efficiency was assessed according to the Response Evaluation Criteria in Solid Tumors (RECIST). Partial response (PR) describes a reduction in tumor mass of more than 50%, complete response (CR) signifies a complete disappearance of measurable disease, and objective response (OR) rate is the sum of the former response categories (Therasse *et al.* 2000). In different cancers OR to PD-L1 antibody ranged between 6% and 17% and for PD-1 between 18% and 28%. Treatment was associated with 9% and 14% of severe drug-related adverse events, with three cases of treatment-related death in the PD-1 antibody group (Brahmer *et al.* 2012; Topalian *et al.* 2012).

The expression of further surface markers specifies the grade of exhaustion. Gene expression profiling of tumor infiltrating lymphocytes (TILs) from human melanoma lesions supported the idea that T cell-exhaustion develops gradually (Baitsch *et al.* 2011). Some of the molecules associated with T cell-exhaustion mediate a mechanism non-redundant with PD-1. Combined blockade of LAG-3 and PD-1 synergistically restored the capacity of exhausted T cells to produce cytokines *in vitro*. This process could even restore proliferation and led to reduced viral burden in a murine LCMV-infection model (Blackburn *et al.* 2009). The synergistic effect of the two mechanisms was confirmed by a report demonstrating significantly accelerated clearance of blood-stage Plasmodium infection by combined blockade of PD-1 and LAG-3 in a murine infection model of *Plasmodium yoelii* (Butler *et al.* 2012). Correspondingly, in an *in vivo* melanoma model the synergistic effects of PD-1 and LAG-3 blockage for tumor rejection have been verified (Woo *et al.* 2012).

Furthermore, Tim-3 and PD-1 co-expression was frequently associated with T cell-exhaustion. Tim-3 is a cell surface molecule predominantly expressed on Th1 cells. Tim-

3/Galectin-9-binding promoted apoptosis and reduced IFN γ -secretion in T cells, as well as prevented EAE induction (Zhu *et al.* 2005). In a mouse model of AML, Tim-3 and PD-1 was co-expressed on chronically stimulated T cells. The combined blockade of both pathways acted synergistically to reactivate T cells. In the same model transferred to a Galectin-9 knock-out mouse, the blockade of Tim-3 did not restore the function of exhausted T cells (Zhou *et al.* 2011). This finding was confirmed in an *in vivo* model of LCMV infection, where T cell-exhaustion was promoted by Tim-3 and PD-1 in a cooperative manner. Blockade of both ligands synergistically acted to control viral load (Jin *et al.* 2010).

CTLA-4 has been shown to be an important factor in the maintenance of central tolerance. When the severe autoimmune phenotype of the CTLA-4 knockout mouse model was examined, it became clear that Tregs stringently depend on the function of CTLA-4 (Wing *et al.* 2008). Likewise effector T cells can mediate potent immune-suppressive function through CTLA-4 expression. Selective CTLA-4 blockade on effector T cells inhibited tumor growth in a murine model of melanoma while selective blockade of Tregs was surprisingly ineffective. Yet CTLA-4 blockade on both cell types retarded tumor growth significantly more (Peggs *et al.* 2009). A CTLA-4 blocking antibody was tested in clinical trials. The first application to nine patients with metastatic melanoma or ovarian cancer caused clear signs of anti-tumor immune response without severe side effects (Hodi *et al.* 2003). Not only did subsequent clinical trials of CTLA-4 blockade frequently induce anti-tumor-activity associated with prolonged overall survival, but also a substantial fraction of treatment-associated severe adverse events including patient death (Hodi *et al.* 2010).

Based on these observations we can clearly ascribe a crucial role to T cell-exhaustion for chronic infections and cancer development. Thus the blockade of immune suppressive signaling pathways could contribute to the efficiency of adoptive cell transfer.

5.6. IMMUNE ESCAPE BY PREVENTION OF ANTIGEN PRESENTATION

Although viruses and tumors use similar strategies for immune escape, they substantially differ in mechanistic details. Whereas tumors gradually acquire escape mechanisms *de novo* through genomic instabilities leading to gain or loss of function mutations, viruses carry a conserved set of evolutionarily refined molecular tools. Several mechanistic categories to prevent effective T cell-responses can be identified.

A common strategy to avoid T cell-activation is to prevent MHC presentation of highly immunogenic T cell-epitopes. For this purpose, the MHC-complex itself frequently becomes a molecular target. The CMV-encoded proteins US2 and US11 translocate to the cytoplasm and promote the degradation of MHC-I heavy chains. US2 furthermore can mediate degradation of HLA-DR and HLA-DM α -chains (Wiertz *et al.* 1996; Wiertz *et al.* 1996; Tomazin *et al.* 1999). The CMV protein US3 prevents egress of MHC-I molecules from the endoplasmic reticulum (Jones *et al.* 1996). In the same manner, the adenoviral protein E3-19K can directly attach to sites on all three α -domains, as well as β 2-microglobulin of MHC class I, and thereby retains the complex in the ER (Burgert *et al.* 1985; Li *et al.* 2012).

The MHC complex is not necessarily a direct target of immune suppressant molecules. Reports demonstrate that the CMV protein US6 could prevent the loading of peptides to MHC-I by inhibiting the transporter associated with antigen processing (TAP) complex. In the same manner the Herpes Simplex Virus protein ICP47 interferes with the TAP complex, only slightly differing in binding site, outside the ER lumen (York *et al.* 1994; Ahn *et al.* 1997). Likewise, EBV inhibits TAP through the protein BNLF2a. Furthermore, this mechanism seems to be highly conserved across the entire gamma-1 Herpesvirus family (Hislop *et al.* 2007).

The HIV-encoded Nef-protein reduces MHC-I surface expression by a different mechanism. Although the clinical relevance of Nef was long known (Deacon *et al.* 1995; Kirchhoff *et al.* 1995; Collins *et al.* 1998), only recent successful crystallography gave clear insight in its mode of action. In contrast to the before mentioned proteins from Herpes- and Adenoviruses, Nef can act downstream of the endoplasmic reticulum. Nef forms a ternary complex with the clathrin adaptor protein complex 1 (AP1) and MHC-I and impairs trafficking emanating from the trans-golgi network (Jia *et al.* 2012).

The Epstein-Barr virus nucleic antigen 1 (EBNA1) uses the most straightforward mechanism to prevent MHC-I presentation. EBNA1 contains a Gly-Ala domain, which prevents

proteasome degradation and furthermore suppresses its own gene expression. In combination, this mediates low and self-limiting presence of protein, protected from proteasome degradation and invisible to MHC-I presentation during viral latency (Levitskaya *et al.* 1997; Yin *et al.* 2003).

Similar mechanisms to suppress MHC presentation have been observed in tumors. Complete absence of antigen processing was observed in small cell lung carcinoma cell lines, caused by a complete deficiency of TAP-1 and TAP-2, as well as the proteasome components LMP-7 and LMP-2. The described phenotype was reversible by IFN γ -stimulation (Restifo *et al.* 1993). However, other deficiencies resulted from gene loss by missense mutations, and thus were resistant to IFN γ -mediated MHC-I upregulation (Chen *et al.* 1996). The most conclusive description of altered MHC presentation in cancer is a recent analysis of 178 small lung cancer carcinoma samples. All samples were analyzed for DNA copy number, somatic exon mutations, mRNA sequence, mRNA expression, and promoter methylation, as well as histopathology. In addition, whole genome sequencing of 19 samples and micro RNA sequencing from 159 samples were conducted. Strikingly, HLA-A was among the 10 most frequently mutated genes (Hammerman *et al.* 2012).

5.7. ADOPTIVE CELL THERAPY

Adoptive cell therapy (ACT) describes the transfer of immune cells to compensate for a qualitative or quantitative insufficiency of a defined function in the recipient. Theoretically, ACT could cure many different conditions like infections, cancers or autoimmune diseases. Because of their diverse functions T cells in particular are highly suitable for this approach.

5.7.1. STEM CELL TRANSPLANTATION AND DONOR LYMPHOCYTE INFUSION

Many reports of adoptive T cell-transfer have proven that this approach can be highly effective. The first bone marrow transplantation as a treatment of human leukemia was reported in 1959. After lymphodepletion by total body irradiation, bone marrow from their respective identical twins was applied to three patients. Adoptive T cell-transfer was performed unwittingly along with the bone marrow stem cells. At the time, T cells were more-the-less unknown and were not depleted from the graft (Thomas *et al.* 1959). This is important because, when donor T cells with specificity for any recipient tissue are activated upon adoptive transfer, Graft versus host disease (GvHD) can occur. This condition results in severe tissue inflammation and immune hyperfunction. For a long time, GvHD was exclusively regarded as an unwanted side effect of bone marrow transplantation, until it turned out to be highly correlated with a reduced risk of leukemia recurrence. This finding coined the idea of a graft versus leukemia (GvL) effect (Weiden *et al.* 1979; Weiden *et al.* 1981).

T cell-depletion from bone marrow grafts resulted in diminished GvHD but more frequent graft rejection and higher probability of leukemia relapse, indicating that T cells mediated the GvL effect (Marmont *et al.* 1991). For patients with previous stem cell transplantation (SCT), the GvL-effect was utilized separately to treat patients with disease relapse. SCT patients become largely tolerant to the donor immune system, which allows engraftment of peripheral blood mononuclear cells (PBMCs) from the donor. This treatment, known as donor lymphocyte infusion (DLI), showed a GvHD-associated GvL-effect that frequently led to leukemia remission (Kolb *et al.* 1990).

Although for leukemia the induction of GvL by transfer of allogeneic T cells has become an effective standard treatment, the corresponding graft versus tumor (GvT) effect is probably not broadly usable. For renal cell carcinoma a GvT effect was reported to yield response rates of up to 57%. However, the high correlation with severe GvHD and treatment-related mortality of up to 33% still hamper broad application. Similarly, GvT response rates of up to 37%, but with a treatment-related mortality of up to 22%, were reported for metastatic melanoma. A number of reports of GvT-treatment for pancreatic and ovarian cancer and several other cancers show highly diverse results (Demirer *et al.* 2008).

5.7.2. TUMOR INFILTRATING LYMPHOCYTES

Previous to Tumor infiltrating lymphocytes (TILs) patient-PBMCs were evaluated as a graft source for adoptive therapy. Similar to TILs PBMCs were *ex vivo* isolated and *in vitro* expanded in the presence of cytokines. This type of cell graft is generally described as Lymphokine activated killer (LAK) cells. The reinfusion of LAKs as a potential regimen for human therapy was evaluated in several models of murine cancer. In a first report, tumor cells were intravenously applied to mice, which were monitored for the appearance of lung metastases. LAK infusion acted synergistically with application of IL-2 for tumor protection (Mule *et al.* 1984). LAK therapy in humans initially achieved OR of 44% of all treated patients with various types of cancer. However, for larger patient cohorts this result was not confirmed (Rosenberg *et al.* 1985). Further trials rather suggested an OR of 27% (Rosenberg *et al.* 1987). When data from several clinical trials were analyzed, the combined application of LAK and IL-2 only induced a slightly better, but not significant, tumor response than IL-2 alone (Rosenberg *et al.* 1993).

Results from mouse studies suggest that TILs can induce strong anti-tumor responses (Yron *et al.* 1980). In one study, a direct comparison of tumor-inhibiting capacities indicated that activated TILs are 50-100 times more effective than LAKs. In addition, a strong synergistic effect of lymphodepletion with cyclophosphamid, prior to cell infusion, was observed and thus, even LAK resistant metastases were sensitive to the combined treatment of TILs, lymphodepletion and IL-2 (Rosenberg *et al.* 1986). Supremacy of TILs over LAKs as a treatment of metastatic melanoma was further confirmed in clinical trials. As a first clinical treatment protocol a median number of 2×10^{11} *in vitro* expanded TILs were infused, followed by 10^5 U IL-2 every eight hours until toxicity prohibited further cytokine application. Nine out of 15 treated patients showed an OR, which equals 60% (Rosenberg *et al.* 1988). The benefit of non-myeloablative lymphodepletion with cyclophosphamid was less pronounced than in the murine studies. OR rate in subsequent trials was 35% with prior treatment, and 31% without (Rosenberg *et al.* 1994). However, in this initial trial only a single dose of 25mg/ml of cyclophosphamid was applied, whereas following treatment protocols applied more intensive lymphodepleting regimens with substantially higher response rates (Dudley *et al.* 2002).

In addition to these milestone observations, numerous clinical trials against different tumor types were conducted in different centers (Topalian *et al.* 1988; Kradin *et al.* 1989; Dillman *et al.* 1991; Rosenberg *et al.* 1994; Schwartzentruber *et al.* 1994; Goedegebuure *et al.* 1995; Ravaud *et al.* 1995; Queirolo *et al.* 1999; Dudley *et al.* 2002; Dudley *et al.* 2005; Dudley *et al.* 2008; Besser *et al.* 2010; Dudley *et al.* 2010; Ellebaek *et al.* 2012; Radvanyi *et al.* 2012). The protocols varied considerably, but many studies applied the same categorization to quantify

treatment efficiency into partial, complete and objective, as defined in the RECIST criteria (Therasse *et al.* 2000). We extracted all data from these categories from the aforementioned reports and summarized them (Fig. 5.1.a and c). As the treatment protocols varied in supplementary treatments, concerning IL-2 doses, pre-conditioning lymphodepletion, infused TIL numbers, cell expansion protocols and most importantly in tumor type and stage the comparison of these results only allows reduced conclusions. ORs ranged between 0% and 72% and complete responses were detected in 0% to 33% of patients per treatment group. Overall weighted average values of 40% for objective responses and 6.9% for complete responses were calculated based on the patient number per treatment group.

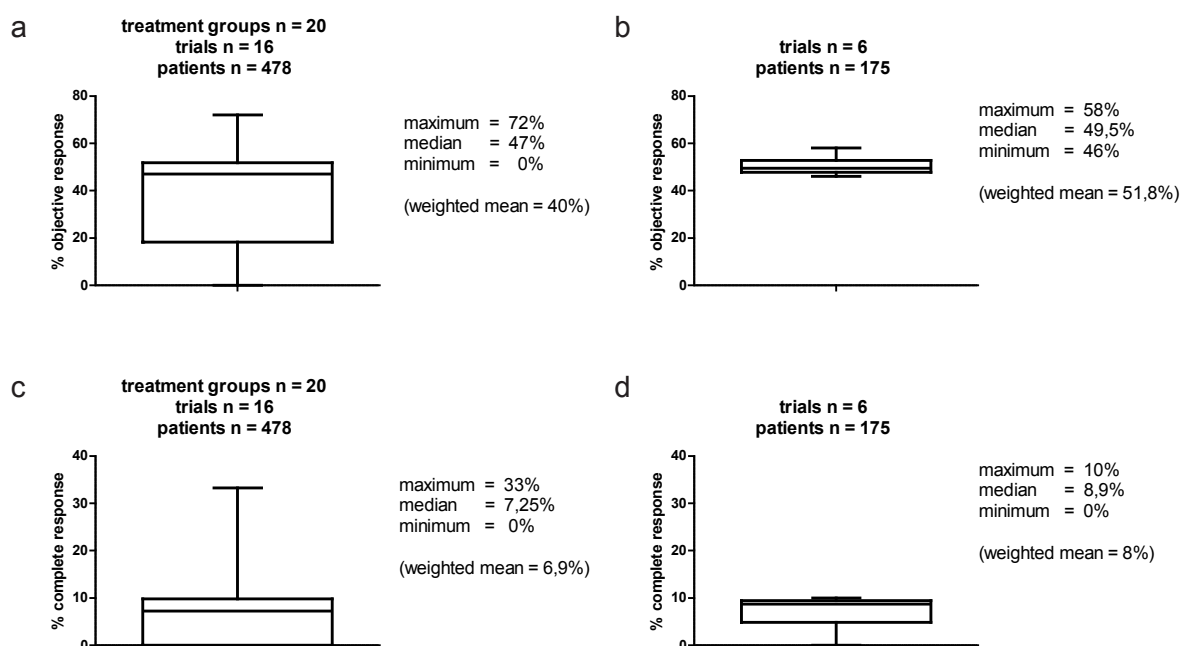


Figure 5.1: Assessment of Response Rates to TIL therapy.

All Pubmed accessible data quantifying objective and complete response rates of TIL therapy were extracted and combined (Topalian *et al.* 1988; Kradin *et al.* 1989; Dillman *et al.* 1991; Rosenberg *et al.* 1994; Schwartzentruber *et al.* 1994; Goedegebuure *et al.* 1995; Ravaud *et al.* 1995; Queirolo *et al.* 1999; Dudley *et al.* 2002; Dudley *et al.* 2005; Dudley *et al.* 2008; Besser *et al.* 2010; Dudley *et al.* 2010; Ellebaek *et al.* 2012; Radvanyi *et al.* 2012). Variation range, interquartile range and median were summarized in box plots. Weighted arithmetic mean was calculated as measure of patients per treatment group. (a,c) Objective or complete response rates respectively from all trials are shown. (b,d) Diagrams combine results from all TIL trials with non-myeloablative pre-conditioning and application of high dose IL-2.

The most broadly applied treatment protocol however includes non-myeloablative preconditioning with Cyclophosphamid and Fludarabin followed by TIL infusion and repetitive application of high dose IL-2, up to the occurrence of dose limiting toxicity. When only considering metastatic melanoma patients treated with this protocol the clinical outcomes

appear far more reproducible and constant. As shown in Fig. 5.1b and d, minimum and maximum OR were 46% and 58% respectively with a median of 49.5% and a weighted average value of 51.8%. A single trial observed 0% of CR, which lies markedly outside the interquartile range. The interquartile range lay near a median value of 8.9%. The weighted arithmetic mean of 8% ranged near the maximum value of 10%. Despite the impressive effect of shrinking tumor mass, the more important parameters to assess the potential of a treatment regimen should consider the endurance of response. For this reason data on overall survival were collected. This measure also enables the inclusion of patients, preemptively treated with TILs post tumor resection. Several studies have conducted a long-term patient follow up (Fujita *et al.* 1995; Ratto *et al.* 1996; Figlin *et al.* 1999; Takayama *et al.* 2000; Ridolfi *et al.* 2003; Gardini *et al.* 2004; Khammari *et al.* 2007; Rosenberg *et al.* 2011). The fraction of overall five-year survival probability was the most commonly described parameter. Analysis of combined data is hampered because of fundamental inconsistency between treatment protocols and type of disease as well as in the choice of parameters to quantify the treatment efficiency. Several studies lack a control group or apply standard therapy as control group, which does not include IL-2 infusion. Despite these limitations some of the published results clearly demonstrate efficacy of TIL treatment as summarized in Table 5.1.

Treatment success was associated with different variables. Several studies report that the response rate was positively correlated with higher counts of infused TILs (Radvanyi *et al.* 2012). Likewise, shorter cultivation time and higher *in vitro* proliferation rates were beneficial (Rosenberg *et al.* 1994; Dudley *et al.* 2005; Besser *et al.* 2010). TILs from subcutaneous melanoma deposits led to significantly more responses than TILs from resected lymph nodes (Schwartzentruber *et al.* 1994). Also the differentiation state of infused TILs based on parameters like expression of CD27-expression on CD8⁺T cells, telomere length and secretion of GM-CSF were potentially predictive for therapeutic success (Dudley *et al.* 2008; Rosenberg *et al.* 2011). Furthermore, one study evaluated the therapy history of their recruited patients. Patients previously treated with a CTLA-4 blocking antibody had a significantly prolonged overall survival (Rosenberg *et al.* 2011).

Pathology	Treatment	Patients	Long-term effect	Ref.
hepatocellular carcinoma post liver resection	TIL	76	5 year OS 68% vs. 62% <u>ns</u> overall recurrence reduced by 41% (<u>$p > 0.1$</u>)	(Takayama <i>et al.</i> 2000)
metastatic renal cell carcinoma post kidney resection	TIL, LD IL-2	81	no benefit of treatment; trial terminated prematurely	(Figlin <i>et al.</i> 1999)
liver metastatic colorectal cancer post liver resection	TIL, LD IL-2	14	5 year OS 25% vs. 38% <u>ns</u>	(Gardini <i>et al.</i> 2004)
stage III melanoma post one or two lymph node resection	TIL, LD IL-2	44	5 year OS 39% vs. 27.2% <u>ns</u>	(Khammari <i>et al.</i> 2007)
one resected lymphnode		15	5 year OS 73% vs. 31.6% <u>($p = 0.0125$)</u>	
post operative non small cell lung cancer	TIL, long-term LD IL-2	56	3 year OS 25% vs. 12.5% (<u>$P < 0.01$; control group without IL-2</u>)	(Ratto <i>et al.</i> 1996)
ovarian cancer post resection and chemotherapy	TIL	35	3 year OS 87,2% vs. 55% (<u>$P < 0.05$</u>)	(Fujita <i>et al.</i> 1995)
stage III and IV melanoma after surgery	TIL, medium dose IL-2	25	5 year OS 44% 5 year DFS 37% <u>(no control group)</u>	(Ridolfi <i>et al.</i> 2003)
metastatic melanoma	TIL, HD IL-2, lymphodepletion,	93	5 year OS 29% <u>(no control group)</u>	(Rosenberg <i>et al.</i> 2011)
initial complete responders	TBI (0,200,1200Gy)	20	5 year OS 93% <u>(no control group)</u>	

Table 5.1 Overall survival after TIL therapy.

All Pubmed accessible data quantifying long-term overall survival (OS) of patients treated with TIL therapy were summarized. Additional application of IL-2, lymphodepleting chemotherapy or total body irradiation is listed under treatment. P-values indicate significant difference in overall mean survival values between treatment group and matched control group. ns= not significant. Other included parameters are disease free survival (DFS) and overall reduced recurrence.

One major obstacle that prevents a broad clinical application of TIL therapy is the integration into daily clinical routine. Original protocols required enormous costs and efforts. This bottleneck has partially been alleviated by protocols with considerably shorter culture periods. TILs generated this way not only produced at least similar, or better clinical response rates as previous protocols, but also drastically reduced overall cell culture time to a mean of 32-35 days (Dudley *et al.* 2010). Further, new bioreactor systems allow simplified, large scale cell cultivation under good manufacturing practice (GMP) grade conditions (Somerville *et al.* 2012). Several clinical trials with such “young” TILs are currently ongoing.

5.7.3. TUMOR-SPECIFIC T CELL-CLONES

Increasing knowledge of the tumor-associated antigens (TAA) that were most frequently recognized by TILs, encouraged efforts to specifically expand and transfer T cells of known epitope-specificity from sources other than tumor infiltrates. Hypothetically different advantages favor this approach. First, *in vitro* expansion of TILs is not always successful. Although the success rate to expand tumor infiltrating lymphocytes has increased, tumors without sufficient infiltrate or lymphocyte growth are observed. Second, no surgical removal of tumor tissue is necessary. Third it has been shown that TILs mostly are functionally impaired (Baitsch *et al.* 2011). Although *in vitro* expansion can restore cell function, there remains doubt about the stability of this effect.

It is generally accepted that different sub-populations of T cells vary in their potential to reconstitute the whole spectrum of the functionally distinct sub-phenotypes, including long-living memory cells. Apart from a subset of central memory T cells termed “memory stem cells”, single naïve T cells can give rise to all progenitor cell types associated with a full-blown and long-lasting T cell-response (Stemberger *et al.* 2007; Gattinoni *et al.* 2011). Similarly, central memory T cell-descendants persisted longer and protected better than effector differentiated T cells, although after *in vitro* expansion they expressed markers of effector T cells (Berger *et al.* 2008). PBMCs contain all T cell-types, including naïve and memory stem cells. Therefore, for adoptive therapy they supposedly constitute a better cell source than TILs.

These arguments favor the approach to use PBMCs as a cell source for adoptive therapy. Antigen-specific T cells were expandable from vaccine-induced T cell-populations, and even from initially undetectable numbers. Surprisingly, the clinical response rates to T cells obtained by this strategy were substantially diminished compared to TILs (Yee *et al.* 2002; Mackensen *et al.* 2006). Lymphodepleting preconditioning with Fludarabin significantly prolonged persistence of infused clones (Wallen *et al.* 2009). Cyclophosphamid-lymphodepletion and high dose IL-2 were clinically evaluated without increased response rates. However, this result is uncertain, as only three patients were treated (Chapuis *et al.* 2012).

Pathology	Treatment	Antigen	Patients	response	Ref.
MM	CD8 ⁺ T cells; LD IL-2	MART-1; gp100	10	minor	(Yee <i>et al.</i> 2002)
MM	CD8 ⁺ T cells; LD IL-2	MART-1	11	1 PR/ 1 CR	(Mackensen <i>et al.</i> 2006)
MM	CD4 ⁺ T cells	NY-ESO-1	1	CR	(Hunder <i>et al.</i> 2008)
MM	CD8 ⁺ T cell; LD IL-2; Flud	MART-1; gp100; Tyrosinase	10	minor	(Wallen <i>et al.</i> 2009)
stage III/IV melanoma	CD8 ⁺ T cells; LD IL-2; IFN α	MART-1	14	4 PR/ 2 CR	(Khammari <i>et al.</i> 2009)
MM	CD4 ⁺ /CD8 ⁺ T cells; IFN α	Nd.	10	1 PR/ 1 CR	(Verdegaal <i>et al.</i> 2011)
MM	CD8 ⁺ T cell	MART-1	9	3 PR/ 1 CR	(Butler <i>et al.</i> 2011)
MM	CD8 ⁺ T cells; HD CyP; LD IL-2;	MART-1; gp100; Tyrosinase	10	1 PR/ 1 CR	(Chapuis <i>et al.</i> 2012)

Table 5.2 Response Rates after infusion of cancer-specific T cell-clones.

All Pubmed accessible data treatment response of patients treated with in vitro expanded clones specific for tumor-associated antigens were summarized. Treated diseases are metastatic melanoma (MM) and stage II/IV melanoma. Additional application of IL-2, IFN α lymphodepleting chemotherapy with Fludarabin (Flud), Dacarbazine (Dac), cyclophosphamid (CyP) is listed under treatment. Partial (PR) response indicates Tumor shrinkage of >50% and complete response (CR) indicates complete tumor disappearance.

The highest response rate to infusion of *in vitro* expanded T cell-clones was observed in a study of stage III/IV melanoma. The treatment protocol included many factors that have not been evaluated in T cell-therapy before. Cell transfer was combined with dacarbazine chemotherapy, infusion of nine international mega-units of IL-2 for 10 days, and IFN α for one month. ORs were assessed in 43% of patients including 2 complete responses (Khammari *et al.* 2009). The authors explain this result by their different pre-selection strategy of T cells for infusion, which was based on the capability to secrete IL-2. To which extent this exceptionally high response rate can further be attributed to the subsidiary treatment or the stage of disease remains unresolved.

The most common combination of supplemental treatments applied in TIL studies, consisting of repetitive, high dose IL-2, cyclophosphamid and fludarabin for non-myeloablative lymphodepletion, so far has not been evaluated in this context. Artificial antigen presenting cells for *in vitro* priming and expansion of T cell-clones can direct T cells towards a memory phenotype. T cells generated with this method displayed a prolonged *in vivo* survival. In this study ORs were achieved in 4/10 patients, among them one complete response (Butler *et al.* 2011).

One case report furthermore describes infusion of a NY-ESO-1-targeted CD4⁺ T cell-line resulting in a complete remission without any additional treatment. Upon T cell-infusion immune responses to other melanoma-associated antigens became detectable (Hunder *et al.* 2008). One study describes the infusion of CD4⁺ and CD8⁺ T cell-lines generated by co-incubation of tumor tissue with autologous PBMCs and additional IFN α -treatment. In 2/10 patients ORs, one complete and one partial were observed (Verdegaal *et al.* 2011).

Transfer of *in vitro* grown T cell-clones has also been applied for treatment of CML. Fourteen Patients in remission after SCT were infused with autologous CD4⁺ and CD8⁺ T cell-clones reactive to the leukemia-associated antigens WT1, PR1 and BCR/Abl. Long-term remissions were achieved. As this was a prophylactic treatment the patient cohort is too small to draw clear-cut conclusions about therapeutic efficacy (Bornhauser *et al.* 2011). All results that describe treatment response are summarized in Table 5.2.

5.7.4. ADOPTIVE TRANSFER OF VIRUS-SPECIFIC T CELLS

Especially under immunosuppressive treatment infections with viruses like CMV, EBV and Adenovirus are a relevant cause of mortality (Boeckh *et al.* 2003; Myers *et al.* 2005; Brunstein *et al.* 2006). Like TILs for different cancers, virus-antigen-specific T cells have been used for adoptive transfer against viral disease. In the setting of stem cell transplantation, donor-derived T cells can engraft after transfer. Transfer of virus-specific T cells as treatment of transplantation-associated viral complications therefore seemed an attractive option. The first report of targeted adoptive transfer against CMV disease after hematopoietic stem cell transplantation in 1995 showed that this approach is highly efficient. For expansion of CMV-specific T cells fibroblasts were infected with CMV in order to stimulate T cells from the bone marrow donor (Walter *et al.* 1995). This approach was translated to EBV in similar fashion. For use as APCs, B-cells were EBV infected and concomitantly immortalized to obtain cell lines mostly called B-lymphoblastoid cell lines (B-LCLs). Bone marrow-derived PBMCs were co-cultured with B-LCLs to expand EBV-specific T cells (Heslop *et al.* 1996). Several clinical trials for CMV-, EBV- and Adenovirus-associated diseases have shown that this strategy is highly effective. Decline in viral load, absence of viral disease and long-term persistence of transferred T cells was frequently described. Protection from disease however is difficult to quantify in these patients, as they suffer from diverse and highly complex symptoms. Many different methods for *in vitro* expansion of antigen-specific cells have been clinically applied. Several of these approaches aim to create T cells for several of the most frequent transplantation-associated infections in parallel, as a preventive therapy (Leen *et al.* 2006). Mostly stem cell donors served as PBMC donors for *in vitro* cell expansion of virus-specific T cells, predominantly from pre-existing cell populations. In addition, also T cell-lines derived from 3rd party donors or haplo-identical family donors led to successful engraftment and clinical responses. Furthermore, EBV-associated malignancies like nasopharyngeal carcinoma and lymphomas have been treated resulting in objective responses and a significant prolongation of mean overall survival (Lucas *et al.* 2004; Bollard *et al.* 2007; Louis *et al.* 2010; Smith *et al.* 2012).

Expansion method	Disease	Donor	Patients	Ref
CMV infected fibroblasts	CMV disease	CMV ⁺ SCD	14	(Walter <i>et al.</i> 1995)
B-LCL; genetic labeling for long-term detection	EBV PTLD	EBV ⁺ SCD	14	(Heslop <i>et al.</i> 1996)
CMV lysate	CMV disease	CMV ⁺ SCD	8	(Einsele <i>et al.</i> 2002)
autologous DCs pulsed with CMV lysate	CMV disease	CMV ⁺ SCD	16	(Peggs <i>et al.</i> 2004)
B-LCL	EBV positive HD	3 rd party partially HLA-matched	6	(Lucas <i>et al.</i> 2004)
B-LCL infected with pp65 (CMV) expressing adenoviral vector Ad5f35pp65	CMV/EBV/AdV disease	SCD	11	(Leen <i>et al.</i> 2006)
autologous DCs pulsed with pp65 peptide	CMV disease	CMV ⁺ SCD	9	(Micklethwaite <i>et al.</i> 2007)
B-LCL-modified for enhanced presentation of latency antigens	EBV positive lymphoma	Autologous	16	(Bollard <i>et al.</i> 2007)
autologous DCs infected with pp65 expressing adenoviral vector Ad5f35pp65	CMV disease	CMV ⁺ SCD	12	(Micklethwaite <i>et al.</i> 2008)
Ad5f35null infection 10 days; expansion with Ad5f35null infected B-LCLs	EBV/AdV disease	EBV ⁺ AdV ⁺ SCD	13	(Leen <i>et al.</i> 2009)
B-LCL	EBV NPC	Autologous	23	(Louis <i>et al.</i> 2010)
B-LCL	EBV disease	3 rd party donor	2	(Barker <i>et al.</i> 2010)
AdE1-LMP poly vector infected autologous irradiated PBMCs	EBV NPC	Autologous	14	(Smith <i>et al.</i> 2012)

Table 5.3 Treatment settings of adoptive therapy with virus-specific T cells.

All published clinical trials of infusion of in vitro expanded clones specific for viral antigens that showed at least one non-redundant feature in the listed categories are summarized. Treated diseases besides virus infection-associated disease are nasopharyngeal carcinoma (NPC), post transplant lympho-proliferative disorder (PTLD) and Hodgkin Disease (HD). Stem cell donor = SCD.

In this setting autologous patient T cells were expanded and re-infused. Table 5.3 summarizes the most important constellations for cell therapy of viral diseases. Despite potent clinical efficacy, broad clinical application of this therapy is prevented by logistic requirements. Extensive GMP cell culture is hardly compatible with clinical routine, therefore more direct and faster methods are necessary. Several strategies for a direct transfer of antigen-specific T cells with no or minimal cell culture have been evaluated. Pre-existing T cell-populations specific for viral antigens have been identified by *in vitro* stimulation with viral antigens and have been isolated based on their capability to secrete IFN γ (Feuchtinger *et al.* 2006; Feuchtinger *et al.* 2010; Moosmann *et al.* 2010; Qasim *et al.* 2011).

Isolation method	Disease	Donor	Patients	Ref
MHC multimer	CMV disease	CMV+ SCD	9	(Cobbold <i>et al.</i> 2005)
IFN γ -secretion; stimulation with AdV infected cell lysate	AdV disease	AdV+ SCD	9	(Feuchtinger <i>et al.</i> 2006)
MHC multimer	EBV PTLD	3 rd party haplo	1	(Uhlin <i>et al.</i> 2010)
IFN γ -secretion; stimulation with pp65 (CMV) protein	CMV disease	CMV+ SCD	16	(Feuchtinger <i>et al.</i> 2010)
IFN γ -secretion; stimulation with EBV peptide pool	EBV PTLD	EBV+ SCD	6	(Moosmann <i>et al.</i> 2010)
reversible MHC multimer	CMV disease	CMV+ SCD	2	(Schmitt <i>et al.</i> 2011)
IFN γ -secretion; stimulation with a ADV infected cell lysate	AdV disease	3 rd party haplo	1	(Qasim <i>et al.</i> 2011)
MHC multimer	CMV/EBV/AdV disease	SCD/ 3rd party HLA-matched	8	(Uhlin <i>et al.</i> 2012)

Table 5.4 Application of ex vivo isolated virus-specific T cells.

All published clinical trials of infusion of directly *ex vivo* isolated T cells specific for viral antigens that showed at least one non-redundant feature in the listed categories are summarized. Treated diseases besides virus infection were disease post transplant lymphoproliferative disorder (PTLD). Donor “Stem cell donor” (SCD).

Other strategies utilized MHC multimers to isolate T cells based exclusively on the specificity of their TCR. Both strategies apply magnetic enrichment to isolate the labeled cells. In general, substantially fewer T cells can be obtained by direct transfer in comparison to in vitro expansion based methods. The clinical outcomes however are comparable if not better (Cobbold *et al.* 2005; Uhlin *et al.* 2010; Uhlin *et al.* 2012). The most promising strategy to obtain virus-specific CD8⁺T cells for adoptive transfer seems to be the application of reversible MHC multimers, which can be detached off the cells after the isolation procedure (Schmitt *et al.* 2011). Cells isolated in this way can be considered as minimally manipulated and can be transferred without any other molecule, which is very important from the regulatory point of view. The mentioned methods that were applied in a clinical setting are summarized in Table 5.4.

5.7.5. GENETIC REDIRECTION OF T CELLS

In 1986 genetic transfer experiments have for the first time conclusively demonstrated that antigen-specificity of T cells is exclusively mediated by the TCR (Dembic *et al.* 1986). Later, first *in vivo* experiments have demonstrated that TCR-redirectioned T cells can persist and produce a functional immune response (Kessels *et al.* 2001). These groundbreaking discoveries paved the way for the first application of adoptive immunotherapy with TCR-redirectioned T cells in a clinical trial (Morgan *et al.* 2006). The transfer of the TCR molecule to autologous patient T cells has several advantages over transfer of cell lines or clones. First the quality of the TCR can be evaluated and remains constant, irrespective of the endogenous immune response. A TCR that yields best clinical response can be selected, which in principle should result in constantly high response rates. Second the host cell type can be pre-defined. Several studies could show that naïve or memory T cells have different capacities to proliferate, persist and confer protection. Third, no tumor biopsies or other sources of antigen-specific T cells are required. And fourth, extensive in vitro expansion is dispensable.

Another argument in favor in this approach over TIL reinfusion is based on recent findings about dysfunctional T cells. The molecular program of tolerant CD8⁺ T cells that have escaped thymic negative selection despite a highly auto-antigen-affine TCR was analyzed. Lymphopenia transiently reversed the immune suppressive function of those cells but soon returned to a tolerant state. This finding indicates that antigen-specific tumor infiltrating lymphocytes, which potentially resemble the examined cell type, become activated by lymphopenia, but will return to their epigenetically hardwired, tolerant phenotype. Therefore,

genetic redirection of functional T cells should be favored over reactivation of dysfunctional T cells (Schietering *et al.* 2012).

Several pre-clinical models have shown that this approach is feasible resulting in several clinical trials that have demonstrated the possibility to induce complete and partial regressions in solid tumors. Several clinical trials are currently ongoing and some results have already been published (Morgan *et al.* 2006; Johnson *et al.* 2009; Parkhurst *et al.* 2011; Robbins *et al.* 2011). All patients that received genetically redirected T cells were treated with cyclophosphamid and fludarabin for non-myeloablative lymphodepletion. Furthermore, all patients received high dose IL-2 infusions until dose limiting toxicity occurred. All published results on adoptive transfer of TCR-redirectioned T cells are summarized in Table 5.5.

Pathology	Antigen	Patients	OR	CR	Ref.
Metastatic melanoma	MART-1 ₂₇₋₃₅	15	13%	0%	(Morgan <i>et al.</i> 2006)
Metastatic melanoma	MART-1 ₂₇₋₃₅	20	30%	0%	(Johnson <i>et al.</i> 2009)
Metastatic melanoma	gp100 ₁₅₄₋₁₆₂	16	19%	6%	
Metastatic melanoma	NY-ESO-1 ₁₅₇₋₁₆₅	11	67%	18%	(Robbins <i>et al.</i> 2011)
Synovial cell carcinoma	NY-ESO-1 ₁₅₇₋₁₆₅	6	45%	0%	
Metastatic colon carcinoma	CAE ₆₉₁₋₆₉₉	3	33%	0%	(Parkhurst <i>et al.</i> 2011)

Table 5.5 Reported clinical application of genetically redirectioned patient T cells.

All Pubmed accessible data quantifying the response rates as measure of tumor shrinkage after infusion of TCR-redirectioned autologous patient T cells were extracted. All patients received high dose IL-2 and non-myeloablative, lymphodepleting chemotherapy. TCRs were specific for different tumor-associated antigens as indicated.

Several TCRs have been and are currently in clinical applications. The binding strength to the cognate MHC-peptide ligand has been identified as an important parameter to successfully trigger T cell-function. Several TCRs that have been used in clinical trials have

been extensively characterized. One TCR-specific for MART-1, generally referred to as DMF4, has been replaced by a different TCR termed DMF5.

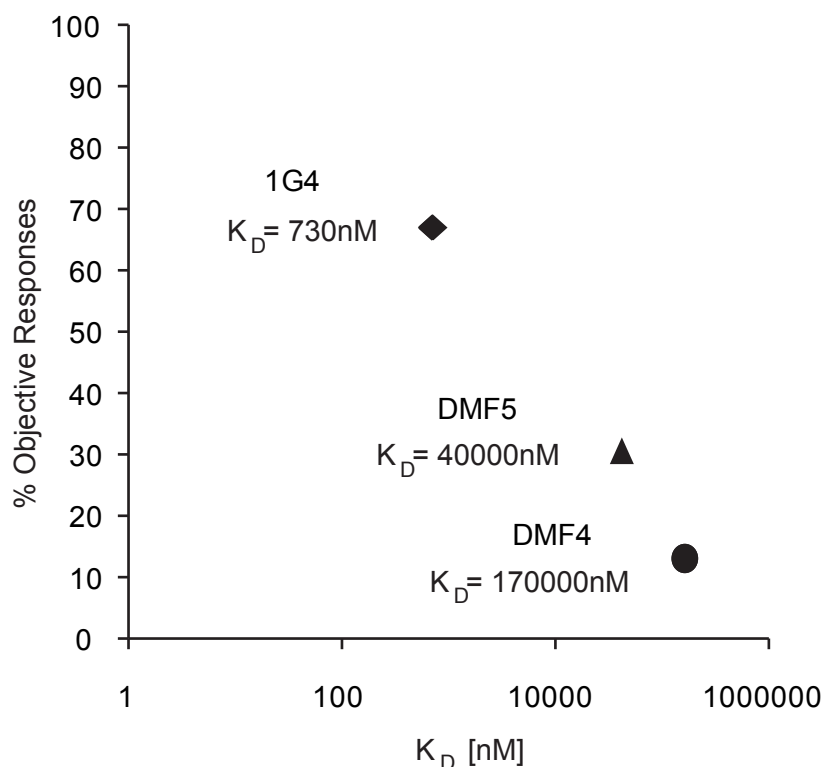


Figure 5.2: Correlation of structural avidity and clinical response"

For several TCRs, which have been tested in clinical trials, dissociation constant (K_D) values have been reported. All Pubmed accessible data quantifying objective tumor response rates after infusion of autologous T cell-redirected with one of these TCRs were pooled and plotted against their dissociation constants.

For both molecules crystal structures and affinity data from surfaces Plasmon resonance have been published (Borbulevych *et al.* 2011). Both TCRs have been used for clinical trials with similar treatment protocols (Morgan *et al.* 2006; Johnson *et al.* 2009). Further, affinity information has been reported for modified versions of 1G4, a TCR-specific for the cancer testis antigen NY-ESO-1, which has first been described in 2000 (Chen *et al.* 2000). In several studies variants of 1G4 ranging in affinities between K_D -values of 2.6pM and 32 μ M have been generated by phage display or site directed mutagenesis (Boulter *et al.* 2003; Li *et al.* 2005; Dunn *et al.* 2006). One variant with two amino acid substitution within the CDR3 α -domain has been clinically applied, with a protocol similar the DMF4, DMF5 trials (Robbins *et al.* 2011).

Antigen	HLA-type	Name	Origin	Modification	Ref.
Tyrosinase ₃₆₈₋₃₇₆	A2	TIL 1383I	Human TIL CD4 ⁺		(Nishimura <i>et al.</i> 1999)
WT1 ₁₂₆₋₁₃₄	A2		Allo-MHC repertoire		(Gao <i>et al.</i> 2000)
p53 ₂₆₄₋₂₇₂	A2		HLA-A2 Mouse		(Cohen <i>et al.</i> 2005)
MART-1 ₂₇₋₃₅	A2	DMF4	Human TIL		(Morgan <i>et al.</i> 2006)
NY-ESO-1 ₁₅₇₋₁₆₅	A2	1G4	Human TIL	CDR3 α TS95LY	(Robbins <i>et al.</i> 2008)
MART-1 ₂₇₋₃₅	A2	DMF5	Human TIL		(Johnson <i>et al.</i> 2009)
gp100 ₁₅₄₋₁₆₂	A2		HLA-A2 Mouse		(Johnson <i>et al.</i> 2009)
CAE ₆₉₁₋₆₉₉	A2		HLA-A2 Mouse	CDR3 α S112T	(Parkhurst <i>et al.</i> 2009)
TRAIL/DR4	non-MHC	HC/2G-1	TIL CD4 ⁺	CDR3 α Y109F/S112K	(Wang <i>et al.</i> 2011)
MAGE-A3 ₁₁₂₋₁₂₀	A2	TCR9W11	HLA-A2 Mouse	CDR3 α A118T	(Chinnasamy <i>et al.</i> 2011)

Table 5.6 Overview of characterized TCRs for clinical applications.

All first descriptions for TCRs that have entered clinical trials have been reviewed and several characteristics were outlined. The position of amino acid modifications are marked by domain, original sequence, amino acid position and exchanged amino acids.

The antigen affinity of this TCR has been quantified with a K_D value of 730nM (Robbins *et al.* 2008). We compared the outcomes of trials with TCRs of known K_D values. The overall results confirm the large body of data that suggests a strong correlation between TCR-antigen avidity and immunogenicity (Fig.5.2). Several other TCRs have been modified for higher binding affinity and are currently under clinical investigation. Table 5.6 summarizes published information on TCRs that have been tested in clinical trials.

An MHC-mismatch was used to tap a TCR repertoire that was not shaped by central tolerance (Gao *et al.* 2000). For some antigens no high avidity TCR could be identified, which led to isolation from the xeno-repertoire of human HLA-A2 transgenic mice. Although among murine TCRs higher tumor-specific cytolytic activity than within autologous immune responses were detected, their structural difference can induce specific antibody development. *In vitro* data show that murine TCRs are strongly inhibited by blood serum of antibody positive patients (Davis *et al.* 2010). Several clinical trials in different centers are currently ongoing but have not published results yet. Currently conducted trials are summarized in Table 5.7.

Antigen	HLA	Trial ID	Pathology	Additional Treatment
gp100	A2	NCT00509496	MM	CyP, Flud; HD IL-2
gp100	A2	NCT00610311	MM	ALVAC; CyP, Flud; HD IL-2
HIV gag	A2	NCT00991224	HIV	
MAGE-A3	A2	NCT01273181	MM	CyP, Flud; HD IL-2
MAGE-A3/ NY-ESO-1	A1/A2	NCT01350401	MM	
MAGE-A3/ NY-ESO-1	A1/A2	NCT01352286	Myeloma	Prevenar-13 Adj
MART-1	A2	NCT00509288	MM	CyP, Flud; HD IL-2
MART-1	A2	NCT00091104	MM	peptide; IFA; G-CSF; CyP, Flud; HD IL-2
MART-1	A2	NCT00612222	MM	ALVAC; CyP, Flud; HD IL-2
MART-1	A2	NCT00706992	MM	ALVAC; peptide; CyP, Flud; HD IL-2

Antigen	HLA	Trial ID	Pathology	Additional Treatment
MART-1	A2	NCT00910650	MM	CyP, Flu; HD IL-2
MART-1/ gp100	A2	NCT00923195	MM	peptide; Montanide ISA 51 VG Adj; irradiation; CyP, Flu; HD IL-2
MART-1	A2	2011-002941-36	MM	Chemotherapy; LD IL-2
NY-ESO-1	A2	NCT00670748	Metastatic Cancer	CyP, Flud; HD IL-2
NY-ESO-1	A2	NCT01697527	Malignant Neoplasm	DC vaccine
NY-ESO-1	A2	NCT01457131	Metastatic Cancer	CyP, Flud; IL-12 transgene
p53	A2	NCT00393029	Metastatic Cancer	G-CSF; CyP, Flud; HD IL-2
p53	A2	NCT00704938	Metastatic Cancer	G-CSF; autologous dendritic cell- adenovirus p53 vaccine
Tyrosinase	A2	NCT01586403	MM	LD IL-2
WT1	A2	NCT01621724	CML;AML	
WT1	A2	NCT01640301	CML;AML	IL-2
CMV pp65	A2	2008-006649-18	CMV disease	

Table 5.7 Overview of currently ongoing clinical trials of adoptive therapy with TCR-redirectioned T cells (status December 2012)"

All currently ongoing clinical trials with TCR-redirectioned cells registered at www.clinicaltrialsregister.eu and www.clinicaltrials.gov at clinical trials were collected. Target antigen, HLA-restriction of the used TCR, Trial ID, disease and supporting therapy are outlined. Abbreviations are CyP for Cyclophosphamid, Flud for Fludarabin, HD/LD for high/low dose and adj for adjuvant.

5.8. TCR ISOLATION STRATEGIES

Molecular cloning of an antigen-specific TCR is complicated by the high diversity of the TCR locus. The TCR is rearranged on the level of genomic DNA. Apart from the outstandingly diverse V(D)J-junction, also the 5' front end is considerably diverse, as different V-segments can potentially exist at this site. Furthermore, mostly one unmodified and one rearranged allele for α - and β -chain are present in each cell. This hampers direct priming to the respective positions of the genomic DNA. Most antigen-specific TCRs have been extracted from their original cells by reverse transcription and PCR amplification, a method generally termed rapid amplification of cDNA ends (RACE)-PCR. This approach uses mRNA as template, which is transcribed to a single stranded DNA-molecule by reverse transcriptase. In case of the TCR only one end of the transcript, the constant region is known. In order to allow PCR amplification of the unknown region outside the C-region, an artificial priming site is generated. Several different methods have been described for this purpose. One uses the enzyme terminal DNA transferase to add a stretch of identical nucleotides to open 3'OH groups of DNA molecules, in a template independent manner (Loh *et al.* 1989). Another very common approach generates an artificial priming site of a defined sequence by using DNA-ligase, to fuse a primer to the open 3' OH end (Bertling *et al.* 1993). Furthermore, direct manipulation of mRNA by RNA-ligases can be applied, ahead of reverse transcription (Liu *et al.* 1993). Another strategy to obtain large parts of the variable part of the TCR sequence makes use of sets of primers that cover all V-segments. Those primers are combined in a multiplex PCR, using cDNA as template. One method was described using forward and reverse priming, with a set of V-specific forward primers and a set of J-specific reverse primers, all in one PCR reaction. Pre-amplified products are split into several reactions with two or three of the V-specific forward primers and a nested set of J-segment-specific reverse primers (Babbe *et al.* 2000). These strategies have found broad application in molecular biology apart from TCR amplification.

To PCR-amplify and clone TCRs, in particular, RACE-PCR based approaches have been applied. Also the first tumor antigen-specific TCR was isolated in this way (Cole *et al.* 1994). Mostly *in vitro* expanded monoclonal T cell-cultures have served to obtain sufficient amounts of template material for TCR isolation, but since not all T cells are expandable under similar *in vitro* culture conditions, *in vitro* culture-based protocols limit access to restricted TCR repertoire compositions. Outgrowth of dominant T cell-clones during five weeks of *in vitro* TIL expansion was observed in several reports (Nishimura *et al.* 1998; McKee *et al.* 2000). By comparing repertoire compositions at different time points after *ex vivo* extraction, complete

disappearance of initially dominant T cell-clones from TILs was observed, which hints at loss of tumor-specific TCRs (Dietrich *et al.* 1997).

6. AIM OF THIS WORK

Adoptive transfer of TCR-redirectioned T cells could become a highly efficient treatment option, as shown by the outcomes of several clinical trials. A better understanding of the mechanisms that cause the diversity in clinical response - and side effect rates, could make this approach more predictable. Important questions to be answered as a step towards broader application address the choice of target antigen and optimum of TCR avidity. To further elucidate the influence of these variables, a broad spectrum of TCRs will be required. However, current approaches for TCR isolation suffer from several drawbacks. Strategies to circumvent thymic selection for low avidity, like the isolation of MHC mismatch restricted TCRs or murine TCRs can introduce cross reactivity. The same limitation occurs for avidity enhancement by mutagenesis. The transfer of murine TCRs to humans can furthermore induce antibody responses. Antigen-specific TCRs expanded from autologous repertoires are limited in diversity and predominantly display low TCR avidities. Basically all current approaches for isolation of antigen-specific TCRs build on T cell-expansion ahead of molecular cloning, which potentially reduces the repertoire of TCRs. TCR repertoire restriction by *in vitro* expansion of T cells could best be overcome by direct *ex vivo* single-cell sorting of antigen-specific T cells and subsequent TCR isolation from individual cells, without the need for any *in vitro* propagation.

In principle, this could be achieved by combining MHC multimer-staining (Altman *et al.* 1996) with single-cell TCR sequencing. Therefore, the first aim of this work was the development of a novel method for single cell PCR amplification of the TCR.

Single-cell-based TCR sequencing efforts have been described, mostly using sets of degenerate primers binding to consensus motifs (Babbe *et al.* 2000; Zhou *et al.* 2006; Junker *et al.* 2007; Dash *et al.* 2011; Kim *et al.* 2012; Wang *et al.* 2012) or rapid amplification of cDNA ends (RACE) PCR (Ozawa *et al.* 2008; Sun *et al.* 2012).. Although these strategies provided single-cell-derived TCR sequences, it has not been shown that correct pairing to functionally reconstruct the receptor of the original cell can be obtained, e.g. by transgenic re-expression of the identified TCR chains. There are several technical concerns that require careful interpretation of sequencing results, without further analysis of the obtained receptor. For example, in the case of consensus primer-based approaches, V-segment domains are

truncated outside the primer binding sites; since single nucleotide polymorphisms (SNPs) within V-segments have been described to influence ligand binding, reliable sequence reconstruction might be limited (Gras *et al.* 2010).

In addition to single-cell-based TCR amplification we aimed to utilize *ex vivo* isolated, unexpanded T cells for TCR isolation, thus preserving the largest possible diversity of TCR-specimen. Although epitope-specific T cell-populations are in many settings extremely rare without pre-expansion, they can be accurately detected through the combination of MHC multimer-based pre-enrichment and combinatorial MHC multimer staining technologies (Moon *et al.* 2007; Obar *et al.* 2008). However, it has not yet been possible to combine MHC multimer staining with single-cell TCR identification, since the simultaneous extraction of both chains of the hetero-dimeric receptor is technically highly challenging.

In summary, this work aims at establishing a novel strategy for the isolation antigen-specific TCRs. Therefore, we want to isolate antigen-specific T cells without previous expansion from the naturally occurring “naïve” T cell repertoire, which theoretically contains the largest TCR sequence diversity. To directly access this repertoire we intend to amplify the TCR from single cells by establishing a novel RACE-PCR based method. We assume that this strategy will be highly valuable for the field of adoptive immunotherapy with TCR-redirectioned T cells.

7. MATERIALS AND METHODS

7.1. MATERIALS

7.1.1. CHEMICALS AND REAGENTS

Reagent	Supplier
Ammonium chloride (NH ₄ Cl)	Sigma, Taufkirchen, Germany
Ampicillin	Sigma, Taufkirchen, Germany
Biocoll Ficoll solution	Biochrom, Berlin, Germany
Bovine serum albumin (BSA)	Sigma, Taufkirchen, Germany
Dimethylsulfoxid (DMSO)	Sigma, Taufkirchen, Germany
Dithiothreitol (DTT)	Agilent, Waldbronn, Germany
dGTP	Roche, Mannheim, Germany
dNTP	Roche, Mannheim, Germany
Ethanol	Klinikum rechts der Isar, Munich, Germany
Fetal calf serum (FCS)	Biochrom, Berlin, Germany
Formamide	Sigma, Taufkirchen, Germany
Gentamycin	Gibco BRL, Karlsruhe, Germany
Guanidine-HCl	Sigma, Taufkirchen, Germany
Glutamax I	Life Technologies, Darmstadt, Germany
HCl Roth,	Karlsruhe, Germany
HEPES	Gibco BRL, Karlsruhe, Germany

Interleukin-2	Novartis, Basel, Switzerland
Igepal CA-630	Sigma, Taufkirchen, Germany
MgCl ₂	Sigma, Taufkirchen, Germany
KCl	Sigma, Taufkirchen, Germany
NaOH	Roth, Karlsruhe, Germany
Penicillin Roth,	Karlsruhe, Germany
Phosphate buffered saline (PBS)	Biochrom, Berlin, Germany
Propidium iodide (PI)	Molecular Probes, Invitrogen,
Retronectin	Takara Bio Europe S.A.S., Saint-Germain-en-Laye, France
RPMI 1640	Gibco BRL, Karlsruhe, Germany
Sodiumacetate	Sigma, Taufkirchen, Germany
Sodiumazide (NaN ₃)	Sigma, Taufkirchen, Germany
Sodiumchloride (NaCl)	Roth, Karlsruhe, Germany
Sodium-EDTA (Na-EDTA)	Sigma, Taufkirchen, Germany
Streptavidin BV421	Biolegend GmbH, Germany
Streptavidin FITC	Molecular Probes, Invitrogen
Streptavidin PE-Cy7	Molecular Probes, Invitrogen
Streptavidin eF450	Molecular Probes, Invitrogen
<i>Strep</i> -Tactin-APC	IBA, Göttingen, Germany
<i>Strep</i> -Tactin-PE	IBA, Göttingen, Germany
Tris-hydrochloride (Tris-HCl)	Roth, Karlsruhe, Germany
tRNA	Roche, Mannheim, Germany
Trypan Blue solution	Sigma, Taufkirchen, Germany

7.1.2. BUFFERS AND MEDIA

Buffer	Composition
FACS buffer	1x PBS 0.5% (w/v) BSA pH 7,45
Cell culture medium	1x DMEM 10% (w/v) FCS 0.025% (w/v) L-Glutamine 0.1% (w/v) HEPES 0.001% (w/v) Gentamycin 0.002% (w/v) Streptomycin
Erythrocyte Lysing Solution	153 mM NH_4Cl 17 mM Tris-HCl
Complete freezing medium (CFM)	FCS 10% DMSO

T cell-culture medium	1x RPMI 1640
	10% (w/v) FCS
	0.025% (w/v) L-Glutamine
	0.1% (w/v) HEPES
	0.001% (w/v) Gentamycin
	0.002% (w/v) Streptomycin
	0.002% (w/v) Penicillin

7.1.3. MHC MULTIMERS

All MHC multimers for detection and purification of antigen-specific CD8⁺ T cells were produced in house according to a previously published standard protocol (Busch *et al.* 1998). Peptide-MHC multimers were generated as described (Altman *et al.* 1996; Knabel *et al.* 2002). In brief, MHC heavy chain was urea denatured and refolding in the presence of peptide and β 2 microglobulin was enabled by progressive dialysis of detergent. Complexes were biotinylated by BirA and were purified by FPLC. Monomeric complexes were multimerized by addition of two types of different backbone molecules labeled with the respective fluorophore. The backbones for multimerization were either Streptavidin, a tetrameric protein complex with one binding site for biotin per monomer. Alternatively a modified version of Streptavidin, generally termed *Strep-Tactin* was utilized. The modifications involve amino acid exchanges in the biotin binding sites, which allows stable interaction with a peptide sequence termed *Strep-Tag* (Skerra *et al.* 1999). As *Strep-Tag* displays a lower binding strength to the *Strep-Tactin* than biotin, the latter molecule can replace *Strep-Tag*, disassembling the multimeric complex. For multimerization, the ratios of MHC/backbone and staining dilution were separately titrated for each reagent to obtain optimal staining intensities.

H2-K ^b / mβ2m/ Ova ₂₅₇₋₂₆₄	SIINFEKL
HLA-A2 / hβ2m/ Her2/neu ₃₆₉₋₃₇₇	KIFGSLAFL
HLA-A2 / hβ2m/ WT1 ₁₂₆₋₁₃₄	RMFPNAPYL
HLA-A2 / hβ2m/ pp65 ₄₉₅₋₅₀₃	NLVPMVATV
HLA-B7 / hβ2m/ pp65 ₄₁₇₋₄₂₅	TPRVTGGGAM
HLA-B8 / hβ2m/ IE1 ₈₈₋₉₆	QIKVRVDMV
HLA-B8 / hβ2m/ IE1 ₁₉₉₋₂₀₇	ELRRKMMYM

7.1.4. ANTIBODIES

Antibody	Clone	Supplier
Human CD3 PE-Cy7	UCHT1	eBioscience
Human CD3 Pacific Blue	UCHT1	Pharmingen
Human CD3 AmCyan	SK7	BD
Human CD8 FITC	RPA-T8	Pharmingen
Human CD8 PE	RPA-T8	Pharmingen
Human CD8 PerCP	SK1	Pharmingen
Human CD8 AmCyan	SK1	BD
Human CD8 APC	RPA-T8	Pharmingen
Human CCR7 FITC	3D12	Pharmingen
Human CD45RA PE-Cy7	L48	BD
Human CD3	Okt3	Orthoclone
Human CD28	37.51	eBioscience

FACS analysis for human V β -Repertoire was carried out with IO Test Beta Mark TCR V Kit from Beckman coulter

All FACS antibodies were titrated for optimal cell labeling.

7.1.5. ENZYMES

Enzyme	Supplier
Affinity Script, Reverse Transcriptase	Agilent, Waldbronn, Germany
EcoRI	Fermentas, Leon-Rot, Germany
Exonulcease I	Fermentas, Leon-Rot, Germany
Expand LT, DNA Polymerase	Roche, Mannheim, Germany
Herculase II, DNA Polymerase	Agilent, Waldbronn, Germany
NotI	Fermentas, Leon-Rot, Germany
SuperscriptII, Reverse Transcriptase	Invitrogen, Darmstadt, Germany
Taq DNA Polymerase	Promega GmbH, Mannheim, Germany
TdT	Promega GmbH, Mannheim, Germany

7.1.6. PRIMERS

Name	5' – 3' Sequence
hTCRBC1	TAGAACTGGACTTGACAG
hTCRBC2	GTATCTGGAGTCATTGAGG
hTCRBC3	CACCTCCTTCCCATTAC
hTCRBC4	CACGTGGTCGGGGAAGAAGC
hTCRBC5	GTGGCCAGGCACACCAGTGT
hTCRBC6	CTGCTTCTGATGGCTCAAAC
hTCRAC1	CTTTCAGGAGGAGGATTC
hTCRAC2	AAGTTTAGGTTCGTATCTG
hTCRAC3	ATAATGCTGTTGTTGAAGG
hTCRAC4	ACACATCAGAATCCTTACTTTG
hTCRAC5	GGTGAATAGGCAGACAGACTT
hTCRAC6	GCTGGTACACGGCAGGGTC
Adaptor 1	ACAGCAGGTCAGTCAAGCAGTA
Adaptor 2	AGCAGTAGCAGCAGTTCGATAA
dC-Anchor PTO	ACAGCAGGTCAGTCAAGCAGTAGCA GCAGTTCGATAAGCGGCCGCCATGG ACCCCCCCCCCV-PTO-N

Pfu-Polymerase based Enzymes have been shown to digest primers that bind DNA sequences over a part of their sequence but not the 3' end. The single stranded 3' end can be degraded leaving a truncated but completely annealed primer. It was shown that this exonuclease activity can be blocked by coupling the nucleotides on the 3' end of a primer over a phosphorothioate (PTO) group (Skerra 1992). The primer dC-Anchor PTO contains a 51bp long overhanging 5' sequence and otherwise consists only of cytosine bases, which

makes false priming very likely. To prevent the elongation of unwanted priming events the 3'-terminal nucleotide of this primer was coupled over PTO.

7.1.7. EQUIPMENT

Equipment	Supplier
AmpliSpeed, Thermocycler	Advantix, München
Cyan Lx Flow cytometer	Beckman Coulter, Fullerton
MoFlo Cell Sorter	Beckman Coulter, Fullerton
FACS Aria	Becton Dickinson, Heidelberg
FACS Calibur	Becton Dickinson, Heidelberg
Microscopes Axiovert S100	Carl Zeiss, Jena
Zeiss LSM 510, confocal microscope	Carl Zeiss, Jena
Leica SP 5, confocal microscope	Leica, Bensheim
Centrifuges Biofuge fresco	Heraeus, Hanau
Multifuge 3 SR	Heraeus, Hanau
Sorvall® RC 26 Plus	Heraeus , Hanau
FPLC	Amersham Biosciences, Europe GmbH, Freiburg
Heating block Thermomixer compact	Eppendorf, Hamburg
HE33 agarose gel casting system	Hoefer, San Francisco
Incubator Cytoperm 2	Heraeus, Hanau
Laminar flow hood HERA safe	Heraeus, Hanau
Mighty Small SE245 gel casting system	Hoefer, San Francisco

Neubauer counting device	Schubert, München
Nano Drop spectrophotometer	Nano Drop, Baltimore
Photometer Bio Photometer	Eppendorf, Hamburg
Shaker Multitron Version 2	INFORS AG, Bottmingen
Thermocycler T Professional Thermocycler	Biometra, Göttingen
Water bath LAUDA ecoline 019	Lauda -Königshofen

7.1.8. KITS

mTRAP mRNA extraction System	Active Motif, La Hulpe, Belgium
PureYield Plasmid Miniprep System	Promega GmbH, Mannheim, Germany
Pure Yield Plasmid Midiprep System	Promega GmbH, Mannheim, Germany
Qiaquick Spin Column	Qiagen, Hilden, Germany
Human IFN γ -ELISA	BD Biosciences, Heidelberg, Germany

7.1.9. CELLS AND CELL-LINES

Hek293T, kidney cancer cell line	ATCC: CRL-11268
SKOV-3, ovarian cancer cell line	ATCC: HTB-77
T2	ATCC: CRL-1992

Jurkat76 T cell-lymphoma cell line was kindly provided by Professor Wolfgang Uckert, MDC for molecular medicine, Berlin. HLA-A2 transgenic SKOV-3 cell line was supplied by M. L. Disis; University of Washington, Seattle, WA, USA.

B-LCLs were kindly provided by Dr. Angela Krackhardt, Institute of Hematology Klinikum Rechts der Isar, Munich.

Blood was taken from healthy donors. Written informed consent was obtained from the donors, and usage of the blood samples was approved according to national law by the local Institutional Review Board (Ethikkommission der Medizinischen Fakultät der Technischen Universität München).

Jurkat 76 cells were grown at 37°C, 95 % humidity, 5 % CO₂ in 1640 RPMI medium supplemented with 10 % fetal calf serum and 100 U/ml penicillin, 100 U/ml streptomycin and gentamycin.

The HER2⁺/HLA-A2⁻ ovarian cancer cell line SKOV-3, the HLA-A2⁺ transfected cell line SKOV-3-A2 and the HEK 293T cell-line were cultured in DMEM medium with Glutamax I supplemented with 10% heat-inactivated fetal calf serum and 100 IU/ml of penicillin/streptomycin. T2 cells and primary T cells were cultured in T cell-medium.

7.1.10. SOFTWARE

Software	Supplier
FlowJo	Treestar
Office	Microsoft
VectorNTI Advance	Life Technologies
Prism 5	Graph Pad
Illustrator	Adobe

7.2. METHODS

7.2.1. FLOW CYTOMETRIC DATA ACQUISITION AND CELL SORTING

For PBMC extraction whole blood was pre-diluted 1:1 with PBS (pH7.4) and was carefully transferred to a layer of Ficoll. Separation of erythrocytes, lymphocytes and serum was accomplished by density gradient centrifugation for 20min at 2000 rpm. The lymphocyte layer was transferred to a fresh tube, washed twice with FACS-Buffer and was counted on a Neubauer Chamber. For phenotypic characterization of cells, a master mix of the respective antibodies was prepared, and was added to the cell sample. During the labeling cells were kept on ice, in the dark for 30min. For additional MHC multimer staining, the reagent was added to the sample without intermediate washing step and was incubated for an additional 30min on ice in the dark. Samples were analyzed using a CyanLx 9 color flow cytometer. Cell sorting was performed on a MoFlo. For single cell sorting to AmpliGrid PCR Slides a Cyclone system was used. FACS data was analyzed with FlowJo v9.5.2 software.


7.2.2. SOLID PHASE cDNA AMPLIFICATION

mRNA extraction, reverse transcription and cDNA amplification were performed as previously described (Hartmann *et al.* 2006). In brief, single cells were transferred to mTRAP lysis buffer with protease. After protease digest, PNAs were added to bind mRNA. Streptavidin coated paramagnetic beads were co-incubated with PNA-mRNA complexes for 45min at room temperature. Complexes were precipitated by magnetic force and were washed twice. Reverse transcription was performed at 44°C and complexes were washed twice. Beads were resuspended in tailing solution and incubated for 60min at 37°C. PCR-mix for cDNA amplification was added and 35 cycles of PCR were performed.

7.2.3. REVERSE TRANSCRIPTION AND PCR OF THE TCR FROM SINGLE CELLS

Reverse transcription was performed on an AmpliGrid Slide from Advantix. Single-cells were spotted with the Cyclone system of a MoFlo cell sorter to pre-defined slide positions and were resuspended in 0.5 μ l of 50 mM Tris-HCl (pH 8.3), 75 mM KCl, 3 mM MgCl₂, 1.6 mM dNTPs, 10 mM DTT, 0.1 mg/ml BSA, 0.1 mg/ml tRNA, 0.25 % Igepal CA-630, 0.8 U/ μ l RNasin Plus, 1 μ M reverse transcription primers each and 0.05 rxn/ μ l Affinityscript reverse transcriptase. Reverse transcription was performed for 20min at 51°C followed by 30min at 70°C on an AmpliSpeed PCR cycler. For primer exonuclease I digest, the reaction volume was filled up to 1 μ l resulting in a final concentration of 67 mM glycine-KOH (pH 9.5), 6.7 mM MgCl₂, 10 mM DTT and 1U/ μ l Exonuclease I. Exonuclease I digest was performed for 30min at 37°C and enzyme was inactivated for 20min at 70°C on an AmpliSpeed PCR cycler. For oligo-dG tailing, complete reaction was transferred to a 96 well plate. Tailing was performed in 5 μ l of a final concentration of 10 mM MgCl₂, 1 mM DTT, 10 mM Tris (pH7.5) and 2 mM dGTP and 0.75 U/ μ l terminal dNTP transferase, tailing reaction was performed for 45min at 37°C and enzyme was inactivated for 20min at 37°C on a Biometra Professional Gradient Cycler. For anchor PCR the reaction volume was filled up to 25 μ l with a final concentration of 1xHerculasell reaction buffer, 0.20 mM dNTPs, 3 % formamide, 0.02 rxn/ μ l Herculasell DNA polymerase and 0.5 μ M of each primer.

PCR program:

94°C	3min		
94°C	15s		24x
60°C	30s		
72°C	45s		
72°C	5min		
16°C	pause		

1 µl of product was transferred to nested PCR amplification in separate reactions for α- and β- chain. Except for primers, PCR conditions for nested PCR round I and II were identical to anchor PCR.


7.2.4. CLONING AND SEQUENCING


PCR products from single T cell-samples were prepared for sequencing by standard blunt end cloning using CloneJet-kit according to the manufacturers recommendations. After ligation, plasmid preparation from transformed DH5α was performed using the Pure Yield Mini column extraction kit. Extracted Plasmids were Sanger sequenced by the commercial provider GATC. Sequencing data was analyzed with Vector NTI Advance and online tools of international ImMunoGeneTics information system for immunoinformatics (IMGT; <http://www.imgt.org>).

7.2.5. RETROVIRAL TRANSDUCTION

PCR products from single-cell PCRs were completed for their truncated constant region by megaprimer PCR. PCR products from α- or β-chain were incubated together with equimolar amounts of PCR product of constant region α- or β- respectively in a PCR mastermix as described for the single-cell PCR protocol.

PCR-Program:

94°C		3min	
94°C		15s	
80°C		1s	
40°C	0.1°C/s	1s	
72°C		45s	

94°C	15s		35x
60°C	45s		
72°C	1min		
72°C	5min		
16°C	Pause		

PCR products were cloned into the retroviral expression vector pMP71. Plasmid DNA was digested with NotI and EcoRI restriction enzymes and was transferred to agarose gel electrophoresis. Successfully digested plasmid was excised from agarose and was extracted with the column based Qiagen gel extraction kit.

For transduction of primary T cells the constant regions of the HER2-specific TCR α - and β -chain were replaced by codon optimized murine sequences harboring mutations to form an additional cystein bridge. Both TCR chains were combined by a 2A peptide linker sequence (P2A) and cloned into the retroviral vector MP71-PRE. Generation of retroviral particles was performed as previously described (Engels *et al.* 2003). In brief, separate pMP71 expression vectors containing TCR α - and β -chain or a pMP71 vector with a TCR cassette, gag/pol plasmid and amphotropic env plasmid were transfected into HEK 293T cells by calcium phosphate precipitation. Viral supernatant was harvested after 24h and 48h and was transferred to Jurkat76 cells and to human PBLs stimulated for two days with plate-bound anti-CD3/CD28 antibodies and 100 IU/ml IL-2. Transduction of target cells was supported by spin inoculation using retronectin-coated plates.

7.2.6. MAGNETIC CELL SEPARATION

MACS enrichment with Miltenyi anti-PE nanobeads was performed on Miltenyi MS-columns according to the manufacturers recommendations. In brief, PE-labeled cells were co-incubated with anti-PE-antibody-labeled paramagnetic beads for 15min at 4°C. Cell suspension was washed once. MACS columns were placed on a magnet and were equilibrated. Cell suspension was transferred to the column and washed twice. Positive cell

fraction was eluted by removal of the column from the magnet. Cells were flushed off the column with pressure.

7.2.7. *IN VITRO* T CELL-EXPANSION

T cells were directly FACS sorted into 96 well cell culture plates containing 1 µg/ml Okt3 antibody, 1 µg/ml anti CD28, 100 U/ml IL-2, B-LCLs irradiated with 50 Gy and human PBMCs irradiated with 35 Gy. Cells were kept at 37°C, 95% relative humidity and 5% CO₂ in a total volume of 200 µl RPMI⁺, 10 % heat inactivated fetal calf serum, Streptomycin, Penicillin, Gentamycin.

7.2.8. FUNCTIONAL ANALYSIS OF T CELLS

TCR-modified PBLs were analyzed in chromium (⁵¹Cr) release assays and interferon (IFN γ)-secretion was measured by enzyme-linked immunosorbent assays (ELISA). To determine cytolytic activity, 2x10³ peptide-loaded T2 cells (1 µM) labeled with ⁵¹Cr were incubated for 4h with TCR-modified PBLs at different effector/target ratios (E/T ratios). T2 cells were pulsed with HER2₃₆₉₋₃₇₇: KIFGSLAFL and WT-1₁₂₆₋₁₃₄: RMFPNAPYL peptides. Spontaneous release was determined using T2 cells incubated without T cells and the transfer of T2 cells directly to the solid scintillator-coated lumaplates without incubation produced maximal release values. All samples were run in duplicates and the specific lysis was calculated as follows: % specific cytotoxicity = [mean sample release (cpm) - mean spontaneous release (cpm)]/[mean maximal release (cpm) - mean spontaneous release (cpm)] × 100. For determination of cytokine release IFN γ was measured after co-culture of 1x10⁵ TCR-modified PBMBs with the same number of T2 cells pulsed with titrated amounts of peptide or with tumor cells for 24h by ELISA according to the manufacturer's instructions. Samples were run in triplicates.

8. RESULTS

8.1. ESTABLISHMENT OF A PCR METHOD FOR V-SEGMENT INDEPENDENT AMPLIFICATION OF TCR α - AND β - CHAIN FROM SINGLE T CELLS

Several obstacles hamper direct PCR amplification of the T cell-receptor genes. The TCR sequence is virtually unique, as somatic rearrangement can theoretically produce up to 2.5×10^{15} different sequences (Davis *et al.* 1988). The human genome contains 43-45 functional $V\alpha$ genes, which can be further divided into 32-34 subgroups. Similarly, there are 40-48 functional $V\beta$ -genes in 21-23 subgroups (Scaviner *et al.* 2000). Although some consensus motifs, which are present in several V-genes, can serve as primer binding site, there still remains considerable complexity. Therefore, to PCR amplify the TCR many different V-specific primers are required to potentially detect every possible V-segment. As the template materials, i.e. mRNA or genomic DNA from a single cell is sufficient only for a single PCR reaction all primers need to function in combination. To reach a sensitivity that can resolve the single cell level, one set of primers is probably insufficient. A second PCR with a set of nested primers, binding inside of the respective first primers, so far was indispensable to reach single cell resolution, as independently shown by several reports (Zhou *et al.* 2006; Dash *et al.* 2011; Wang *et al.* 2012). One reported method utilizes genomic DNA instead of mRNA. Whether the higher stability of DNA compared to mRNA can compensate for the larger number of transcripts in the latter case is unclear. For DNA-based amplification, the organization of the genetic locus furthermore necessitates the use of several combined J-segment-specific reverse primers, in addition to multiplexed forward priming. A large space of intervening sequence between the recombined part of the gene and the constant region prevents priming in the latter domain. For clarification this is representatively shown for the human α -chain locus in Fig. 8.1 (Babbe *et al.* 2000).

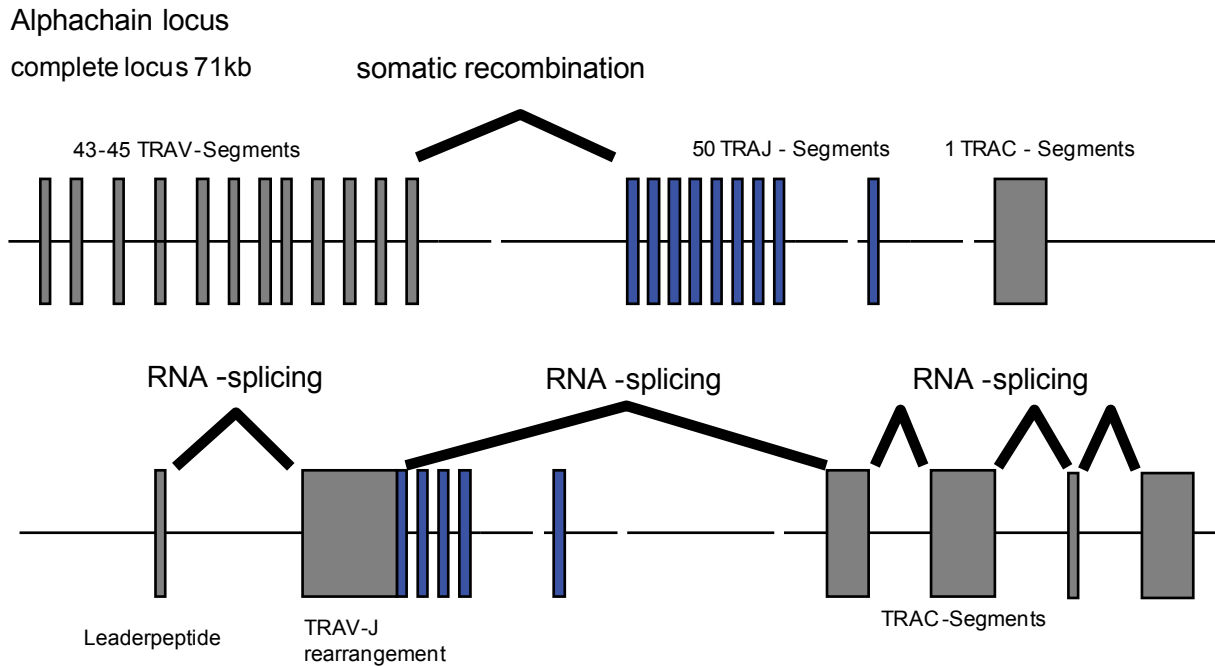


Figure 8.1: TCR, genomic locus.

Scheme of the genomic locus of the TCR α -chain before (top row) and after somatic recombination (bottom row).

The mentioned reports prove the feasibility of single cell PCR of the TCR. It is a major disadvantage of those multiplex primer-based approaches nonetheless that the resulting PCR products are truncated within the V-segment. This is straightforward for characterization of TCR repertoires, but for translation to a productive protein the complete sequence, including the start codon is necessary. Completion of the V-segment based on published sequence information bears the risk to introduce SNPs that formerly were not contained. Single amino acid exchanges in the V-segment have been demonstrated to potentially influence ligand binding (Gras *et al.* 2010). To avoid the introduction of errors by adding variant sequences, we chose a strategy to reverse transcribe and PCR amplify the complete mRNA sequence, without a priori knowledge of the V-segment sequence. For less sensitive applications than single cell amplification, RACE-PCR is a broadly applied tool to determine the sequence of unknown loci.

8.1.1. SOLID-PHASE COUPLED cDNA-AMPLIFICATION

Initially we focused on a way to propagate cDNA amounts derived from a single cell. We followed a method for single cell complete cDNA amplification for microarrays (Hartmann *et al.* 2006). To accomplish exchange of reaction conditions for several subsequent enzymatic modifications to the same template, mRNA was coupled to paramagnetic beads via a stretch of modified oligothymidin peptide nucleic acids (PNA)s. PNAs are multimerised over a glycin instead of phosphate backbone, which results in a strongly increased binding affinity of the coupled nucleic acid base towards its respective complementary base. Single cells were picked under a microscope and transferred to a strong denaturing agent for cell lysis and for binding to the PNA stretch. These harsh conditions denature mRNA-degrading enzymes and thus increase mRNA stability. The bead-bound mRNA was extracted and washed by magnetic sedimentation and was similarly treated for several buffer exchange steps as outlined in Fig. 8.2.

For reverse transcription (RT) we used gene-specific primers with a terminal overhang of 15 dC-residues. (Fig. 8.2.b) After mRNA-extraction and RT, an artificial priming site of several dG-nucleotides was added to the cDNA. The enzyme terminal DNA-transferase (TDT) couples dNTPs to 3' terminal OH groups of cDNA molecules in a template independent manner. As uniquely dGTP was provided in the reaction the nascent artificial priming site consisted of guanine only (Fig. 8.2.c). At this point the cDNA contained oligo-dC overhang on the 5'end, which was derived from the RT-primers and an enzymatically generated oligo-dG-overhang on the 3' end. A complementary single primer was therefore enough to PCR amplify the modified cDNA in both directions (Fig. 8.2.d). Up to the first PCR amplification step a complex of mRNA, cDNA and biotinylated PNA, coupled to paramagnetic beads was theoretically maintained. This is of special relevance, as after each enzymatic reaction two washing steps were performed by magnetic retention of the beads. A successful transfer of cDNA from one step to the next was strictly dependent on the integrity of this complex (Fig. 8.2.c). The disruption of this complex was only permitted during the first PCR amplification step, as from this point on the template was sufficiently multiplied to allow the transmission, by passing on a small volume to subsequent steps. Although RT-priming was TCR-confined, the specificity of the protocol after one round of PCR was insufficient. Gel electrophoresis exhibited a diffuse smear of DNA rather than a band of defined size (data not shown).

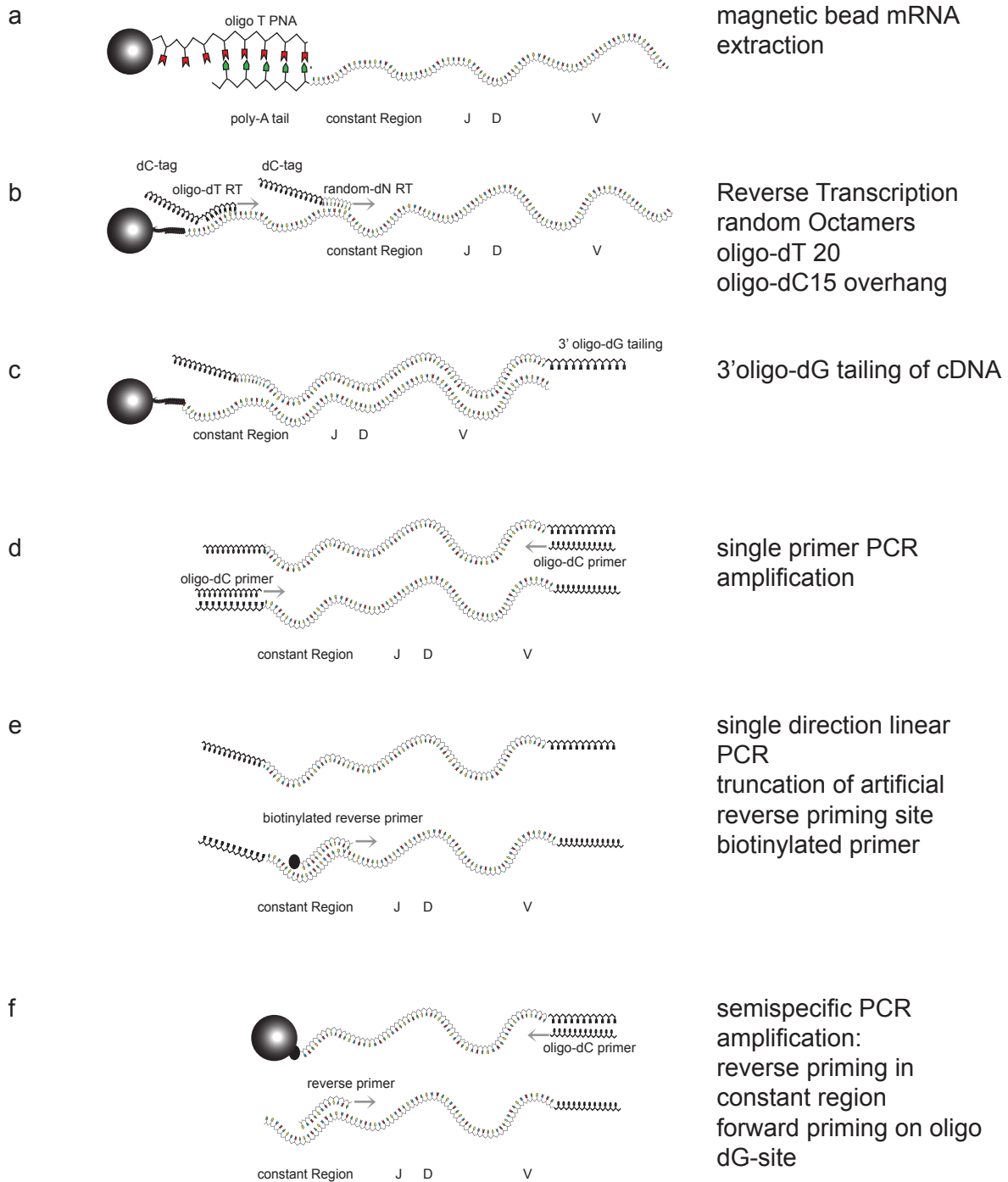


Figure 8.2: Schematic overview of the single cell PCR strategy using solid phase coupled cDNA amplification"

(a) PNA-coupled paramagnetic beads are used to bind mRNA poly-A tails. (b) RT of bead bound mRNA with gene-specific primers with oligo-dC overhang. (c) After RT, open cDNA 3'OH end is prolonged by oligo-dG. (d) single oligo-dC primer is used to amplify cDNA. (e) 5' artificial priming site is truncated by linear PCR with a biotinylated nested primer binding inside the constant region. (f) Biotinylated PCR products are attached to streptavidin coated paramagnetic beads. After washing of bead coupled PCR products, distinct primers on both ends can be used for PCR.

In order to increase the specificity and to obtain a clear-cut product a round of semi-nested amplification was necessary. For this purpose, the artificial priming site needed to be removed from the template. This was accomplished by a PCR reaction, using a single, biotinylated primer, specific to a site of the constant region that was still present after RT (Fig. 8.2.e). The truncated product was selected by coupling of the biotinylated product to streptavidin-coupled beads and two sequential washing steps. The resulting product only had an artificial priming site on one end and a conserved sequence on the other end. This allowed further product amplification with two distinct primers (Fig. 8.2.f). Thereby, the specificity was sufficiently increased to yield a clearly detectable PCR product.

Initially the sensitivity of the cDNA amplification (Fig. 8.2.c) was tested with single murine OT1 T cells. Pre-amplified cDNA was used as template for V-segment-specific PCRs (Fig. 8.3.a). Sequencing of the PCR-product yielded the expected OT1-TCR sequence (data not shown). The complete protocol as outlined in Fig. 8.2 was then tested on single human CMV-specific T cells, which were identified and isolated based on labeling with staining B8/IE1₁₉₉₋₂₀₇ MHC multimer.

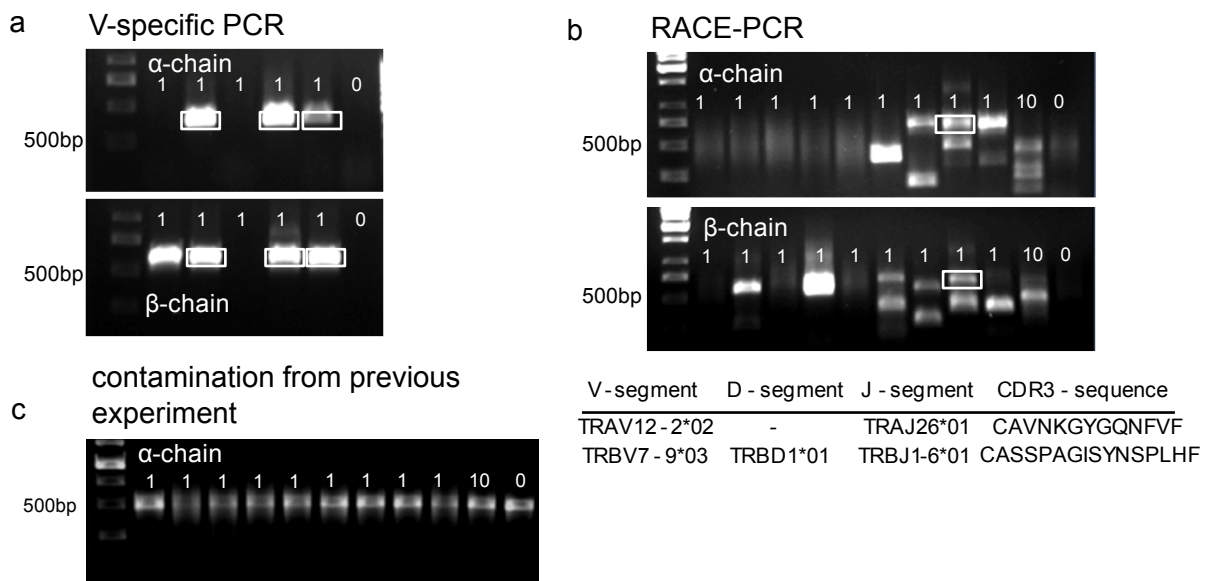


Figure 8.3: Results from solid phase coupled cDNA amplification protocol.

(a) Single cell amplified cDNA was generated from OT1-T cells as shown in Fig. 8.2. V-segment-specific PCR was performed to evaluate efficiency of previous steps. Upper row shows α -chain products and bottom row β -chain products. (b) Pre-amplified cDNA from single human T cells were amplified as shown in Fig 8.2. Upper row shows α -chain products and bottom row β -chain products. White box indicates successful amplification of α - and β -chain from the same cell. Rearrangement of TCR sequence is described in the table below (c) Single cell PCR was performed as shown in Fig 8.2. All samples including zero cell control show identical bands indicating false positive results.

Although the PCR product size was variable the method turned out to be highly specific for TCRs. Bands smaller than the expected 600bp to 750bp were found to be truncated fragments of TCR chains by sequencing. Similarly the sequences of double bands were identical but truncated within the V-segment, in the smaller fragment. This strategy readily provided single cell-derived TCR sequences (Fig. 8.3.b) but could not be broadly applied due to several restrictions. During the washing steps of the bead bound template, cross-contaminations between samples and even between subsequent experiments by aerosol formation were in our hands not controllable (Fig. 8.3.c). A second limitation of this approach was the low sample throughput owed to the time consuming washing steps.

8.1.2. GENE-SPECIFIC cDNA AMPLIFICATION WITHOUT WASHING STEPS BY VOLUME UPSCALING

To avoid formation of aerosols, we decided to dispense washing steps. The washing steps between different enzymatic reactions were substituted by volume upscaling. This allowed us to evaluate a different strategy as previously suggested Ozawa et al (Ozawa *et al.* 2008). However, we could not reproduce the efficiency of the previously published method, therefore we modified and optimized the original protocol.

It was not possible to accurately position single cell samples in 96 well PCR plates, most probably due to electrostatic interactions between the sort droplet and the plastic. We solved this problem by using plane PCR glass slides and a suitable thermal cycler. The extraction of mRNA turned out to be dispensable when the cells were spotted and exsiccated on the glass slides. We directly performed RT in a reaction volume of 0.5 μ l by simply adding the reaction mixture onto the glass slide. Hydrophilic spots on the slide-surface served to deposit small amounts of aqueous solutions. The spots were covered by an oil droplet and a hydrophobic followed by a hydrophilic ring kept the two phases in place (Fig. 8.4.a and b). For the sequence of enzymatic steps the volume was increased from 0.5 μ l to 1 μ l, 5 μ l and 25 μ l as shown in Fig. 8.4. Buffer substitution diluting the previous reagents produced optimal conditions for the following enzyme. The first two steps were performed on the slide before the complete reactions were transferred to 96 well plates. After reverse transcription we digested the residual primers with exonuclease I. As described for our original protocol we used TDT tailing to generate an artificial priming site (Fig.8.4.d). The oligo-dG stretch served as an anchor to attach a defined sequence by PCR using an oligo-dC-primer with a long

overhang (Fig 8.4.e). After this anchor step one micro liter of the reaction was transferred to two separate PCR reactions for further amplification of α -chain or β -chain respectively. The forward priming site was the overhang generated by anchor PCR and the reverse primer bound within the constant region. This step was repeated with a pair of nested primers for each chain (Fig. 8.4.f, g).

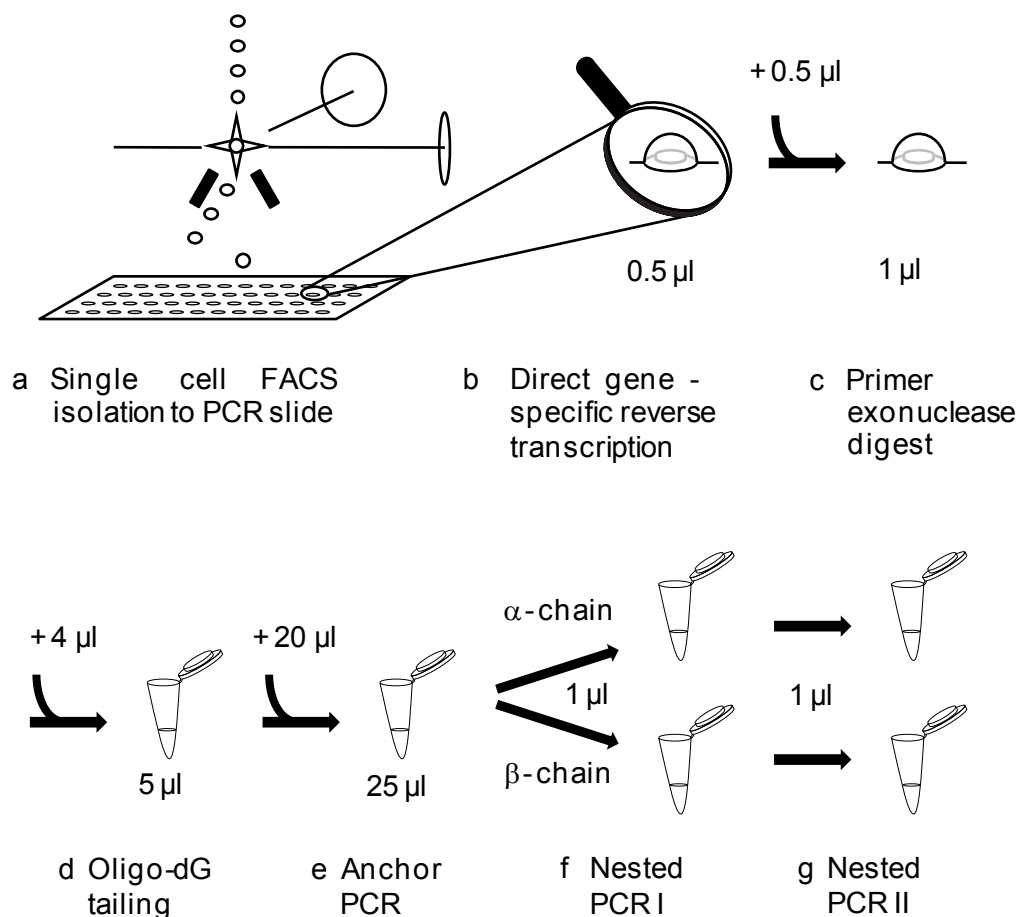


Figure 8.4: Sketch of the basic principle of the novel single-TCR sequencing strategy.

Reverse transcription and exonuclease digest were consecutively done on slides by upscaling volumina. Complete reactions were transferred to 96 well plates for tailing, anchor PCR and nested PCR round I and II. Alpha and beta chains were pre-amplified together during anchor PCR and in separate reactions for nested PCRs I and II.

8.1.3. PRIMING

The undoubtedly most critical step within the entire procedure was the conversion of mRNA to cDNA, as the minute amounts of template mRNA is prone to RNase degradation and incomplete RT. Besides obvious factors like addition of RNase inhibitors and *dithiothreitol*, several other parameters turned out to have essential influence of the efficiency.

To test whether gene-specific priming is more efficient than non-specific priming several different strategies were tested. We compared the combined use of random octamers and oligo-dT primers, one single gene-specific primer as published (Ozawa *et al.* 2008) , and several serial gene-specific primers per TCR-chain (Fig. 8.5.a). We performed the protocol as outlined in Fig. 8.4 for all three conditions with decreasing numbers of template cells. The use of random and oligo-dT primers produced PCR products in the expected size down to a number of 5 cells, whereas several serial gene-specific primers resulted in a product, only down to 50 cells. The use of a single gene-specific primer for RT did not result in any PCR product.

We hypothesized that residual RT-primers might interfere with later amplification steps by non-specific priming events and primer dimer formation. For this reason, we tested whether exonuclease digest of residual primers after RT could reduce the formation of non-specific smear. This effect had been proposed in a report about cDNA amplification for single cell microarrays (Kurimoto *et al.* 2007).

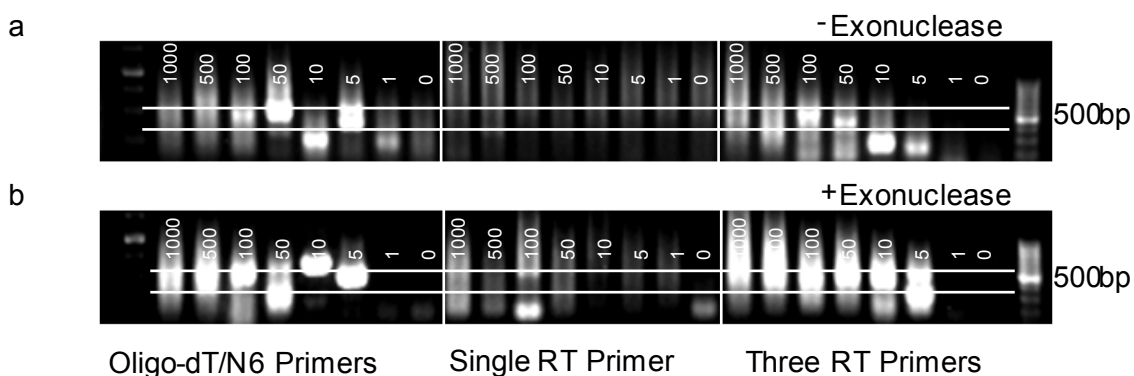


Figure 8.5: Evaluation of priming strategies for Reverse Transcription"

Different priming strategies (standard oligo-dT/random octamers, one gene-specific primer and three gene-specific primers per TCR chain) were tested with and without extra exonuclease-I digest of residual RT-primers. Decreasing numbers of human T cells, from 1000 to 1 as indicated served as template. (a) Protocol without exonuclease I digest. (b) Protocol with exonuclease I digest.

Our results confirmed this finding and even indicated a positive influence on sensitivity (Fig. 8.4.c). Exonuclease III is used to digest all single stranded nucleic acids i.e. residual RT primers. Specific cDNA at this point is still bound to the complementary mRNA and is therefore protected from digestion.

A general tendency towards more total PCR product yield was observed in all exonuclease groups. The most prominent influence was found in combination with three gene-specific RT-primers. Although in this experiment no PCR product was generated from a single cell, we successfully tested this condition on a larger number of single cell samples, however with low efficiency (data not shown).

8.1.4. OPTIMIZATION OF SENSITIVITY BY THREE ROUNDS OF EXPONENTIAL TEMPLATE AMPLIFICATION

The strategy proposed by Ozawa et al. included as a first PCR step a linear amplification that solely served to add an overhang to the previously formed oligo-dG stretch at the cDNA 3'-end. We reasoned that additional antisense priming during this reaction would either improve the sensitivity of the protocol or would generate more non-specific products. Therefore, we evaluated the addition of a reverse primer, binding in the constant region to turn the linear into an exponential amplification.

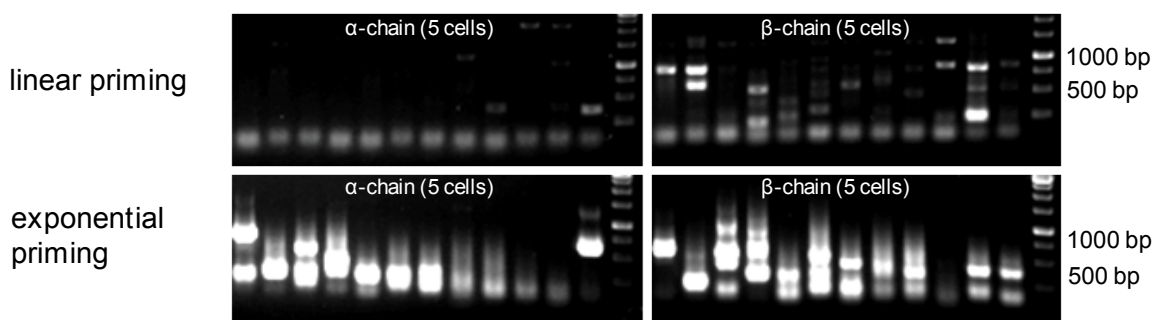


Figure 8.6: Test of third round of PCR amplification.

The RACE-PCR protocol as outlined in Fig 8.4 was performed with 5 cells per sample. Anchor PCR was tested without reverse primer in “linear” mode (top row) and with reverse primer in “exponential” mode of amplification (bottom row).

We chose to use 5 cells as template to detect subtle improvements of efficiency as very few single cell samples resulted in a PCR product with the protocol at this stage. The comparison

between the groups with priming in only one direction (i.e. linear PCR) and priming in both directions (i.e. exponential PCR) during anchor PCR (Fig. 8.4.e) clearly showed an improved efficiency for the latter condition (Fig.8.5.).

8.1.5. RT-TEMPERATURE

Annealing temperature during reverse transcription is generally believed to be optimal in the highest possible range, as the stability of mRNA secondary structures decreases with temperature. For this reason we initially used the highest possible temperature according to the manufacturers' recommendations. To empirically validate this assumption we tested a variety of RT-annealing temperatures using ten cells per sample in order to obtain a reliable signal. As lower temperatures to our surprise did not result in a reduced sensitivity (Fig. 8.7.),

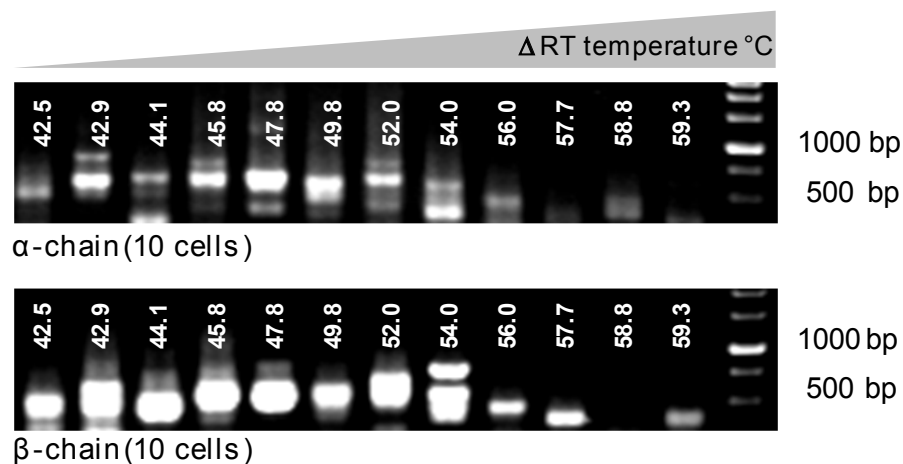


Figure 8.7: Optimization of RT-temperature.

The RACE-PCR protocol as outlined in Fig 8.4 was performed with 10 cells per sample. Reverse transcription was performed over a temperature gradient from 42.5°C to 59.3 °C

we changed our standard RT-temperature from 55 to 51°C. We hypothesized however, that a temperature increase during RT might resolve secondary structures and might allow continuation of interrupted transcription of reverse transcriptase molecules that still might remain bound to mRNA.

To test this hypothesis, we performed RT at 51°C for 30min and raised the temperature to 70°C for 20min. The latter temperature results in a strongly reduced half life of reverse transcriptase. However, a strikingly increased PCR efficiency on the single cell level was

found as representatively shown in (Fig. 8.8.a). In total 144 single cell samples were processed with an RT-temperature of 51°C. The recovery of alpha and beta-chain sequences from the same cell that contained the translation start in total was 0.7%, which equals one single sample. With the modified two-temperature RT-strategy 63 out of 266 single cell samples provided TCR sequences with complete coverage of the variable domain. In 32.3% of all samples the sequence of the α -chain and 45.7% of the β -chain was identified. In total 23.7% of all single cell samples delivered both TCR-chains (Fig. 8.8.b).

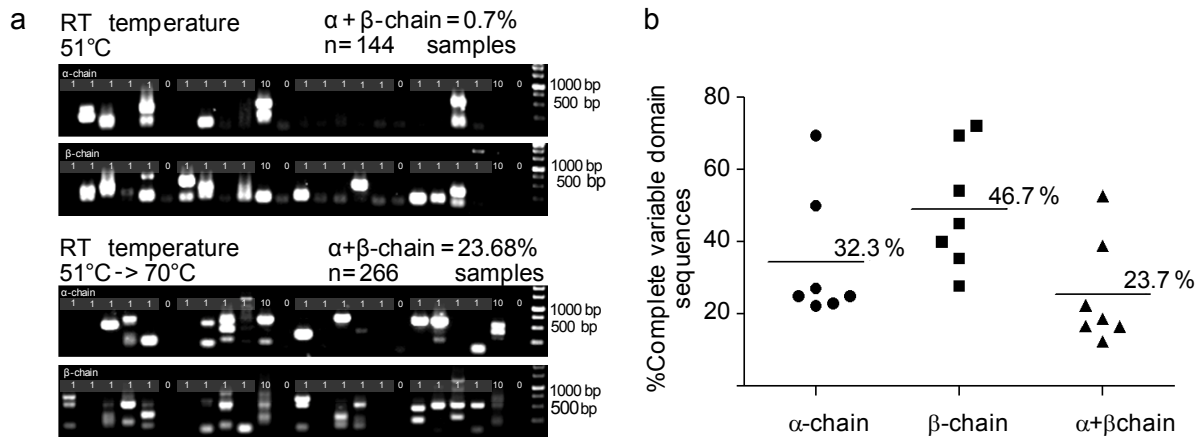


Figure 8.8: Efficiency of Single cell PCR protocol.

(a) Temperature switch during reverse transcription was tested. RT at a constant temperature of 51°C was compared with a temperature increase from 51°C for 30min to 70°C for 20min. (b) In seven independent single-cell PCR experiments a total number of 266 samples were processed. Numbers of samples yielding α - and/or β - chain products above the evaluated full-length cut-off size were calculated as a percentage of total samples per experiment. Mean values for all experiments taken together are indicated by horizontal lines.

8.1.6. PRECAUTIONS FOR PREVENTION OF CROSS-CONTAMINATION

The protocol we developed includes three subsequent PCR amplification steps with specificity for the TCR. This results in an extremely high sensitivity, which, on the one hand is necessary, but on the other hand harbors the risk that minute amounts of starting material can lead to cross contaminations. Although standard precautions like spatial separation between master-mix preparation, PCR cycling, and PCR product analysis were fulfilled all through the establishment process, cross contaminations between samples and even between experiments was observed (Fig. 8.3.c). Two types of precautions were taken to reduce the burden of cross contamination. First, we tried to identify the prevalence of false positive samples. In every experiment several samples (16.67% of all samples) were negative controls i.e. samples without cell. Furthermore, all obtained sequences were entered into a database and all new sequences were compared with the previously identified ones. These measures enabled us to quantify the grade of cross contamination. The other type of measure addressed the prevention of cross contaminations. A very stringent lab protocol was designed that included UV-irradiation steps between subsequent steps. After every step waste bags were sealed, UV-irradiated and discarded. All pipettes and plastic materials were irradiated and were exclusively used for specified steps, which were assigned to defined areas. To reduce the formation of aerosols, PCR oil was used instead of the common PCR foils. Furthermore, cross-contamination by personal was avoided. All master-mixes were prepared by a person that was precluded from all areas where PCR product preparation and further processing took place. For optimal spatial separation the ventilation system in the building was considered. All steps downstream of the PCR amplification were therefore performed in a separate floor of the building to exclude air exchange through the ventilation system. By those measures we were able to reduce the burden of false positives to a minimum. Most experiments were completely devoid of cross contamination according to our detection methods.

8.2. TCR-SEQUENCE ANALYSIS OF CMV-SPECIFIC T CELL POPULATIONS

To ascertain whether our protocol was suitable to describe the TCR composition of a defined T cell-population we analyzed CMV-specific T cells. Donor 1 showed a T cell-population positive for MHC multimer B7/pp65₄₁₇₋₄₂₆, which was used to FACS-sort single cells to PCR slides for TCR amplification, as shown in Fig. 8.9.a. In this experiment, 22.2% of all single cell samples resulted in a full-length product for both TCR chains as indicated by the white boxes (Fig. 8.9.b). All samples were sequenced and analyzed. We repeatedly identified the same TCR α/β -pairing in all but one sample, indicating clonal dominance (Fig. 8.9.c). To exclude cross contamination, we isolated MHC multimer-positive T cell from the same donor once more and propagated T cell-clones by limiting dilution. In total we analyzed the TCR of six clones that were completely MHC multimer-positive (Fig. 8.9.d) by PCR and exclusively identified the dominant sequence that we had previously found on the single cell level. Surprisingly, we discovered that the rearrangement of the second TCR pairing that we sequenced in this population had previously been reported to be part of a CMV-specific public repertoire among HLA-B7 positive-donors (Weekes *et al.* 1999).

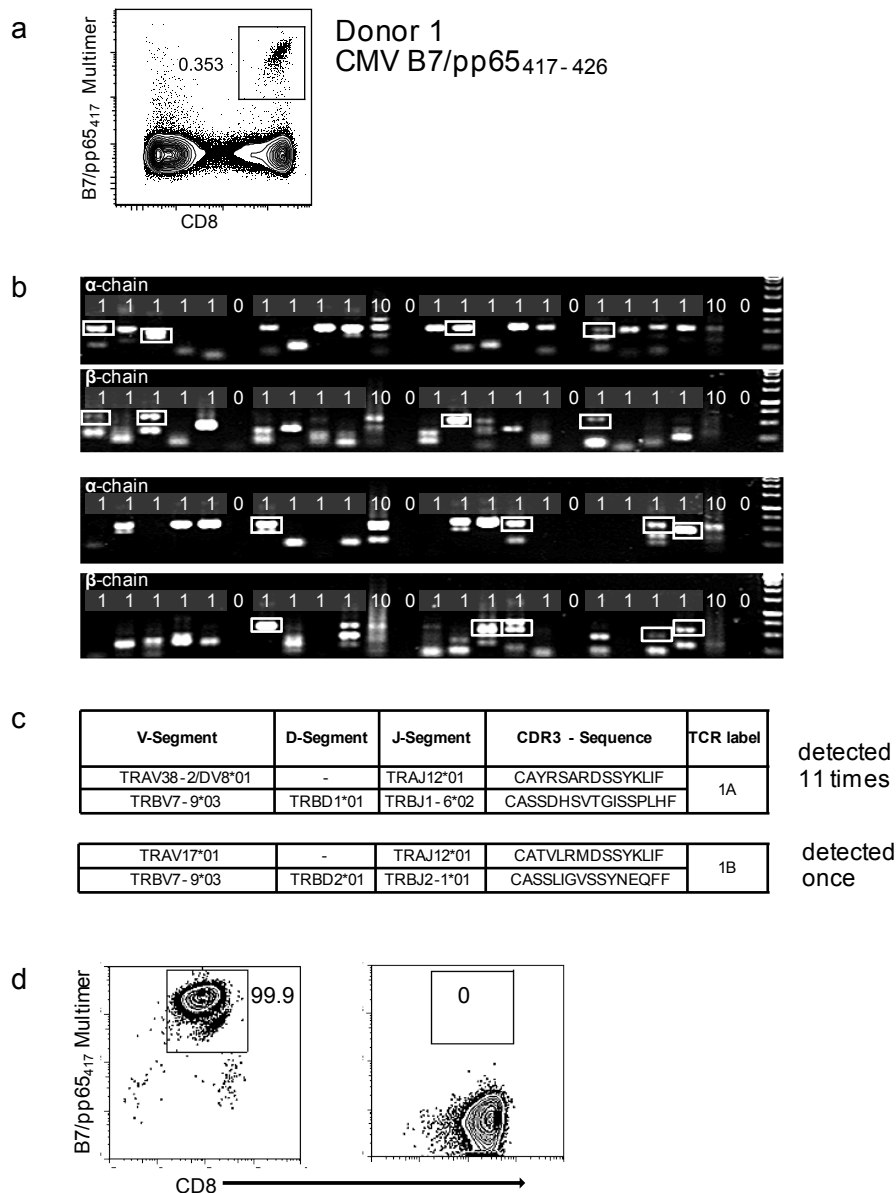


Figure 8.9: Single cell PCR analysis of CMV Donor 1.

(a) PBMCs from Donor 1 were recovered and stained with HLA-B7/pp65₄₁₇₋₄₂₆ multimers. The positive gate shows the further analyzed CD8 and MHC multimer double-positive cell population. Cells were pre-gated on live lymphocyte (propidium iodide-negative, and CD3-positive). (b) Single antigen-specific T cells from Fig. 8.9 (a) were FACS-isolated and used for single-cell TCR sequencing as described in Fig. 8.4. The image shows a representative agarose gel with PCR products. White boxes indicate samples that yielded full-length TCR α - and β - chain products. (c) PCR products from Fig. 8.9c were cloned and sequenced. TCR1A was identified 11 times and TCR 1B was detected once. (d) MHC multimer-positive T cells from the same donor were *in vitro* expanded and six T cell-clones were successfully maintained. All clones contained TCR1A. The left FACS plot shows HLA-B7/pp65₄₁₇₋₄₂₆ staining and the right FACS plot shows staining with an irrelevant MHC multimer.

8.3. REPERTOIRE ANALYSIS AND DEMONSTRATION OF SINGLE CELL -DERIVED TCR-SPECIFICITY BY GENE TRANSFER.

We analyzed a second CMV-specific T cell-population from a different donor. We used the HLA Multimer B8/IE1₁₉₉ to detect CMV-specific T cells and directly sorted single cell samples as shown in Fig. 8.10.a. Single cell PCR yielded 10% full length TCR α/β -pairings. Once again, we found the same pairing in all sequenced samples. In order to exclude cross contamination the experiment was repeated twice and a total of 25 pairings was analyzed. We only identified a different TCR sequence in one sample (Fig.8.10.c). Similar to donor 1, this strongly indicated prevalence of a dominant clone. To verify this result by a different method, we stained the MHC multimer-positive T cell-population with an antibody that was specific for the expected V β -segment. More than 80% of the MHC multimer-specific T cells had the V β -type that we detected by single cell TCR sequencing, thus confirming the existence of a dominant clone (Fig. 8.10.d). Altogether, due to the complete absence of false-positive control samples or previously detected sequences and exclusive pairing of the same α - and β -chains in several independent experiments, we exclude cross contamination. These findings suggest that the TCRs we isolated by single cell PCR are antigen-specific. To conclusively demonstrate this, we decided to transfer the TCR-gene from the dominant clone to other cells. We cloned TCR 2A (Fig. 8.10.c) into the retroviral expression plasmid MP71 and generated viral particles to transduce a T cell-line. As host cells we chose the T cell-lymphoma cell line Jurkat76, which does not express an endogenous TCR, thus formation of chimeric TCRs and competition for cell surface expression is prevented. Furthermore, the cell line is modified to express the CD8 co-receptor α -chain, which interacts with the TCR/MHC complex during antigen binding. This molecule assists TCR-pMHC-interaction and is necessary for successful MHC multimer staining of most TCRs. As shown in Fig. 8.10.e, a substantial fraction of Jurkat76 cells became MHC multimer-positive upon transduction. There seems to be a correlation between CD3 expression and MHC multimer staining intensity. As CD3 only appears on the cell surface in complex with TCR this indicates that all TCR expressing, and therefore successfully transduced T cells, can bind MHC multimer. This experiment for the first time demonstrates successful, genetic redirection of T cells with a TCR gene, isolated by single cell PCR, and proves the operational reliability of our approach.

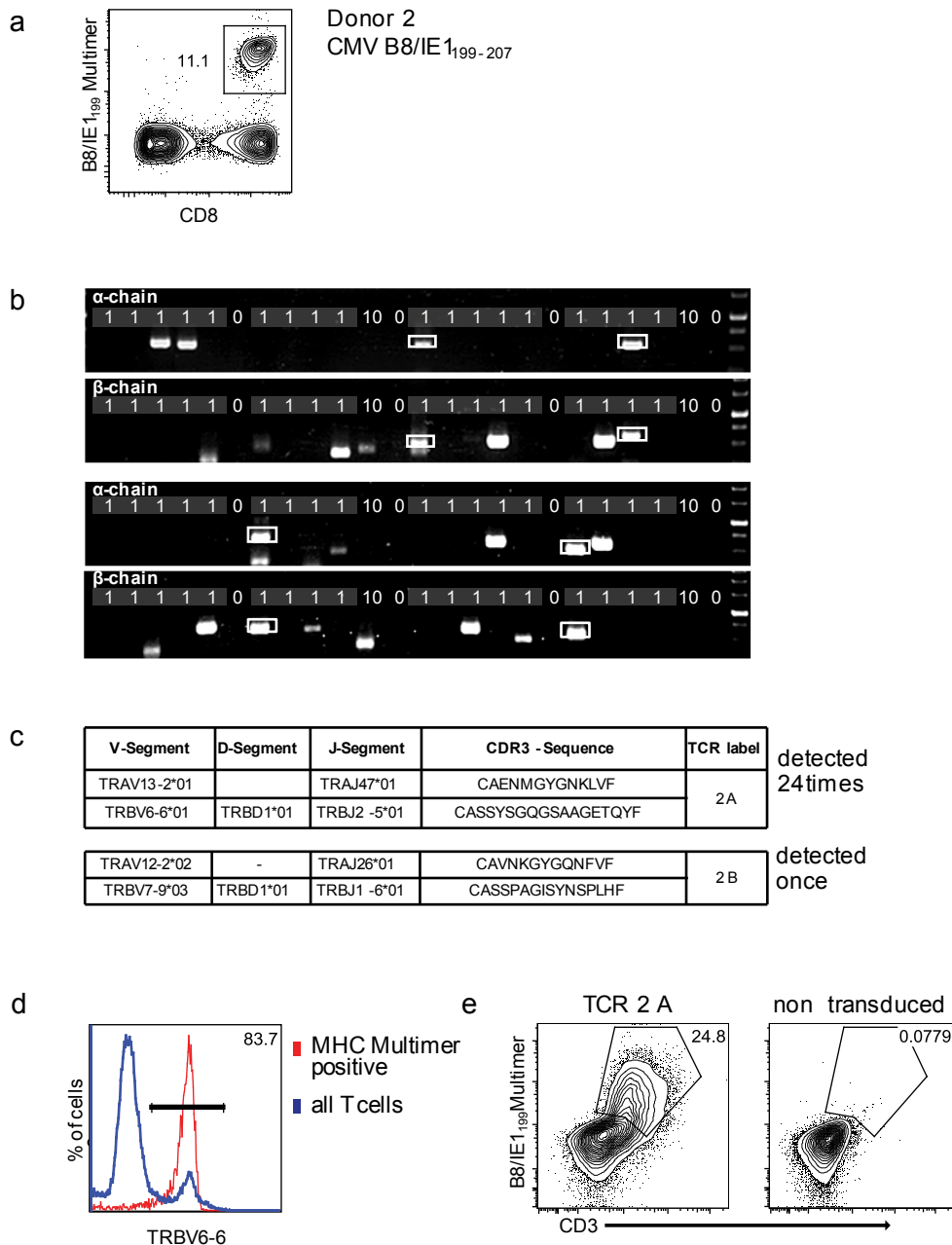


Figure 8.10: Single cell PCR analysis of CMV Donor 2"

(a) PBMCs from donor 2 were recovered and stained with HLA-B8/IE-1₁₉₉₋₂₀₇ multimers. The positive gate shows the further analyzed CD8 and MHC multimer double-positive cell population. Cells were pre-gated on living lymphocytes (propidium iodide negative and CD3 positive). (b) Single antigen-specific T cells from Figure 8.10 (a) were FACS-isolated and used for single-cell TCR sequencing. (c) PCR products were sequenced. TCR 2A was detected 24 times; TCR 2B only once. (d) PBMCs from Donor 2 were labeled with MHC multimer and antibody binding to V-segment of TCR 2a V β 6-6. Red line shows MHC multimer-positive cells. Blue line shows total T cells. (e) The identified TCR sequence from TCR 2A was expressed in Jurkat76 T cells by retroviral gene transfer. Transduced (left FACS plot) and non-transduced (right FACS plot) Jurkat76 T cells were analyzed for expression of CD3 and MHC multimer binding.

These experiments provide a proof of concept of our approach, but for TCR analysis of populations as large and oligoclonal as the ones that we examined so far, single cell PCR would not have been necessary. The specific strength of our approach is the possibility to analyze few cells. For that reason we analyzed a comparably small CMV-specific T cell-population of less than 0.1% of all T cells (Fig. 8.11.a). Again single cells were FACS sorted, based on MHC multimer-staining and single cell PCR was performed. 22.2% of all single cell samples delivered full-length TCR α - and β -chain sequence information (Fig. 8.11.b). The experiment was repeated twice and a total of 16 single cell samples were sequenced and in total 9 different TCRs were detected (Fig. 8.11.c). For one TCR (TCR 3H) we only identified the β -chain and for another TCR (TCR 3G) the α -chain rearrangement turned out to harbor a frame shift and probably could not promote successful translation to a protein. Most likely the original T cell expressed a second, functional α -chain that we did not detect. Finally, to prove antigen-specificity we chose three TCRs and transduced them to Jurkat76 cells (Fig. 8.11.c). All three TCRs recognized the MHC multimer B8/IE1₈₈ that was also originally used for T cell-isolation. Again, there was a clear correlation between CD3 surface expression and TCR expression. This indicates that all TCR positive cells are antigen-specific, and that the variability of percentages of MHC multimer-positive T cells reflects differences in transduction efficiency rather than in antigen-specificity.

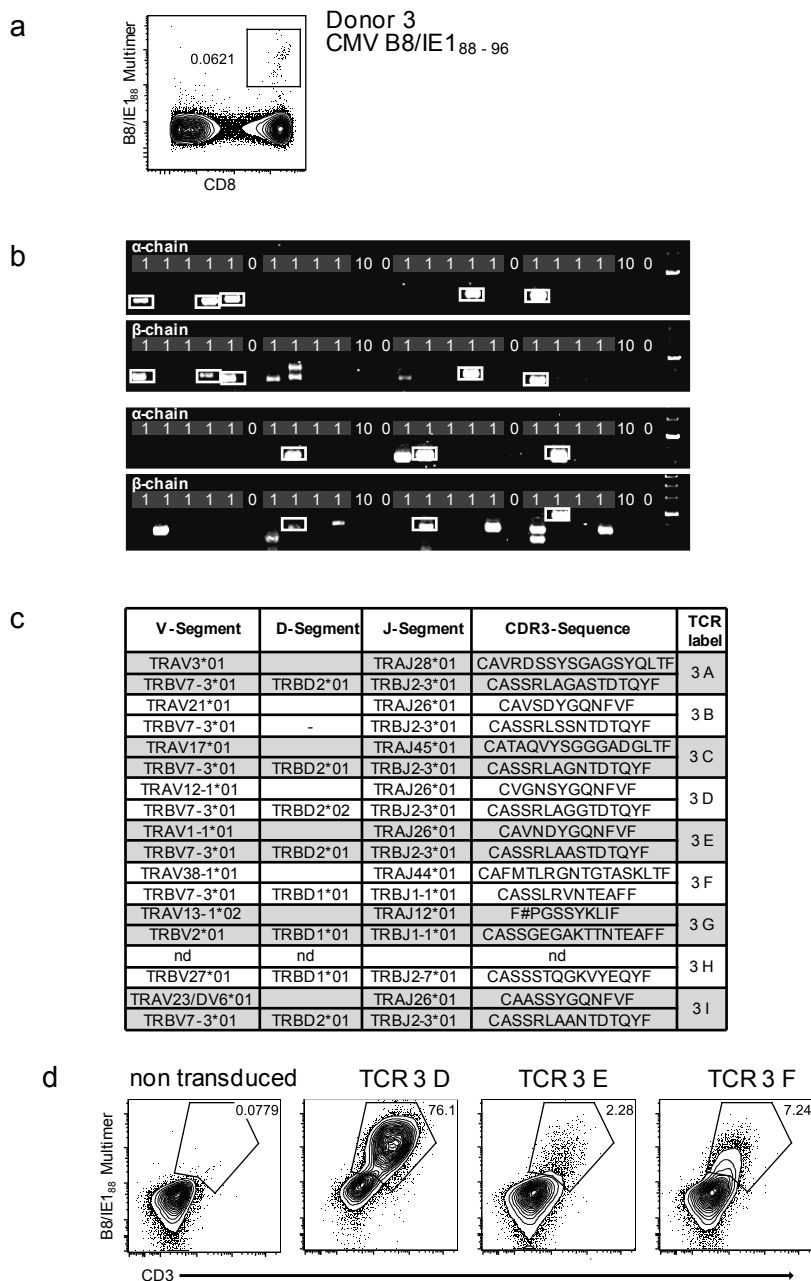


Figure 8.11: Single cell PCR analysis of CMV Donor 3.

(a) PBMCs from donor 3 were stained with HLA-B8/IE-1₈₈₋₉₆-multimers. The positive gate shows the further analyzed CD8 and MHC multimer double-positive cell population. Cells were pre-gated on living lymphocytes (propidium iodide-negative and CD3-positive). (b) Single antigen-specific T cells from Fig. 8.12 (a) were FACS-isolated and used for single-cell TCR sequencing. (c) PCR products from Figure 8.12 (b) were cloned and sequenced. 9 different TCR sequences were identified. (d) Sequences from TCR 3D, 3E and 3G were expressed in Jurkat76 T cells by retroviral gene transfer. Non-transduced (left FACS plot) and transduced Jurkat76 T cells were analyzed for expression of CD3 and MHC multimer binding.

All control samples without cell were negative, the TCR sequences we identified had not been amplified before and α -, β -chain pairings occurred only in the same combinations; therefore, we exclude presence of cross contamination. Clonal dominance as found in the previously analyzed CMV-specific T cell-populations was not detected. However, a high degree of similarity within V β -usage and CDR3 regions of different TCRs was found. The majority of V β -chains had the TRBV7-3*01 segment. We also analyzed the V β -repertoire by FACS. For TRBV7-3*01 no antibody was available, so probably only the smaller part of the V β -repertoire is represented by this method (Fig. 8.12.d). We subjected the CDR3 amino acid sequences separated for α - and β -chain to multiple sequence alignment, and computed a dendrogram to illustrate the grade of CDR3 sequence similarities. Paired α - and β -chain sequences grouped in clusters of closely related sequences with highly conserved sequence motifs. The sequence motifs YGQNF, TDTQ and S*nTEA were reported previously for T cells, binding this particular epitope (Trautmann *et al.* 2005; Wang *et al.* 2012). Interestingly, we exclusively detected pairing of α -chain YSGnG and YGQNF with the β -chain motif TDTQ. To depict these sequence correlations, we brought α - and β -chain similarity trees face to face (Fig. 8.12.b). The highest degree of sequence similarity was found in the pairings of TCRs 3B, D, E and I. All β -chains were identical in V-segment type. Here all α -chain CDR3 domains uniformly consisted of 12 amino acids and associated β -chain CDR3 domains consisted of 15 amino acids. More than 66% and 80% of all positions were identical for α - and β -chains, respectively. The grade of resemblance considering similar chemical properties among different amino acids for both chains was even 100% (Fig. 8.12.c). Surprisingly their corresponding α -chains were completely different in V-segment usage.

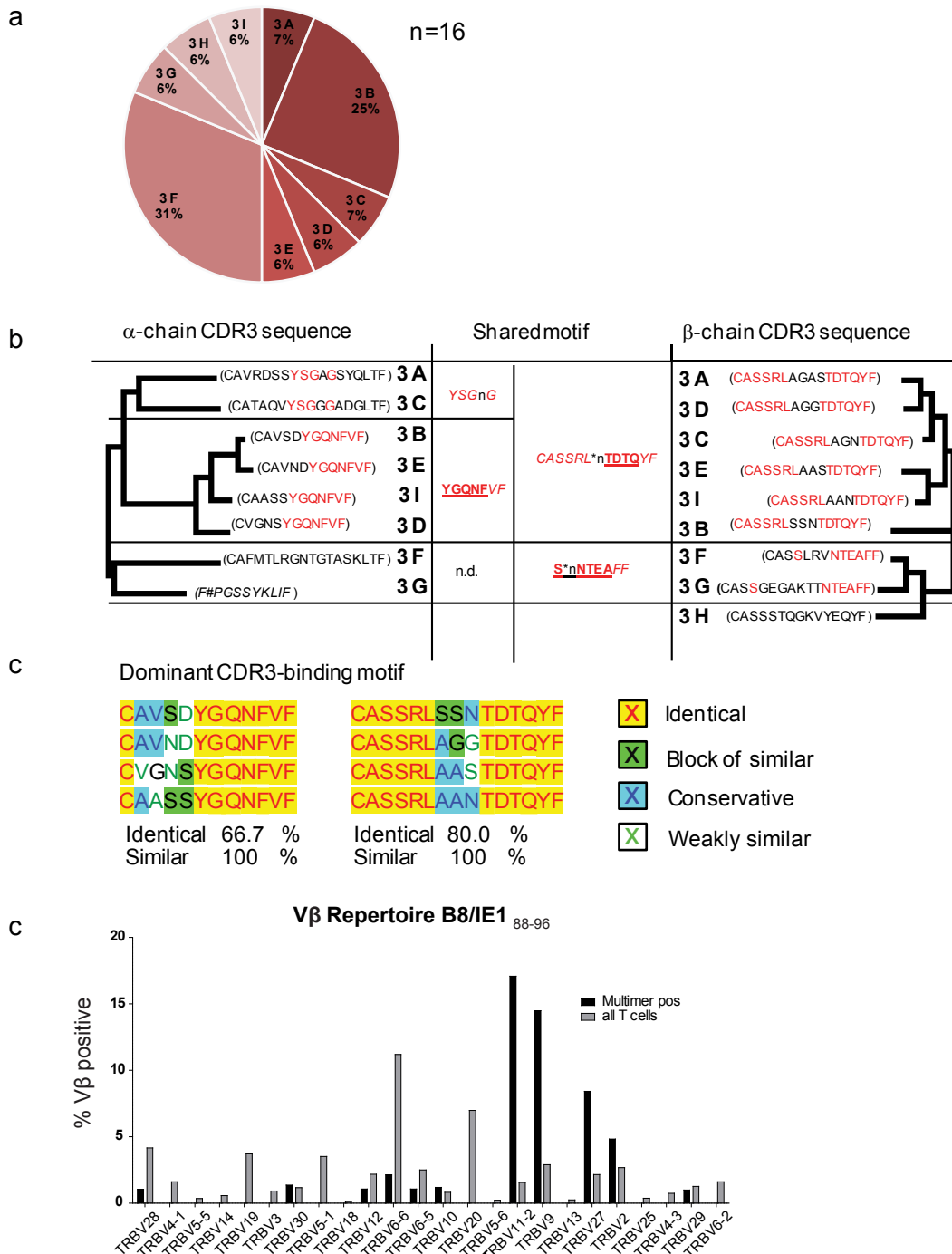


Figure 8.12: Repertoire analysis of CMV-specific T cells from Donor 3"

(a) Clonal composition of the analyzed CMV-specific population; data are derived from a total of 16 single cells samples. (b) Dendrogram of CDR3 sequences from Fig 8.12(c) Length and distance of branches indicate grade of similarity among compared CDR3 sequences. Red indicates identical sequence parts among identified TCRs. Bold letters mark previously described public motifs. (c) CDR3 sequences from four closely related TCR of identical length as shown in Fig 3e were compared by multiple sequence alignment. Grade of identity and similarity was calculated by matrix blosum62mt2 under Vector NTI. (d) Vβ-repertoire analysis of the MHC multimer-positive cells from Donor3. Grey bars indicate the percentage of Vβ-type among complete T cells and black bars MHC multimer-positive T cells

All CMV-specific TCRs that we transduced to Jurkat cells were in parallel transferred to human PBMCs. However, only TCR2A and TCR3D showed significant MHC multimer-staining upon transduction. We explain this effect by competition for surface expression with the endogenous TCR. This phenomenon has been described before, however the mechanistic details of mutually suppressed surface expression between TCRs have not been elucidated yet (Sommermeyer *et al.* 2006). The two TCRs that successfully redirected PBMCs displayed different staining patterns. TCR2A exclusively bound MHC multimer on CD8⁺T cells, whereas TCR3D also bound MHC multimer on CD4⁺ T cells, which indicates that the avidity of this TCR to pMHC was high enough to bind without the co-receptor CD8 (Fig. 8.13). The capacity of CD8-independent MHC multimer binding has previously been suggested as an indicator of high TCR binding affinity (Pittet *et al.* 2003). By measurement of TCR/pMHC dissociation-kinetics we could confirm the difference in binding strength between the two TCRs (Nauerth *et al.*, submitted).

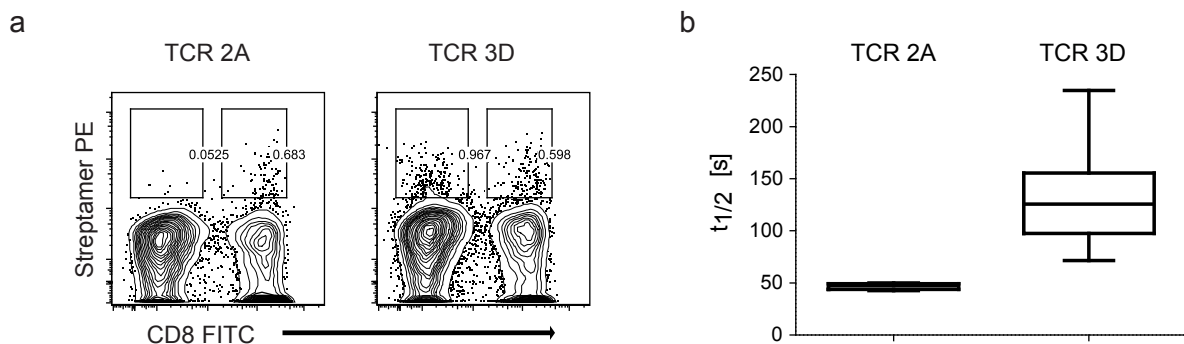


Figure 8.13: Avidity measurement of transduced TCRs.

TCR 2A and 3D were transduced to human PBMCs. (a) FACS plots show CD8 and MHC multimer staining. Gates specify *Streptamer*-positive cells (b) pMHC-dissociation was microscopically measured to calculate fluorescence half life time. The half life times from several single cell samples from TCR2A and TCR3D transduced cells were pooled and are shown as box-plots.

8.4. ENRICHMENT OF TUMOR ANTIGEN SPECIFIC T CELLS FROM THE NAÏVE REPERTOIRE OF HEALTHY DONORS.

To this point we have demonstrated that it is a feasible approach to isolate TCRs from single MHC multimer-specific T cells by single cell PCR, and that we can hereby access very small T cell-populations. We furthermore proved that these TCRs can be used to redirect other T cells. The specificities we chose for this purpose were CMV-epitopes. TCR transfer to redirect the specificity of patient T cells to a CMV-epitope is currently under clinical evaluation (Table 5.7). However, especially in therapy against tumors adoptive transfer of genetically-modified T cells has shown promising results. We reasoned that direct access to *ex vivo*-derived, rare antigen-specific T cells might contain a broad variety of TCRs that was inaccessible by conventional strategies of TCR isolation. We used a strategy that was previously described to quantify the precursor frequency of antigen-specific T cells in the mouse (Obar *et al.* 2008).

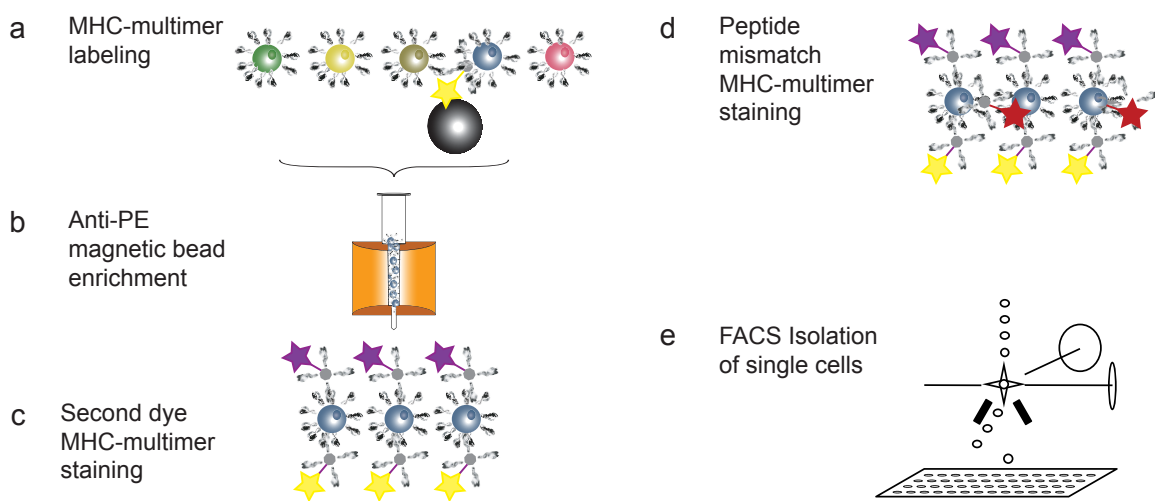


Figure 8.14: Schematic overview of MHC multimer based isolation of rare antigen-specific T cells.

(a) PBMCs were labeled with MHC multimer and bound to anti-PE antibody coated paramagnetic beads. (b) MHC-multimer positive cells were enriched by MACS. (c) The eluted positive fraction was labeled with a differently labeled MHC multimer. (d) Dual-labeled cells were incubated with an MHC-matched, irrelevant MHC multimer coupled to a different fluorophore. (e) MHC multimer positive cells were isolated FACS sorting.

The described method uses magnetic enrichment of MHC multimer-labeled cells. Additionally, dual labeling with MHC multimer of identical specificity but with diverging label was described to reduce the rate of false positive cells. In addition to this, we intended to use a third MHC multimer with identical MHC-complex but with an irrelevant peptide. We reasoned that cross-reactive cells that primarily bind to the MHC-complex would be labeled also by the irrelevant MHC multimer (Fig. 8.14.d).

In total, MHC multimer labeling with three different fluorophore labels was necessary. We tested several commonly used fluorophores, which were broadly applied for antibody labeling. Fluorescein (FITC) MHC multimer-labeling did not yield sufficient resolution to distinguish MHC multimer-labeled cells (data not shown). By labeling with PE-Cy7 and eF450 we could detect CMV-specific T cells. However, in comparison to PE and APC the fluorescence intensity was drastically reduced and provided rather a slight shift from auto-fluorescent cells than a clearly positive and negative signal. In order to improve the signal quality we titrated the amount of fluorophore-labeled Streptavidin backbone over a constant amount of peptide MHC (pMHC) monomeric complexes. This purely empirical procedure was necessary, as neither the exact molecular weight nor the molarity of the fluorochrome-labeled Streptavidin reagents could be determined. We co-incubated a constant amount of pMHC complexes with different amounts of Streptavidin backbone to find the best multimerization conditions. The Streptavidin-concentrations ranged between 0.05 and 1 $\mu\text{g}/\mu\text{l}$, while pMHC concentration was always 40 $\mu\text{g}/\text{ml}$. After 1h of co-incubation we used the multimerized complexes at a dilution factor of 1:5 to label PBMCs from a CMV-positive donor. After multimer labeling we stained the cells with further phenotyping antibodies and determined the geometric mean fluorescence intensity of MHC multimer-labeled cells by FACS. Whereas the optimal concentration of Streptavidin was 1 $\mu\text{g}/\mu\text{l}$ with lower staining intensities at decreasing concentrations for PE, the best results for APC were achieved with 0.25 $\mu\text{g}/\mu\text{l}$. For eF450 and PE-Cy7 best separation of positive and negative cells was detectable with the lowest concentrations of Streptavidin. For both fluorophores, 0.01 $\mu\text{g}/\mu\text{l}$ yielded the best distinction. However the staining intensities for the latter two labels were so drastically reduced as compared to PE and APC that positive and negative cells could not be sufficiently separated (Fig. 8.15.a, b). To identify a third dye for MHC multimer staining, we tested a new type of molecule, which had recently been commercialized. BV421 turned out sufficiently bright for MHC multimer staining. We titrated the multimerization conditions in the same way as for all previous reagents (Fig. 8.15.c).

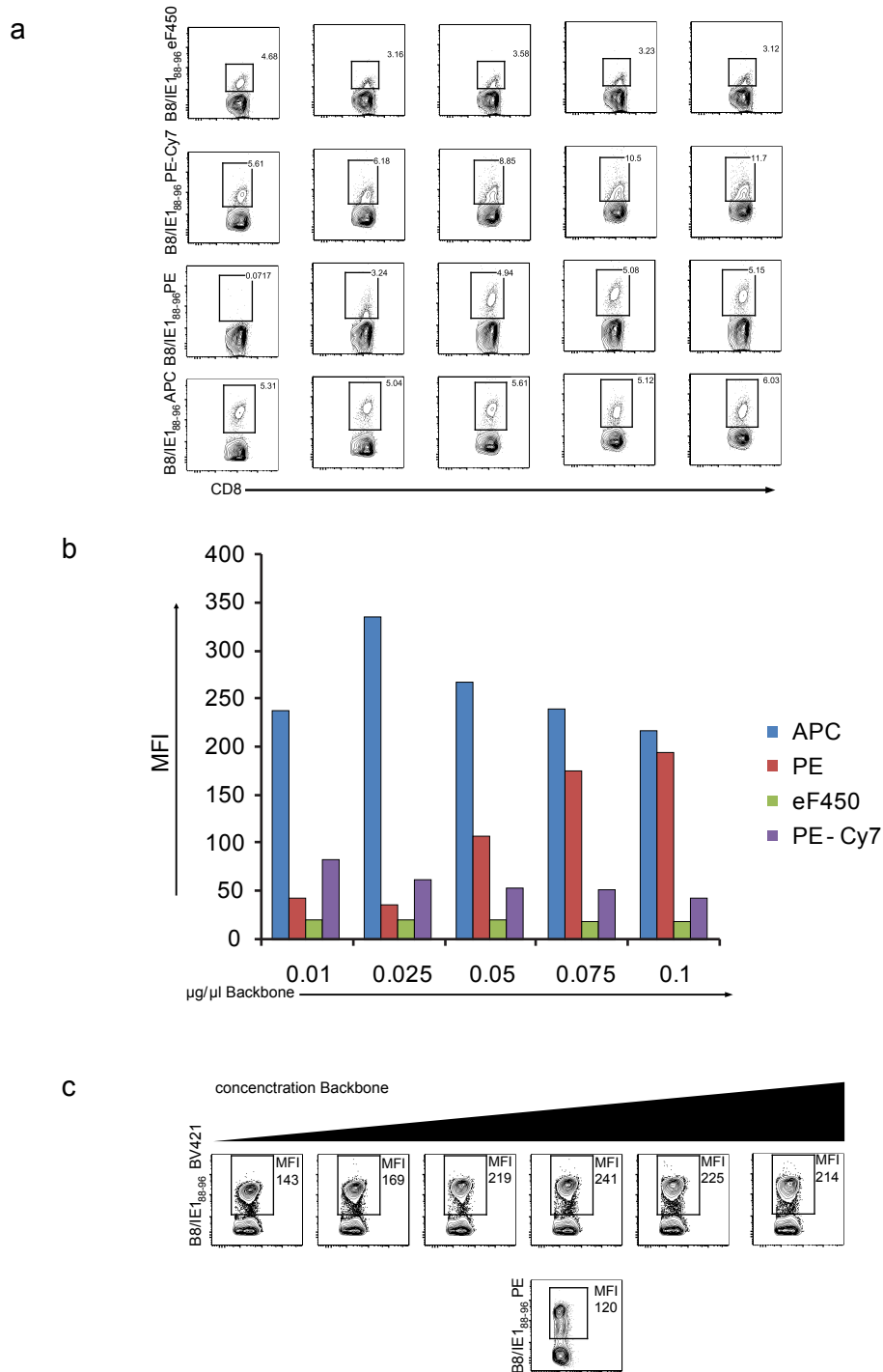


Figure 8.15: Identification of fluorophores for MHC multimer staining"

(a) Conditions for MHC multimerization were titrated. Amount of pMHC was kept constant and Streptavidin/ *Strep*-Tactin was modified for several differently labeled backbone molecules (increasing concentrations from left to right) (b) Bars quantify the MFI-values for MHC multimer-positive cells from 8.15.a. (c) Titration of Streptavidin BV421 over a constant amount of MHC multimer. Bottom plot shows staining with *Strep*-Tactin PE MHC multimer generated by previously optimized conditions.

Similarly, we could identify an optimal ratio for multimerization and found an even better resolution than for PE, which was used under the optimized conditions we had previously determined. The maximal MFI for BV421 was 241 whereas for PE only 120 (Fig. 8.15.c). Next, we tested whether several competing MHC multimers for the same binding partner will mutually decrease their signal intensities. We performed single and double MHC multimer stainings with PE and APC labels and compared the MFI.

In fact the staining intensities decreased for both signals, when two competing MHC multimers were used. However, the decrease in staining intensity did not result in a loss of clearly separable signals (Fig. 8.16.a, b).

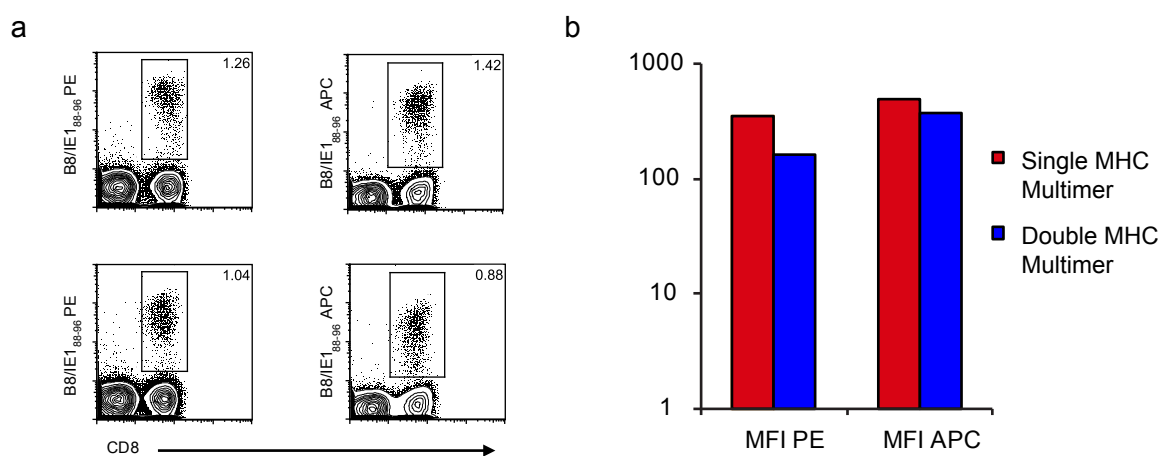


Figure 8.16: Sequential labeling with two MHC multimers does not prevent labeling.

(a) CMV-specific T cells were single (top row) or dual (bottom row) labeled with B8/IE1₈₈₋₉₆ multimers. PE-labeled MHC multimer was used before APC-labeled MHC multimer. (b) Mean fluorescence intensities of MHC multimer-positive cells were determined.

To test whether the MHC multimers for the enrichment of T cells specific for tumor-associated antigens were functional and specific, we sorted single MHC multimer-positive cells. We multimerized pMHC-monomers with fluorophore-labeled streptavidin as previously determined (Figure 8.17). The staining intensities using A2/WT1₁₂₆ were considerably lower as compared to A2/Her2₃₆₉. This is most likely due to the TCR expression on the control cell-line that we used. We never observed a more distinct staining than shown here. However, during the enrichment experiments we observed clearly separable positive and negative signals. Three differently labeled MHC multimers were tested for A2/WT1₁₂₆₋₁₃₄ (top row) and A2/Her2/neu₃₆₉₋₃₇₇ (bottom row).

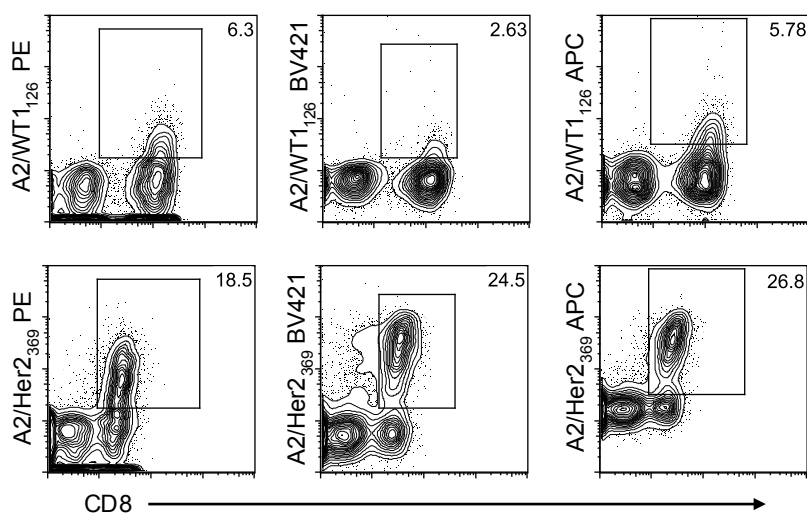


Figure 8.17: Test of reagents for enrichment.

The multimer-reagents used for enrichment of rare antigen-specific cells were tested on antigen-specific T cell-lines. Three differently labeled MHC multimers were tested for A2/WT1₁₂₆₋₁₃₄ (top row) and A2/Her2/neu₃₆₉₋₃₇₇ (bottom row).

We assumed that the number of T cells specific for a defined tumor antigen would be extremely low under steady state conditions. In order to explore to which extent we could isolate T cells by anti-PE MACS in a sensitive scope, we spiked samples of 2×10^8 PBMCs with 1000 CD8 PE and CD8 PerCP antibody-labeled cells. The spiked PBMCs were labeled with MHC multimers for A2/Her2₃₆₉ PE or *Strep*-Tactin PE. We performed anti-PE MACS-enrichment and analyzed the enriched fraction by FACS. The CD8 PerCP label was used to differentiate the spiked cells from endogenous T cells. Three samples were analyzed and 242,160 and 162 cells of the 1000 initial cells were detected after enrichment (Fig. 8.18). From the number of recovered T cells an efficiency of approximately 19% was calculated. These observations indicate that we could detect approximately one fifth of all antigen-specific T cells with our strategy.

After functional testing and optimization of the respective reagents, we performed the complete enrichment procedure as described in Fig.8.14. Fig. 8.19 depicts the signal of the BV421-labeled from the secondary MHC multimer staining, by means of which we quantified antigen-specific T cells at different stages of the purification route. We processed PBMC samples from one HLA-A2 positive and one negative donor. To measure false positives among the extracted cells, we labeled 2×10^8 PBMCs with *Strep*-Tactin PE backbone in a concentration equal to the MHC multimer sample. Before magnetic enrichment the fraction of PE positive cells was similar in the MHC multimer-sample and the control sample. After the

MACS enrichment step the MHC multimer samples showed a higher percentage of PE-positive T cells compared to the *Strep*-Tactin sample.

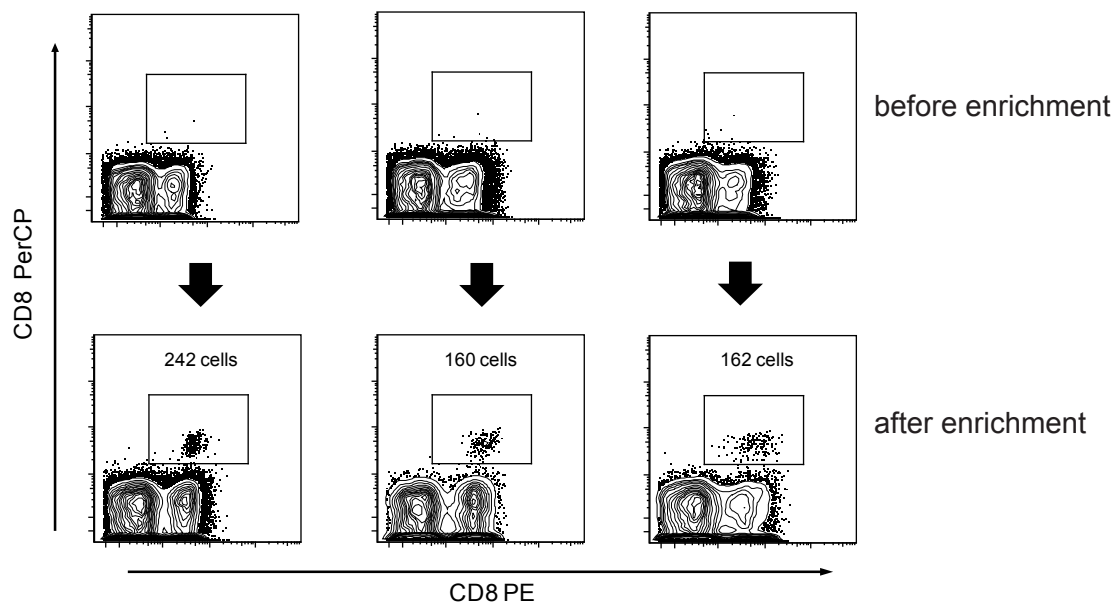


Figure 8.18: Sensitivity of MACS enrichment.

To estimate the sensitivity of MHC multimer MACS enrichment, PBMCs from the donor were isolated and labeled with CD8-specific PE and PerCP-labeled antibodies and were MACS enriched with anti-PE beads. Cells were counted and 1000 cells were transferred to a sample of 2×10^8 PBMCs from the same donor. Enrichment as outlined in Figure 8.14 was performed, and the number of recovered cells of transferred cells was determined by FACS.

Nevertheless, a substantial number of false-positive cells were still detectable, as demonstrated by the backbone sample. B cells are a frequent cause of false-positive labeling in flow cytometry. To assess whether the PE-positive cells in the backbone sample were B cells, we labeled the B cell marker CD19 with a specific antibody. After exclusion of CD19⁺ B cells from the analysis, the fraction of false-positive cells in the *Strep*-Tactin-PE sample was further decreased. Similarly, in the specific samples the fraction of positive cells was reduced, which indicates that numerous false-positive cells were rejected by B cell exclusion. Finally, after inclusion of only PE-positive cells corresponding to the primary MHC multimer label, the percentage of false-positive cells in the *Strep*-Tactin-PE sample was decreased to 0%. In contrast, the fraction of positive cells in the specific samples showed more than 80% or 60% of positive cells.

To further demonstrate that the enriched T cells were antigen-specific, we FACS-sorted single cell samples and performed single cell PCR. From the HLA-A2-negative donor we were able to obtain ten samples that were successfully sorted for PCR. Of these we succeeded to sequence one full length TCR pairing (Fig. 8.19.b).

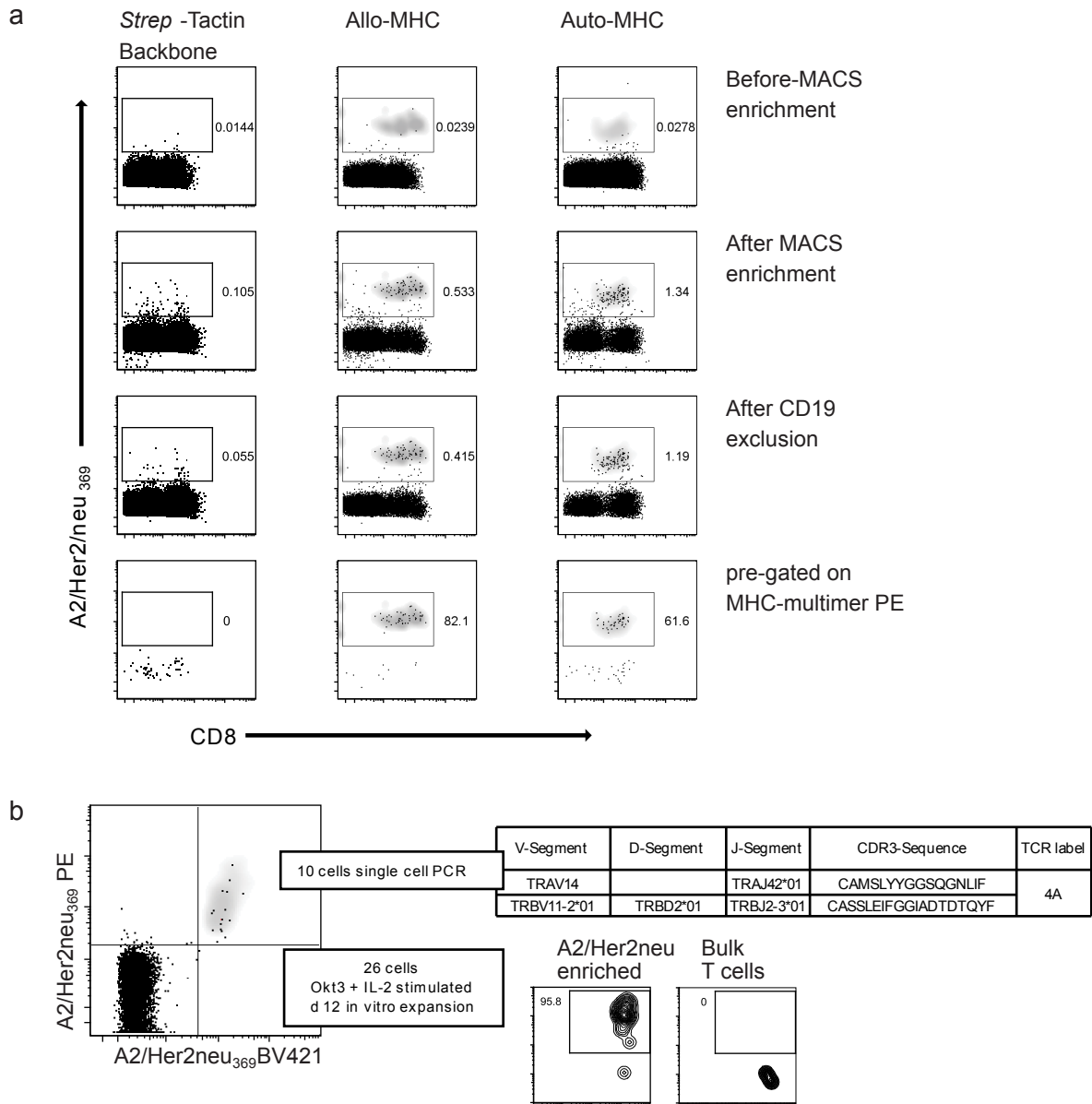


Figure 8.19: Isolation of rare antigen-specific T cells from MHC-matched and MHC-mismatched repertoires"

(a) MHC multimer-based enrichment of rare T cells specific for Her2/neu₃₆₉₋₃₇₇ was performed as described in Figure 8.13. Samples from and HLA-A2⁺ and an HLA-A2⁻ donor were processed side by side. A control sample was primary-labeled with PE-labeled *Strep*-Tactin backbone. The purities of antigen-specific T cells at different points of enrichment and FACS gating are demonstrated as indicated. (b) Sorting gate for specific T cells is shown. 10 single cell samples were sorted for single cell PCR and 26 cells were sorted for *in vitro* expansion. Table shows rearrangement of a Her2₃₆₉-specific TCR from a single cells sample. Bottom row FACS plots show *in vitro* cultured Okt3/IL-2 stimulated cells at day 12 after sorting.

We sorted the remaining 26 cells into a 96 well cell culture plate and stimulated them with Otk3 antibody and IL2 in the presence of γ -irradiated feeder cells. 12 days after stimulation the cells had just sufficiently proliferated for FACS staining. We stained the cells with MHC multimer Her2/neu₃₆₉ and CD8 antibody. More than 95% of all living cells were positive for the MHC multimer, whereas the control group, consisting of non- antigen-specific T cells, remained completely negative (Fig. 8.19.b).

Fig. 8.20.a outlines the FACS gating used for identification of the positive cell fraction. First, forward (FS) and side-scatter (SS) signals were used to exclude dead cells and to reduce the fraction of non-lymphocytes. To exclude residual dead cells, propidium iodide (PI) staining was used. Together with dead cells we discriminated CD19⁺ B-cells with an antibody coupled to the fluorophore PE-A610, which emits a signal of similar wavelength as PI, as a “dump-channel”. Next CD3 negative cells were discriminated. Among CD3⁺ cells we did not separate CD8 negative and positive cells. We assumed that especially in the HLA-A2-negative PBMCs CD4⁺ cells might become MHC multimer positive. This would indicate a TCR with an affinity high enough, to bind the pMHC complex without CD8 co-receptor help, and for this reason would be of special interest. Finally, we used the two MHC multimer signals from PE and BV421 to reach the highest possible purity.

Separate exclusion of B cells has turned out to be crucial to detect rare cell populations, as a large number of B cells bind PE. Although this effect is less pronounced for other fluorophores, still a considerable portion of B cells become multiple false positive, which finally leads to a misinterpretation of results. Especially the magnetic enrichment that is exclusively dependent on PE caused a drastic enrichment of B cells. Fig. 8.20.b describes this effect in more detail. In the sample, stained with *Strep*-Tactin PE, magnetic bead enrichment increased the fraction of PE positive B cells from 0.136% to 5.3% and in the MHC multimer stained sample from 0.778% to 17.3% of all living lymphocytes.

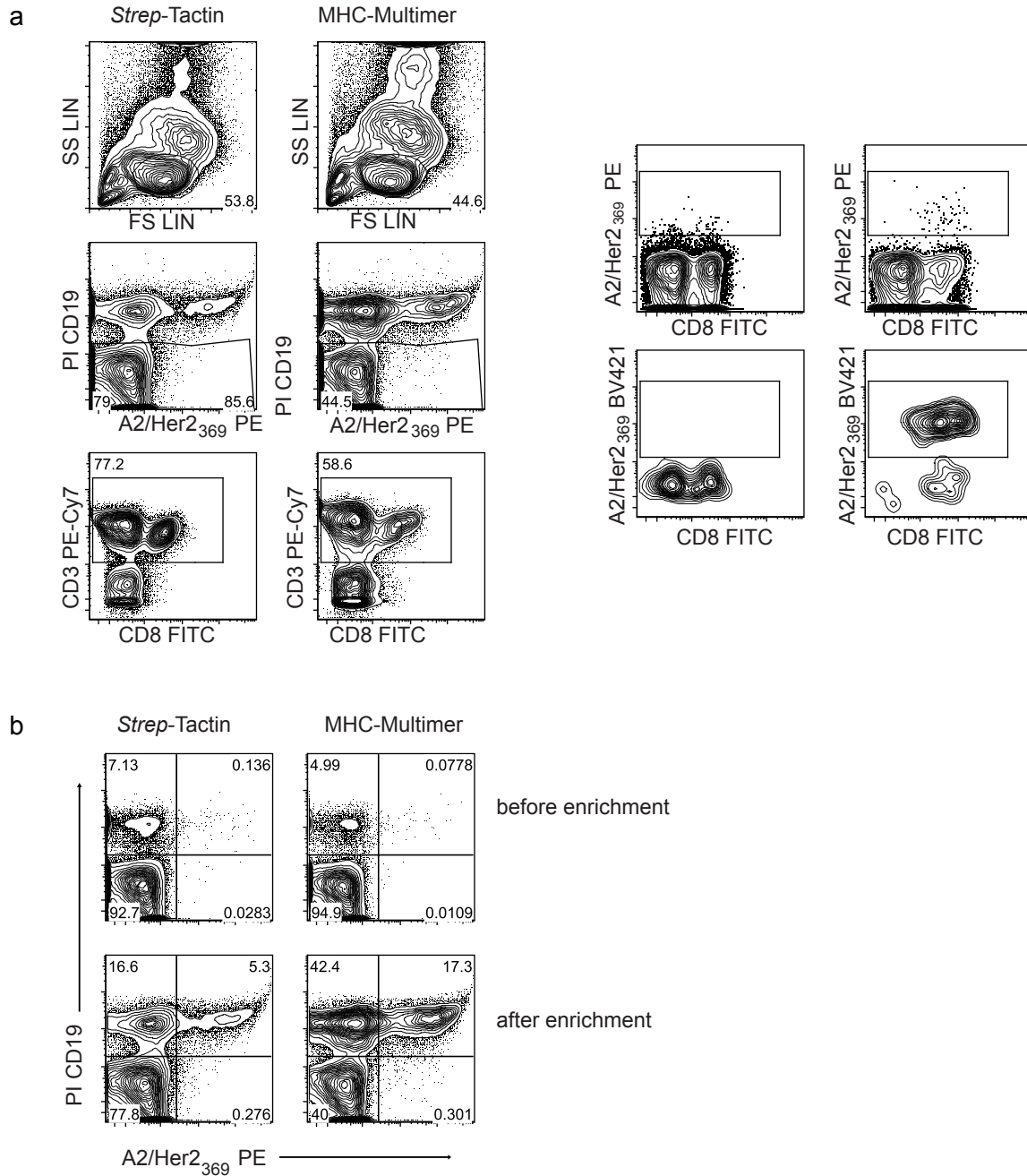


Figure 8.20: FACS isolation of rare antigen-specific T cells.

(a) Gating strategy for enrichment of antigen-specific T cells in (Fig. 8.19 (b)). FACS sorted cells were gated for lymphocytes, dump channel (PI and CD19) negative, CD3 positive, MHC multimer PE positive and MHC multimer BV421 positive. Left column shows data from MHC-independent and right column from MHC multimer enrichment. (b) A2/Her2/neu₃₆₉₋₃₇₇ and CD19 positive T cells are shown before and after MACS enrichments step as described in Fig. 8.14.a. Left column shows data from MHC-independent and right column from MHC multimer enrichment.

We assumed that the multimer-positive cells would exhibit a naïve phenotype. To confirm this conjecture, we performed a separate experiment using an alternative marker panel,

which included antibodies to CD45RA and CCR7 for FACS. These markers are broadly accepted for differentiation of T cells into naïve, effector and memory T cells (Sallusto *et al.* 1999). CD45 can be expressed in different variants produced by alternative splicing. Before activation naïve T cells express the CD45RA variant, whereas upon antigen encounter and activation the CD45RA variant disappears and the CD45RO variant is expressed. CCR7 is involved in transmigration of T cell to lymph nodes, which is a property of naïve and memory, but not effector T cells.

We purified T cells specific for A2/Her2/neu₃₆₉ as described before and stained with antibodies to CD45RA and CCR7 in addition to the previous marker panel. 87.9% of all extracted cells were double positive for CD45RA and CCR7 and therefore showed the naïve phenotype. Only 3% demonstrated an effector phenotype, defined by absence of CD45RA and CCR7. Another 3% were CD45RA-negative and CCR7-positive, which identifies the memory compartment (Fig. 8.21).

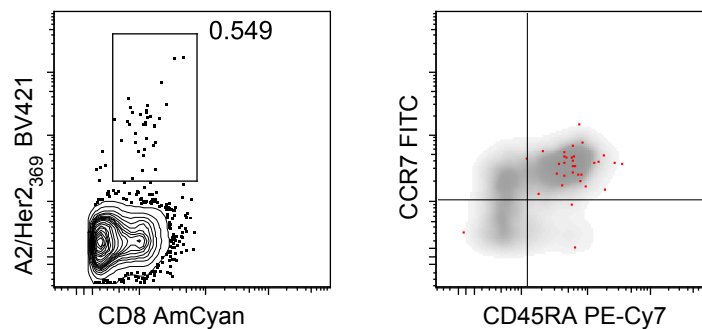


Figure 8.21: Differentiation state of isolated T cells"

In a separate experiment enrichment for A2/Her2₃₆₉-specific T cells was performed with an antibody panel for T cell-differentiation. MHC multimer-positive cells (left plot) were analyzed for expression of CCR7 and CD45RA (right plot)

MHC-mismatch constellations have repeatedly been suggested as a source of TCRs with increased antigen avidity. The idea that negative selection against a defined pMHC combination cannot take place, if the respective HLA-molecule is absent, led to this approach. We reasoned that the MFI of the MHC multimer staining during the purification procedure could serve as a predictor of TCR avidity for pMHC. In addition, we asked whether binding of an HLA-matched MHC multimer with an irrelevant peptide would identify TCRs which rather bind MHC than the peptide component. In order to test these hypotheses, we included an additional labeling step with an irrelevant MHC multimer (A2/WT1 APC) to our purified cell fractions from one HLA-A2-positive and one -negative donor. After MACS

enrichment and gating for true positive cells, we plotted the A2/Her2 MHC multimer signal against the irrelevant MHC multimer. T cells from the A2⁻ donor revealed an increased tendency to bind the irrelevant MHC multimer, as compared to T cells from the A2⁺ donor (Fig. 8.22.a). Similarly, the MFIs for the A2/Her2 multimers on the average were higher for cells from the HLA mismatched than from the matched donor (Fig. 8.22.b).

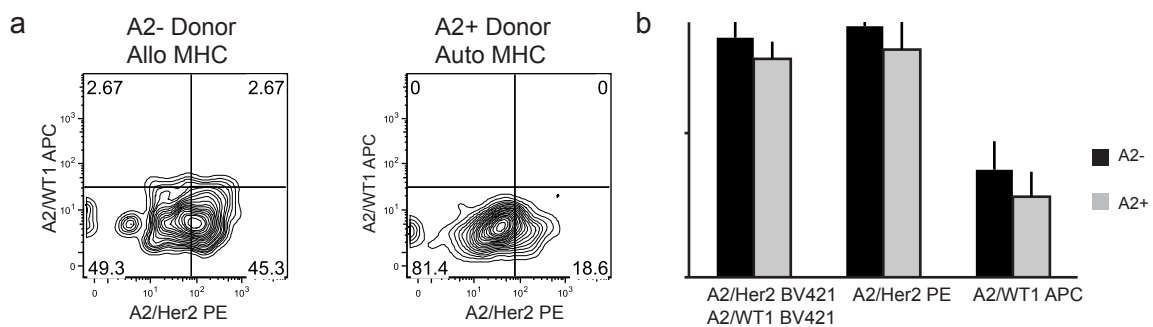
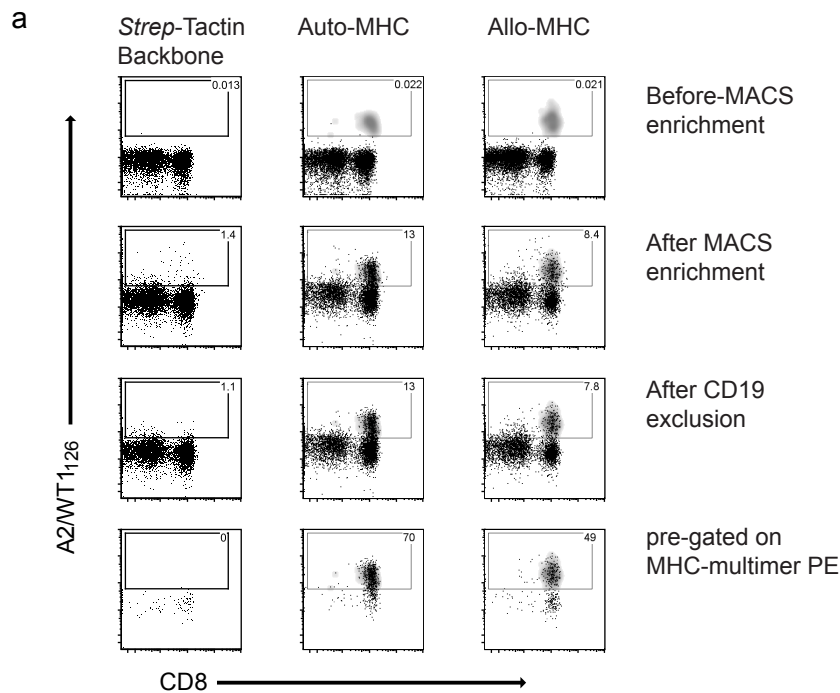


Figure 8.22: Comparison of specificity and binding strength of auto and allo-repertoire.

A2/Her2₃₆₉-specific T cells were purified from an HLA-A2-negative and a -positive donor. In addition to dual labeling with A2/Her2 MHC multimer we additionally performed staining with an irrelevant MHC multimer. (a) Specific multimer PE was plotted against irrelevant MHC multimer A2/WT1 APC. (b) MFIs for all MHC multimer stainings were extracted and compared between A2 negative and positive donor.

These results clearly demonstrate that purification of antigen-specific cells from the naïve repertoire of healthy donors is a feasible method to obtain TCRs targeting tumor-associated antigens. To find out if this strategy works for other antigens as well, we repeated the experiment by an MHC multimer-specific for the leukemia-associated antigen WT1. As already shown for Her2/neu, we performed MHC multimer staining with 2×10^8 PBMCs from one healthy HLA-A2 positive and one negative donor. To control for non-specific enrichment, we similarly stained additional 2×10^8 PBMCs with PE-coupled *Strep*-Tactin backbone. Figure 8.23.a illustrates the stepwise increase of the A2/WT1 BV421-labeled cell fraction.



b

Sample Name	V-Segment	D-Segment	J-Segment	CDR3
allo alpha 18	TRAV14/DV4*01		TRAJ34*01	CAMREVLVNTDKLIF
allo beta 18	TRBV2*01	TRBD1*01	TRBJ1*01	CASSDLDSGVNTEAFF
allo alpha 40	TRAV29/DV5*01		TRAJ50*01	CAASLYDKVIF
allo beta 40	TRBV12-4*01	TRBD2*01	TRBJ2*01	CATAQGLSSYEQYF
allo alpha 46	TRAV38-2/DV8*01		TRAJ41*01	CAYWDSGYALNF
allo beta 46	TRBV30*01	TRBD1*01	TRBJ2*01	CACPGPLTYEQYF
<hr/>				
auto alpha 15	TRAV12-2*02		TRAJ45*01	CAVNDQGGGADGLTF
auto beta 15	TRBV6-2*01	TRBD1*01	TRBJ2-2*01	CASSWWDTGELFF
auto alpha 36	TRAV8-4*03		TRAJ20*01	CAVSEGGDYKLSF
auto beta 36	TRBV28*01	TRBD2*01	TRBJ2-7*01	CAWGTLATEQYF
auto alpha43	TRAV12-2*02		TRAJ45*01	CAVNDQGGGADGLTF
auto beta 43	TRBV6-2*01	TRBD1*01	TRBJ2-2*01	CASSWWDTGELFF
auto alpha46	TRAV12-2*02		TRAJ45*01	CAVNDQGGGADGLTF
auto beta 46	TRBV6-2*01	TRBD1*01	TRBJ2-2*01	CASSWWDTGELFF

Figure 8.23: Isolation of rare antigen-specific T cells from MHC-matched and MHC-mismatched repertoires"

(a) MHC multimer-based enrichment of rare T cells specific for A2/WT₁₂₆₋₁₃₄ was performed as described in Figure 8.14. Samples from an HLA-A2⁺ and an HLA-A2⁻ donor were processed side by side. A control sample was primary-labeled with PE-labeled *Strep*-Tactin backbone. The successive enrichment of antigen-specific T cells at different points of the purification is shown as indicated. (b) Amino acid sequence of the CDR3 domain and V-, D- and J- segment types are listed. Matching pairs are highlighted by white or grey background color. Upper part of the table shows allo-MHC restricted samples and bottom part shows auto-MHC restricted samples.

The cell number extracted with A2/WT1 multimers was considerably larger than for Her2/neu. We detected 495 cells from the HLA-A2⁺ and 150 cells from the HLA-A2⁻ donor. From both groups one PCR slide with 36 single cell samples was used for TCR amplification. From the allo MHC-restricted cells we could isolate 3 different completely functional TCRs. In addition, one sample only showed a non-productive α -chain and from one TCR we could only isolate a truncated β -chain, although according to the band size a longer product should have been sequenced. We assume that a mixture of a truncated and a full length PCR-product was insufficiently separated for sanger sequencing. From the auto-MHC restricted samples we only obtained two different TCR sequences. To our surprise we identified one TCR in several pairings. Actually we identified the β -chain from this TCR in four different samples. In three of these we sequenced the corresponding, presumably functional α -chain. Moreover, we identified an additional non-productive α -chain with these chains. In two samples we sequenced all three chains, two more samples yielded the functional β -chain and the non-productive α -chain and one sample delivered only the non-productive α -chain. In all but one sample we detected chains with the same rearrangement. This indicates that the cells we have isolated from the auto-MHC setting were oligoclonal. Together with the outstandingly large number of purified cells this suggests that this population consisted of expanded clones.

We had included antibodies for CCR7 and CD45RA in the FACS panel, in order to analyze the differentiation state of the isolated T cells. Fig. 8.24 shows the MHC multimer staining and the signals for CCR7 and CD45RA. More than 96% and 94%, respectively, of all MHC multimer-positive cells were double positive for CCR7 and CD45RA. This indicates an antigen naïve state of these T cells. In theory this is expected, but as the auto-MHC-specific samples demonstrated a strongly restricted TCR repertoire it seem likely that they have proliferated. It is generally accepted that under steady state conditions clonal expansion is driven by antigen encounter, which in turn drives the dividing cells to change the surface markers of the naïve phenotype. Therefore the finding of a restricted TCR repertoire and an naïve phenotype contradict each other and need further exploration.

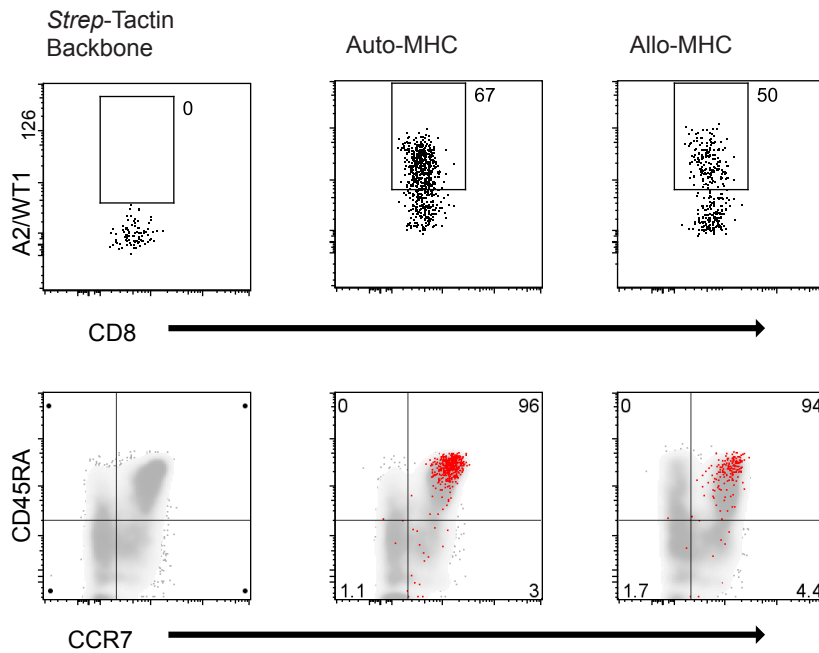


Figure 8.24: Differentiation state of isolated T cells.

PBMCs from an HLA-A2-positive (Auto-MHC) and -negative donor (Allo-MHC) were labeled with PE-labeled A2/WT1₁₂₆₋₁₃₄ multimers or *Strep-Tactin* backbone. Cells were pre-gated for lymphocytes, CD19 negative, living, CD3 positive and A2/WT1 PE positive. FACS plots depict A2/WT1 BV421 and CD8 staining (upper row). Lower row shows the corresponding CCR7 and CD45RA staining. Red dots indicate MHC multimer-positive cells. Grey shades indicate all CD3⁺ cells.

As previously shown for Her2/neu-specific T cells, we compared the mean fluorescence intensities of the MHC multimer staining between the allo- and auto-MHC-specific cell enrichment. As shown in Fig. 8.25a, the MFI values for the MHC multimer PE and BV421 staining was higher in the allo-MHC-specific T cells than in the auto-MHC restricted samples. This confirms our observations from the Her2/neu-specific cell purification. In order to rule out the possibility that the unequal staining intensities are a secondary effect of a generally higher TCR expression level in one of the donors, which could cause more intense labeling, we compared MFI values for CD3 and CD8. None of the two markers were as clearly distinct as the MHC multimer signals, which contradicts the assumption of a secondary effect of variable TCR expression (Fig. 8.25.a).

Assuming the variability in MHC multimer staining intensity is based on differences in CD3 or CD8 expression, MFIs should be positively correlated. To test this hypothesis we plotted the MFIs of the MHC multimer labels against the MFIs of the corresponding CD8 or CD3 staining. We tested for linear regression and could not detect any positive correlation (Fig. 8.25.b).

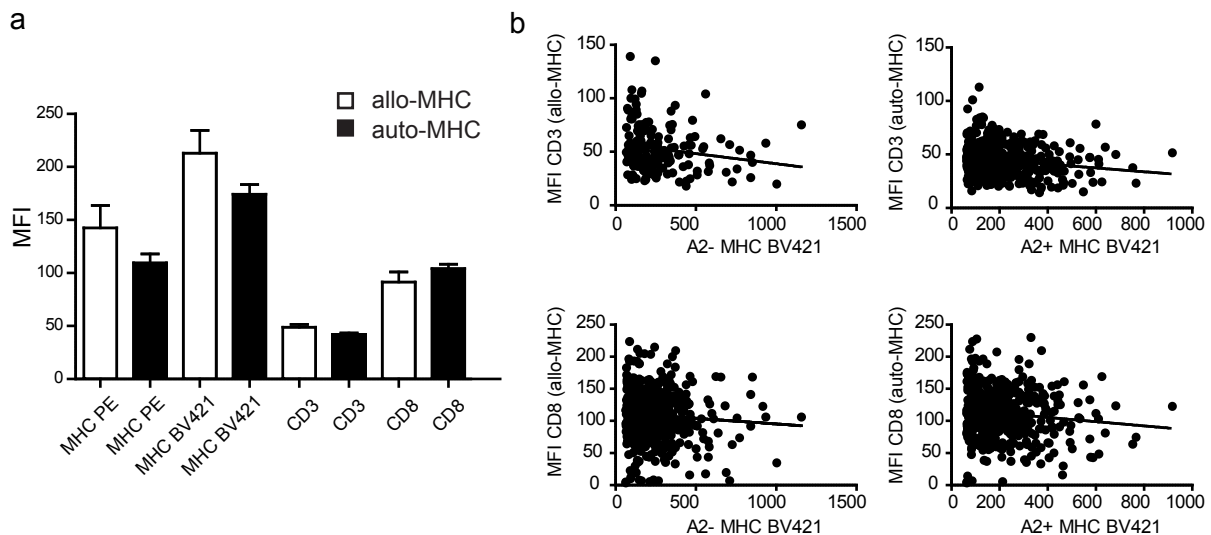


Figure 8.25: Evaluation of MFI as an indicator of avidity.

Mean fluorescence intensities of MHC multimer staining differ between allo- and auto-MHC-restricted samples independent of CD3 and CD8 expression. (a) MFI values with standard deviation for MHC multimer A2/WT1₁₂₆₋₁₃₄ PE and BV421 stainings as well as CD3 and CD8. (b) Correlation between MFIs of MHC multimer PE or BV421 staining from allo- or auto-MHC-restricted samples.

To confirm that the sequences we obtained from the naïve T cell compartment enriched by MHC multimer labeling were specific for their cognate antigen we cloned several TCRs into the retroviral expression vector MP71. To improve the surface expression of the transgenic TCR we substituted the constant regions with the respective codon-optimized murine sequences. Each, α - and β -chain contained an amino acid substitution against cystein at previously described positions to form a second intermolecular disulfide-bond (Cohen *et al.* 2006; van Loenen *et al.* 2011). By retroviral transfer we expressed WT1-specific TCRs in human PBMCs. We chose two TCRs from the allo-MHC and two from the auto-MHC restricted samples. In order to verify their antigen specificity we performed MHC multimer staining. Three of the TCRs conferred MHC multimer binding as shown in Figure 8.26. Interestingly all TCRs demonstrated a variable capability to bind MHC multimer without co-expression of CD8 co-receptor, which indicates a relatively high structural avidity.

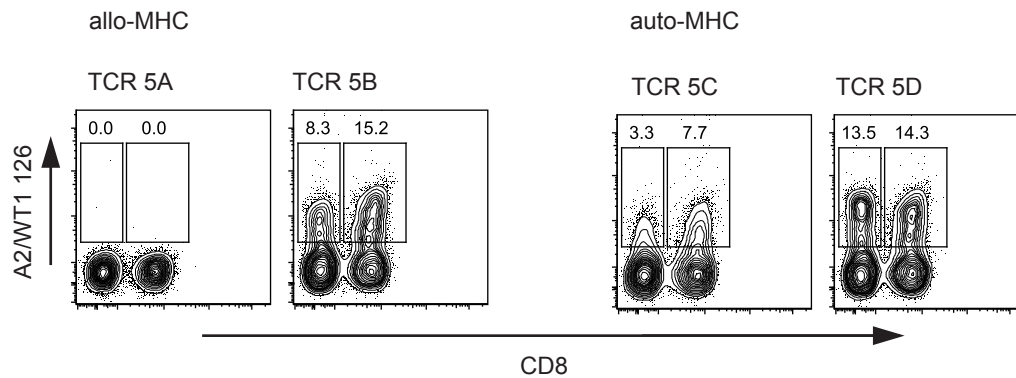


Figure 8.26: Transgenic expression of WT1-specific TCRs.

Four TCR sequences described in Figure 8.23b were expressed in human PBMCs by retroviral gene transfer. FACS-plots show MHC multimer plotted against CD8 staining.

8.5. FUNCTIONAL CHARACTERIZATION OF A TUMOR ANTIGEN-SPECIFIC TCR

We have already shown that the T cells we purified from the naïve repertoire retained their antigen-specificity during *in vitro* expansion. Furthermore, we wanted to verify the antigen-specificity of TCR4A, which we had sequenced after single cell PCR from an A2/Her2₃₆₉-specific T cell (Fig. 8.19.b). For this purpose, we fused α - and β -chain PCR-products to codon optimized, murine constant regions with corresponding insertions of cystein residues, which form an additional intermolecular disulfide bridge. These modifications have previously shown to improve surface expression when competing with an endogenous TCR (Cohen *et al.* 2006; van Loenen *et al.* 2011). We prepared retroviral particles to transduce Jurkat76 T cells. Upon transduction, 18% of all living cells specifically bound Her2/neu₃₆₉multimer (Fig. 8.27.a). As this TCR is of principal therapeutic interest because of the target-specificity, we determined whether the antigen binding was sufficient to initiate T cell effector functions. As Jurkat76 cells do not secrete cytokines or lyse target cells in response to TCR stimulation, we retrovirally transduced human PBMCs. After transduction 13.4% of living lymphocytes became positive for the specific MHC multimer, but not for an irrelevant MHC multimer, which confirms the TCR4A's antigen-specificity as well as the capability for surface-expression despite competition with endogenous TCRs. This was expected but not self-explanatory because TCR4A was directly isolated from the naïve repertoire, without any antigen-contact driven pre-selection. Similarly, we intended to confirm that this TCR can be functional and capable of inducing antigen-specific cell lysis by a chromium release assay. Chromium⁵¹-labeled T2 cells were pulsed either with specific peptide, irrelevant peptide or no peptide and

were co-incubated with the TCR4A -transduced T cells, as shown in Fig. 8.27.b. Lysis was above the background levels was only observed when TCR4A -transduced T cells and specific peptide was used (Fig. 8.27.c). As a second read-out, IFN γ -secretion upon stimulation with peptide-loaded T2 cells was measured. The amount of peptide was titrated from 10^{-5} to 10^{-9} M demonstrating IFN γ -secretion down to a peptide concentration of 10^{-8} M. This indicates that TCR4A can mediate cytotoxic as well as inflammatory function. The most important question however was whether tumor cells with a physiological expression of the Her2 oncogene and immune escape mechanisms can be lysed by TCR4A-transduced T cells. For this reason an HLA-A2-negative and HLA-transgenic version of the Her2/neu expressing tumor cell line SKOV3 were used. Tumor cells were co-incubated with transduced PBMCs and IFN γ -secretion was detected by ELISA. Fig. 8.27.e clearly demonstrates that TCR4A can induce cytokine secretion in an antigen-, as well as HLA-A2-specific manner.

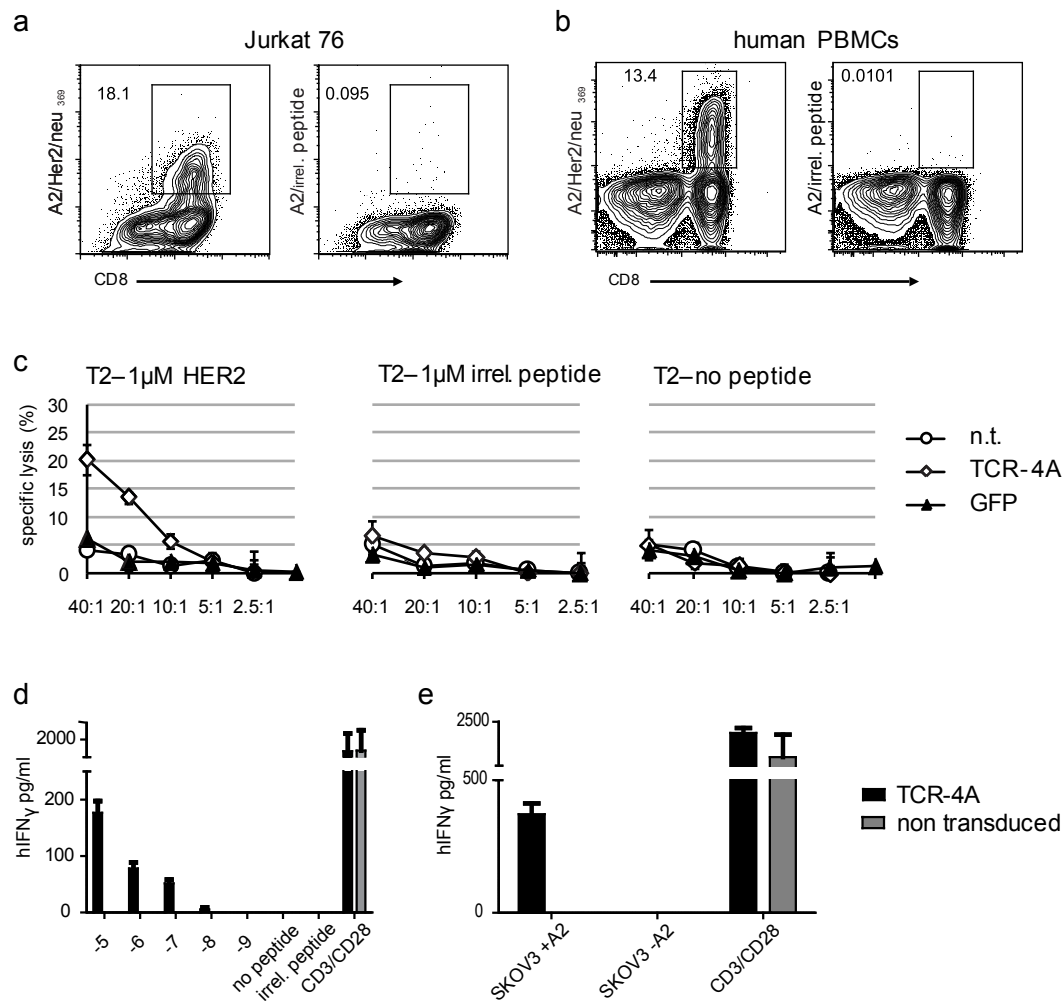


Figure 8.27: Functional characterization of a single cell-derived TCR.

(a) Sequence from TCR 4A was expressed in Jurkat76 T cells by retroviral gene transfer. Left FACS plot shows A2/Her2/neu₃₆₉₋₃₇₇ staining and right FACS plot shows staining with an irrelevant MHC multimer. (b) Sequence from TCR 4A was expressed in human PBMCs by retroviral gene transfer. Left FACS plot shows A2/Her2/neu₃₆₉₋₃₇₇ staining and right FACS plot shows staining with an irrelevant MHC multimer. (c) For functional testing 2×10^3 peptide-loaded T2 cells ($1 \mu\text{M}$) labeled with ^{51}Cr were incubated for 4h with TCR-4A-modified PBLs at different effector/target ratios (E/T ratios). After 4h free chrome [51] was quantified in the supernatant. TCR-specificity was controlled by co-incubation with GFP-transduced and non-transduced (n.t.) PBMCs. All conditions were tested in duplicates. (d) For detection of peptide-specific release, 1×10^5 T2-cells were pulsed with an equal number of Her2/neu peptide titrated from 10^{-5} – 10^{-9}M concentration. Equal numbers of transduced (black bar) and non-transduced (grey bar) T cells were co-incubated for 4 hours and IFN γ -concentration in the supernatant was measured by ELISA. As positive control T cells were stimulated with CD3/CD28 and as control for peptide-specificity T2-cells were pulsed with $1 \mu\text{M}$ of an irrelevant peptide. IFN γ -concentration in the supernatant was measured by ELISA (e) For detection of tumor-specific activity 10^5 tumor cells and equal numbers of transduced (black bar) and non-transduced (grey bar) human PBMCs were co-incubated for 4 hours and IFN γ -concentration in the supernatant was measured by ELISA. As positive control T cells were stimulated with CD3/CD28. All conditions were tested in triplicates.

9. DISCUSSION

With this work we provide a novel tool for quick and efficient TCR isolation. We describe the establishment and validation of a highly sensitive RACE-PCR to obtain the sequences of TCR α - and β -chains on the single cell level. Reverse transcription priming and removal of residual primers have turned out to be of great importance for the efficiency of this protocol. We progressively set up stricter rules to prevent cross contamination, which occurred between samples, and even between experiments. Our method has the advantage over multiplex PCR protocols to deliver the complete V-segment sequence. Hence, we could directly transfer the TCR without the need of reconstruction of the variable part, preserving all polymorphisms of the original sequence. Furthermore, as retroviral transfer of our TCR sequences to other T cells permitted subsequent MHC multimer labeling, we proved their antigen-specificity. To our knowledge, we are the first to conclusively demonstrate the isolation of antigen specific and functional TCRs from single T cells by gene transfer experiments.

We validated our method with a small population of hCMV-specific T cells, which we isolated using conventional MHC multimer labeling and demonstrated that we can access extremely small cell populations with this strategy. Numerous reports have shown that during *in vitro* as well as *in vivo* expansion the TCR repertoire is shaped towards defined characteristics, which involves a reduction of TCR composition (Dietrich *et al.* 1997; Nishimura *et al.* 1998; McKee *et al.* 2000). This might prevent access to the therapeutically most effective TCR sequences. Similarly, it has recently been reported that chronic infection can lead to dominant expansion of low-avidity T cell-populations, which may be less effective for immunotherapy (Khan *et al.* 2010). As chronic antigen stimulation by tumor tissue creates a similar situation for tumor-infiltrating lymphocytes, *in vivo* TCR repertoire changes probably restrict successful identification of highly effective TCR sequences for immunotherapy. Although a progressive TCR avidity decrease among TILs has not conclusively been proven, large screenings for high-avidity TCRs were often unsuccessful, leading to screening of xeno- or allo- MHC-repertoires. Naïve T cell-repertoires that have not been shaped by antigen exposition at all should contain a maximum of diversity.

It is generally accepted that priming of naïve cells initially leads to preferential expansion of TCRs with high avidity (McHeyzer-Williams *et al.* 1995; Busch *et al.* 1999). However, until now no detailed information about the alteration of the TCR composition from the naïve T cell-pool to the antigen-experienced status has been generated. With our strategy we can analyze these initial steps of antigen-priming. We propose to thoroughly isolate antigen-

specific T cells from the naïve repertoire and to analyze the paired TCR α/β -chains with the intention to gain a complete overview of the potential TCR pool for a given antigen. With this knowledge, we will be able to describe the changes of clonal composition during the progress of an immune response through expansion and contraction to long-term memory in settings of chronic antigen stimulation, or after pathogen clearance. We predict that antigen clearance after acute infection will result in memory T cells with increased TCR avidities, whereas chronic antigen stimulation will functionally exhaust the pool of high-avidity T cells and progressively recruit and expand low avidity T cells (Buchholz *et al.* 2011).

9.1. CHOICE OF TCR SOURCE

As we have already discussed, we assume that the structural avidities of TCRs differ between T cell-subtypes. As high avidity is of special interest for adoptive T cell-therapy different T cells sources have been evaluated to identify therapeutically effective TCRs.

9.1.1. ALLO-MHC-RESTRICTION

Earlier reports recommended the employment of allo-MHC restriction to isolate TCRs with high structural avidity. This describes the isolation of T cells specific for a peptide MHC complex that is not present in the donor and thus is not affected by negative selection in the thymus (Obst *et al.* 1998; Munz *et al.* 1999; Moris *et al.* 2001). Using our novel strategy, we detected both, auto- and allo-MHC-restricted auto-antigen-specific T cells in naïve repertoires of healthy donors, and isolated TCRs from both sources.

Whether or not the allo-MHC repertoire is the optimal source of TCRs for adoptive immunotherapy is still a matter of debate, since the circumvention of negative selection permits MHC-dominant binding, making cross-reactivities with other T cell epitopes a potential threat. In several clinical trials, HLA-A2 restricted TCRs have been applied to patients who were solely matched in one HLA-type. Unlike in allogeneic stem cell transplantation, obvious signs of graft versus host disease have not been observed so far. Signs of autoimmunity were mostly discussed as “off site”-effects that result from antigen expression in other tissue than the tumor (Morgan *et al.* 2006; Parkhurst *et al.* 2011; Robbins *et al.* 2011). Even xeno-derived TCRs restricted to human HLA-A2 (Johnson *et al.* 2009)

and TCRs modified by amino acid substitution to confer raised avidity (Robbins *et al.* 2008; Parkhurst *et al.* 2009; Chinnasamy *et al.* 2011; Wang *et al.* 2011) have been applied clinically without causing off-target effects. So far no clinical data on safety and efficacy of T cells redirected with an allo-MHC-restricted TCR have been published. However, one clinical trial is currently ongoing (NCT01621724).

9.1.2. AUTOLOGOUS ANTIGEN-SPECIFIC T CELLS

The prevalence of T cells for defined non-self epitopes in naïve mice has been quantified in earlier reports (Moon *et al.* 2007; Obar *et al.* 2008). The repertoire analyses in this report provide further insights, as, not only auto-antigen-specific T cells are quantified, but also naïve, human repertoires are addressed. Furthermore, we provide the first insight into the clonal composition of naïve T cells. Although the common paradigm suggests a low TCR avidity for those cells, this question remains unresolved. With the approach presented here, we can conclusively elucidate this subject in future studies.

It was recently demonstrated that T cells with low avidity TCRs can escape negative selection and enter the periphery without any functional restrictions (Enouz *et al.* 2012). Our own data confirm the persistence of auto-antigen-specific T cells with naïve phenotype in peripheral blood. Furthermore, the comparison of MFIs from auto-MHC and allo-MHC-restricted T cells provides a first indication that in the auto-MHC-restricted setting, T cells show a lower average avidity than in the allo-MHC setting. Surprisingly, we observed a large range of values that was similar between auto- and allo-MHC-restricted T cells (Fig. 8.22 and 8.25). Although MFI might not be the most accurate measure of avidity, this finding suggests that the auto-repertoire can display a broad range in TCR binding strength. In contrast to xeno-derived, sequence-modified and allo-MHC-restricted T cells, these autologous T cells have gone through normal thymic selection and therefore offer a safe and readily available source of antigen-specific T cells. Even stronger evidence for the prevalence of T cells with high avidity within the auto-repertoire is the discovery of CD8 independent binding of the WT1 restricted TCRs TCR 5C and TCR5D. We still have to determine the exact binding avidity of these TCRs by more sensitive methods. However, if this finding can be decisively confirmed and would turn out to be representative for the autologous repertoire it would challenge the paradigm of central tolerance and would raise many questions and options for future research.

Based on these observations, we propose to build up a bank of auto-MHC-restricted TCRs from HLA-typed donors, to offer completely HLA-matched TCRs for adoptive therapy. This strategy mimics the setting of autologous TILs, which to date has shown superior therapeutic efficacy and safety (Rosenberg *et al.* 2011).

9.1.3. AUTO-REACTIVE REGULATORY T CELLS

As an alternative source of T cell-receptors with high avidity we propose the regulatory T cell-compartment. It is generally accepted that high avidity T cell-receptor signaling during thymogenesis can trigger T cells to pursue regulatory differentiation (Jenkins *et al.* 2010). Despite the fact that the majority of natural regulatory T cells (nTregs) are CD4⁺, a small number are triggered to become CD8⁺ in a MHC-I-dependent manner and are detectable in lymphoid tissue (Fontenot *et al.* 2005). Induced regulatory T cells (iTregs) have been identified as an important mechanism of peripheral tolerance, not redundant with natural, thymus-derived nTregs (Haribhai *et al.* 2011).

Clear evidence about an antigen-specific activity was promoted by the finding that TCRs isolated from mucosa-associated iTregs were antigen-specific for commensal bacteria (Lathrop *et al.* 2011). Although most reports about iTregs focus on CD4⁺ T cells, there is accumulating evidence about the importance of CD8⁺ iTregs. In a murine model of GvHD approximately 70% of all iTregs were CD8⁺FoxP3⁺ and could induce tolerance (Sawamukai *et al.* 2012).

Like CD4⁺iTregs, CD8⁺iTregs revealed antigen-dependent functionality, and thus could prevent allograft rejection upon adoptive transfer (Guillonneau *et al.* 2007). To this point no commonly accepted phenotypic marker molecule for CD8⁺ iTregs has been identified. However, absence of CD45RC expression was suggested as a marker for CD8⁺ iTregs in rats (Xystrakis *et al.* 2004). Similarly, a CD8⁺ CD122⁺ T cell-population displayed suppressive function in a murine colitis model (Endharti *et al.* 2011).

Furthermore, intracellular markers have been proposed to distinguish iTregs. Besides FoxP3 expression it has become evident that the transcription factor Hopx is necessary for the functional stability of iTregs (Hawiger *et al.* 2010). Equally, the transcription factor Helios was suggested to differentiate iTregs from thymus-derived nTregs (Thornton *et al.* 2010). Additionally extensive expression profiling led to the identification of the transcription factor DKK3 as an important functional element of iTregs. Even antibody blockade was possible, which led to recovery of T cell effector functionality, which underlines the importance of this molecule (Papatriantafyllou *et al.* 2012).

9.2. CHOICE OF TARGET ANTIGEN

As a result of this research, TCRs specific for two well-characterized tumor-associated antigens have been isolated from the antigen-naïve repertoire and have been transgenically expressed. For adoptive cell therapy of established tumors, several criteria influence the choice of antigen.

Immunogenicity of the T cell-epitope is one key variable for the efficiency of TCR-redirection T cells. On the one hand it is a prerequisite for recognition, however high immunogenicity bears the risk of inducing GvHD if an antigen is also expressed in other tissue. Overexpression in tumor cells was definitely shown for several antigens. However, the complete absence of expression in any other tissue can hardly be proven. Thus, several trials have shown off site effects caused by antigen recognition in other tissues. Hearing loss, uveitis, and vitiligo were frequently observed in adoptive T cell-transfers targeting melanocyte differentiation antigens (Johnson *et al.* 2009). Severe colitis was observed when a TCR specific for carcinoembryonic antigen (CEA) was used for therapy against colon carcinoma. Because of this problem the trial was stopped after the third patient. It is unclear whether off site or off target effects were the cause (Parkhurst *et al.* 2011). To date, no treatment-associated patient deaths were reported for trials with TCR-redirection T cells.

Apart from TCRs, Chimeric antigen receptors (CARs) have been used to redirect T cell-specificity. CARs consist of an antibody-derived Fab-domain fused to TCR signaling domains and, like TCRs, were tested in clinical trials. In contrast to TCRs, therapy with CAR-redirection T cells has caused patient death. One out of five CLL patients treated with CAR-redirection T cells that targeted CD19 died by treatment-associated side effects. This reaction probably originated from immune hyperstimulation, rather than an antigen-specific effect (Brentjens *et al.* 2010). However, CAR-rearranged T cells targeting ERBB2, an antigen frequently overexpressed in colon carcinoma, mediated an immune response in the lung that resulted in a patient death. The CAR was derived from the antibody Herceptin, which was previously clinically tested without off site effects (Morgan *et al.* 2010). These unforeseen incidents clearly demonstrate the dangers associated with high target immunogenicity.

One of the TCRs described in this work targets the same antigen as Herceptin, which in this report is called Her/neu, but is also known as ERBB2. Although T cells redirected with a CAR for this antigen caused a severe adverse event it is unclear whether T cell-redirection with a TCR instead of a CAR would cause similar problems.

9.3. ROLE OF TCR AVIDITY

Apart from MHC-restriction, one general difference between antibody and TCR binding is the target binding strength. Most published K_D -values for naturally occurring TCRs range between $1\mu\text{M}$ and $100\mu\text{M}$, whereas antibodies rather display K_D -values in the nanomolar range (Price *et al.* 1998; van der Merwe *et al.* 2003; Miles *et al.* 2010). A K_D -value of 19.2nM was reported for Herceptin, which is still approximately a factor of 20 lower than the highest affine TCR in a clinical trial (Fig 5.2) (Monfregola *et al.* 2009). However, increased avidity has been found to be highly correlated with improved TCR functionality in an “*in vivo*” model of autoimmunity (Gronski *et al.* 2004). Data from several clinical trials as summarized in Fig. 5.2 also support this theory.

Using mutated TCRs, the correlation between avidity and functionality has even been found with non-physiologically high TCR avidities in “*in vitro*” experiments (Holler *et al.* 2003). Conversely, a strong decline in ligand-specificity has been observed in TCRs with hyperphysiologic avidities (Zhao *et al.* 2007). In contrast to these findings, it was recently shown that even an extremely low affinity with a K_D value of more than $250\mu\text{M}$ can efficiently activate T cells (Bulek *et al.* 2012). This raises several questions about immunogenicity and affinity. On the one hand, the increase of affinity might compensate for low immunogenicity. On the other hand, it is unclear how high TCR avidity influences T cell-function and differentiation. Thus, it cannot be excluded that excessively high avidity results in tolerance induction. Apart from binding strength, other variables, like conformational changes induced by different binding modes might also account for diversity in TCR efficiency. To conclusively answer these questions, the characterization of a large number of TCRs specific for the same epitope but unequal in other aspects could be helpful. Unlike antigen-expanded T cell-populations, the naïve repertoire might hold sufficient diversity to address these subjects.

9.4. TCR ANALYSIS OF ANTIGEN-SPECIFIC REPERTOIRES

Technical progress in the field of sequencing has opened the possibility to analyze TCR repertoires in high resolution. Several strategies for deep sequencing of TCR-repertoires have been reported. Roche 454 sequencing of TCR β -chains was used to characterize the composition of HCMV- and EBV-specific MHC-Tetramer-positive T cell-populations (Klarenbeek *et al.* 2012), SIV-specific T cell-populations (Bimber *et al.* 2009; Burwitz *et al.* 2011), and to analyze the overlap between naïve, memory, and effector populations (Wang *et al.* 2010; Venturi *et al.* 2011). Illumina sequencing, at the time limited to read lengths of 36bp or 50bp, was applied to sequence the complete TCR β -chain repertoire from pooled mRNA of 550 different donors. To obtain complete sequence information, cDNA was first concatemerized and then sheared to produce a library of short overlapping fragments (Freeman *et al.* 2009). In a similar way, direct sequencing of the CDR3 region was evaluated. A consensus motif within the J-segment was used as a primer binding site, which enabled to sequence the complete CDR3 region, with a read length of only 54bp (Robins *et al.* 2009). With advanced read lengths of 100-150bp, Illumina sequencing could be directly used to sequence the CDR3-region of TCR β -chains by priming in the constant region (Warren *et al.* 2011). Repertoire analysis has also been evaluated using the Ion Torrent sequencing platform (Bolotin *et al.* 2012). So far, no next-generation sequencing strategy for paired TCR α - and β -chains has been reported. We suggest adding the same, unique DNA-barcode to each single cell-derived α - and respective β -chain. This would allow us to combine and sequence all samples in parallel as a library. Not only could matched chains thereby be assigned to each other after sequencing, but also could the sequences be related to their respective single cell PCR sample and conclusively to the respective data point during FACS isolation. With this approach we will be able to perform high throughput analyses of antigen-specific TCRs within naïve repertoires. Large amounts of sequence information for TCRs of same antigen-specificity could help to further elucidate common rules of binding properties, which might assist TCR binding prediction with *in silico* structure simulation approaches (Leimgruber *et al.* 2011).

To achieve this, we are currently modifying our protocol to realize higher throughput. We are restricted to a maximum of 48 samples per experiment, which is the number of positions on our PCR glass slide. After subtraction of positive and negative controls, only 36 samples remain in our standard experimental setup. In order to increase our throughput, we are transferring our protocol to 384 well PCR plates and in a further step to 1536 well plates.

For this purpose we need to refine our FACS sorting technology, as exact positioning to the bottom of the tube is required. This is a critical factor, as our protocol depends on sequential up-scaling of reaction volumes, with an initial starting volume of only 500nl. The planar geometry of the 48 sample glass slides made this possible.

For 384 different barcodes we are evaluating two different strategies. The easier but very costly approach would be to label our PCR products during the last round of amplification with 384 different primers containing the respective barcode. For this purpose separate primers for α - and β -chain would be necessary, which adds up to 768 primers.

Alternatively, we propose to generate a barcode library within a plasmid, containing a highly efficient cloning site for the TCR chains. In a ligation step, we plan to position our PCR products upstream of the barcode site and to use flanking primer binding sites to amplify those products. This would yield a library that can directly be transferred to next-generation sequencing.

The easiest approach certainly would be to obtain a barcoding kit for deep sequencing from a commercial provider. However, to our knowledge such a product is not on the market, until now.

9.5. ALTERNATIVE METHODS TO DETECT ANTIGEN-SPECIFIC TCRs

With our current strategy to isolate cells from antigen-naïve donors we depend on MHC multimers for defined epitopes. In principle, the enrichment process using anti-PE antibody coated magnetic beads for MACS is not saturated, as our enriched fraction only contains 25-500 cells (data not shown). In order to increase the throughput on this level of the process, we are currently exploring, whether combined enrichment, using several different MHC multimer-specificities simultaneously is feasible. In principle it should be possible to perform parallel enrichment with one label, e.g. PE, and to use a combinatorial staining matrix with several secondary labels to differentiate different MHC multimer-specificities. A similar approach has been previously applied to detect a variety of T cell-specificities by combining the respective MHC multimers (Andersen *et al.* 2012).

Many of the most prevalent HLA class-I types have successfully been used to generate MHC multimers. MHC class II multimers are still less common; however, recent reports have demonstrated that isolation of extremely rare antigen-specific cells can be facilitated with

MHC class II multimer reagents (Moon *et al.* 2007). On the one hand our dependence on MHC multimer reagents for T cell-identification might be a disadvantage, as specific reagents need to be available, and one report claims that binding of MHC multimers is not a safe way to guarantee antigen-specificity (Lyons *et al.* 2006). On the other hand a major advantage of MHC multimers is the capability to identify antigen-specific T cells irrespective of cellular functionality. Anyhow, our method does not necessarily rely on a single identification technique. It is possible to use functional readouts like upregulation of CD137 (Wehler *et al.* 2007; Wehler *et al.* 2008) or IFN γ -secretion (Becker *et al.* 2001) as marker for antigen-specific cells upon short-term *in vitro* restimulation.

9.6. EXTENSION OF TCR ISOLATION FOR ACT TO OTHER HLA- RESTRICTIONS

Most TCRs in clinical trials are restricted to HLA*02:01. In Caucasoid populations between 33% (Cuba) and 51% (Spain, Catalonia) of all individuals are positive for HLA*A2:01 but only between 2% (China, Province Han) and 39% (Tibet) in oriental populations (frequencies were calculated from allele frequencies taken from the AFN Database (Gonzalez-Galarza *et al.* 2011)). First efforts are being made to isolate TCRs restricted to other HLA-types. Recently an HLA-A1-restricted TCR for the cancer testis antigen MAGE-A3 has been tested in a clinical trial (NCT01352286).

A further reason to extend the clinically applicable TCR repertoire to other HLA-restrictions is the finding that nonsense mutations in the HLA-A locus is among the most frequent sites of nonsense mutations in non-small lung cancer. This suggests targeting of HLA-B- and C-restricted epitopes in these particular cases (Hammerman *et al.* 2012). Furthermore, members of the HLA-B and C group function as NK-cell killer inhibitory receptors (KIRs), which means that their downregulation can induce NK cell activation (Moretta *et al.* 1996). A large body of knowledge about disease-associated antigens and respective epitopes for numerous HLA-types has accumulated over the last decades. Even for the expert it is challenging to survey the associated literature. Therefore, databases with collections of published information have become indispensable tools for researchers. The immune epitope database (IEDB) includes thousands of epitopes for infectious or autoimmune diseases and

cancers. Additional information on associated HLA-restrictions, original discovery and confirming reports are comfortably accessible (Vita *et al.* 2010). Another database that should be mentioned is the Cancer Genome Atlas (TCGA). Since 2005, different types of cancer tissue samples were systematically analyzed with state-of-the-art genomic methods like whole genome sequencing, exome sequencing, SNP mapping, and methods for detecting epigenetic modifications. The largest part of those data are available to the public (Deus *et al.* 2010). This project gives unprecedented insight into common profiles of antigen expression in different types of cancers and will foster targeted pre-screening for individual patients. Such information can further increase the efficiency of adoptive immunotherapy with TCR transgenic T cells.

10. SUMMARY

Taken together, with this report we describe the first successful isolation of full-length TCR sequences from single T cells with confirmed antigen-specificity. We prove that it is possible to isolate rare antigen-specific T cells from the naïve repertoire by MHC multimer labeling and to directly extract functional, antigen-specific TCRs from single cell samples. Initially, we evaluated a strategy to amplify complete cDNA according to a published method for generation of single cell microarrays as a pre-stage for nested PCR. Although we identified single cell-derived TCR sequences with this method, we had to change the method extensively; for example, as a key element of the previous strategy, 'solid phase coupling' of template turned out to cause an unacceptable grade of cross-contamination by aerosol formation.

To overcome the problems of currently described approaches to reach single cell resolution, we have optimized individual steps of a RACE-PCR protocol. The most important improvements of sensitivity were accomplished by modification of the priming strategy and by optimizing reaction temperatures

We evaluated this method with three CMV-specific T cell-populations. We attained an overall efficiency of 23.7% of full-length PCR products of both TCR chains from 266 single cell samples in seven independent experiments. In two of the CMV-specific T cell-populations that we examined, we observed clonal dominance. As we intended to use this method for the isolation of clinically relevant TCRs, we wanted to confirm the antigen-specificity of the PCR products we obtained. To test this, we completed the fragments for the truncated constant region and cloned the resulting products into a retroviral expression vector. Upon viral transduction with those constructs we could redirect Jurkat cells and human PBMCs to MHC multimer-specificity. One of the TCRs we transduced displayed CD8 co-receptor independent binding, which indicates high TCR avidity. We confirmed this assumption by measuring the dissociation kinetics of MHC-monomers off the TCRs by a novel assay that we have recently developed (Nauerth et al., submitted). In total we confirmed the antigen-specificity of four CMV-specific TCRs by transducing Jurkat T cells and human PBMCs. All Jurkat cells that expressed TCR after transduction could specifically bind their respective MHC multimer.

By these experiments we proved that our method for single cell PCR of the TCR is a valid tool to isolate functional and specific TCRs from *ex vivo* isolated T cells without any *in vitro* cell culture.

To isolate TCRs for tumor-associated antigens we wanted to know if it is possible to enrich antigen-specific T cells from the unbiased repertoire of healthy donors. To achieve this, we used PE-labeled MHC multimers for the tumor-associated antigen Her2/neu to tag antigen-specific T cells in PBMCs of healthy donors. We enriched the PE positive cell fraction by MACS. By dual MHC multimer labeling and exclusion of B cells we attained highly pure MHC multimer-labeled T cells. Using this strategy we were able to reproducibly extract Her2/neu-specific T cells from PBMCs of healthy donors, irrespective of their HLA-type. Hence, we could show that this method is useful to extract auto- and allo-MHC restricted T cells with auto-antigen-specificity.

To prove that MHC multimer-specificity is a reliable marker to isolate rare antigen-specific T cells, we first *in vitro* expanded these cells in bulk cell cultures. After *in vitro* expansion they retained MHC multimer-specificity. In a separate experiment we purified T cells for the same epitope and labeled the isolated cells with antibodies for CCR7 and CD45RA. Thus, we could describe the differentiation state of the purified cells. The vast majority of isolated cells were positive for both markers indicating an 'antigen-naïve' phenotype.

As we could isolate auto- and allo-MHC-restricted T cells from healthy donors, we wanted to know whether allo-MHC-restricted TCRs confer higher antigen avidity than auto-MHC-restricted TCRs. We compared the MFI of MHC multimer labels of side by side purified T cells from HLA-A2 positive donors (i.e. auto-MHC restricted) and HLA-A2 negative donors (i.e. allo-MHC restricted). We discovered that the MFI of all positive cells was higher on allo-MHC restricted T cells than on auto-MHC-restricted T cells. However, the range of fluorescence intensities of single cells was similar in both cases, which could imply that high avidity T cells for auto-antigens are present in the autologous repertoire of healthy donors.

To test whether allo-MHC-restricted T cells are more prone to HLA-dominant binding, we additionally stained with an MHC-matched MHC multimer with irrelevant peptide-specificity. In fact allo-MHC-restricted T cell displayed a higher MFI for this MHC multimer than auto-MHC restricted T cells.

We successfully repeated the purification experiments for a second tumor-associated auto-antigen named WT1. Similar to Her2/neu we readily detected antigen-specific T cells in HLA-A2-positive and -negative donors. Again, allo-MHC-labeled T cells showed a higher MFI than the auto-MHC-labeled T cells. There was no detectable correlation with the MFIs for CD3 or CD8 labels, thus we assume that the divergence between the MHC multimer labels was not an indirect effect of variable TCR surface expression or co-receptor expression. Both types of extracted T cells displayed a naïve phenotype. By single cell PCR we identified three different full length TCRs among the allo-MHC-specific T cells and two among the auto-MHC-restricted T cells. Surprisingly, we detected the same TCR sequences several times in auto-MHC-restricted T cells, which indicates that these cells are clonally restricted and might have undergone clonal expansion for unknown reasons.

We transferred one Her2/neu-specific TCR to Jurkat T cells and human PBMCs, and could confirm antigen-specificity by MHC multimer staining. As a further proof of functionality, we stimulated transduced PBMCs with peptide loaded T2 cells. We proved that Her2/neu TCR-modified T cells secreted IFN γ and could lyse target cells in an antigen-specific manner.

In summary, with this work we report a novel tool to obtain antigen-specific TCRs for clinical application from a previously inaccessible source, i.e. the naïve repertoire. We assume that this method is applicable for most T cell-epitopes and could be useful to make TCR-redirected, adoptive T cell-therapy broadly accessible.

11. BIBLIOGRAPHY

- Ahn, K., A. Gruhler, et al. (1997). "The ER-luminal domain of the HCMV glycoprotein US6 inhibits peptide translocation by TAP." Immunity **6**(5): 613-621.
- Altman, J. D., P. A. Moss, et al. (1996). "Phenotypic analysis of antigen-specific T lymphocytes." Science **274**(5284): 94-96.
- Andersen, R. S., P. Kvistborg, et al. (2012). "Parallel detection of antigen-specific T cell responses by combinatorial encoding of MHC multimers." Nat Protoc **7**(5): 891-902.
- Babbe, H., A. Roers, et al. (2000). "Clonal expansions of CD8(+) T cells dominate the T cell infiltrate in active multiple sclerosis lesions as shown by micromanipulation and single cell polymerase chain reaction." J Exp Med **192**(3): 393-404.
- Baitsch, L., P. Baumgaertner, et al. (2011). "Exhaustion of tumor-specific CD8(+) T cells in metastases from melanoma patients." J Clin Invest **121**(6): 2350-2360.
- Barker, J. N., E. Doubrovina, et al. (2010). "Successful treatment of EBV-associated posttransplantation lymphoma after cord blood transplantation using third-party EBV-specific cytotoxic T lymphocytes." Blood **116**(23): 5045-5049.
- Becker, C., H. Pohla, et al. (2001). "Adoptive tumor therapy with T lymphocytes enriched through an IFN-gamma capture assay." Nat Med **7**(10): 1159-1162.
- Berger, C., M. C. Jensen, et al. (2008). "Adoptive transfer of effector CD8+ T cells derived from central memory cells establishes persistent T cell memory in primates." J Clin Invest **118**(1): 294-305.
- Bertling, W. M., F. Beier, et al. (1993). "Determination of 5' ends of specific mRNAs by DNA ligase-dependent amplification." PCR Methods Appl **3**(2): 95-99.
- Besser, M. J., R. Shapira-Frommer, et al. (2010). "Clinical responses in a phase II study using adoptive transfer of short-term cultured tumor infiltration lymphocytes in metastatic melanoma patients." Clin Cancer Res **16**(9): 2646-2655.
- Bimber, B. N., B. J. Burwitz, et al. (2009). "Ultradeep pyrosequencing detects complex patterns of CD8+ T-lymphocyte escape in simian immunodeficiency virus-infected macaques." J Virol **83**(16): 8247-8253.
- Blackburn, S. D., H. Shin, et al. (2009). "Coregulation of CD8+ T cell exhaustion by multiple inhibitory receptors during chronic viral infection." Nat Immunol **10**(1): 29-37.
- Boeckh, M., W. Leisenring, et al. (2003). "Late cytomegalovirus disease and mortality in recipients of allogeneic hematopoietic stem cell transplants: importance of viral load and T-cell immunity." Blood **101**(2): 407-414.

- Bollard, C. M., S. Gottschalk, et al. (2007). "Complete responses of relapsed lymphoma following genetic modification of tumor-antigen presenting cells and T-lymphocyte transfer." Blood **110**(8): 2838-2845.
- Bolotin, D. A., I. Z. Mamedov, et al. (2012). "Next generation sequencing for TCR repertoire profiling: Platform-specific features and correction algorithms." Eur J Immunol **42**(11): 3073-3083.
- Borbulevych, O. Y., S. M. Santhanagopalan, et al. (2011). "TCRs used in cancer gene therapy cross-react with MART-1/Melan-A tumor antigens via distinct mechanisms." J Immunol **187**(5): 2453-2463.
- Bornhauser, M., C. Thiede, et al. (2011). "Prophylactic transfer of BCR-ABL-, PR1-, and WT1-reactive donor T cells after T cell-depleted allogeneic hematopoietic cell transplantation in patients with chronic myeloid leukemia." Blood **117**(26): 7174-7184.
- Boulter, J. M., M. Glick, et al. (2003). "Stable, soluble T-cell receptor molecules for crystallization and therapeutics." Protein Eng **16**(9): 707-711.
- Brahmer, J. R., S. S. Tykodi, et al. (2012). "Safety and activity of anti-PD-L1 antibody in patients with advanced cancer." N Engl J Med **366**(26): 2455-2465.
- Brentjens, R., R. Yeh, et al. (2010). "Treatment of chronic lymphocytic leukemia with genetically targeted autologous T cells: case report of an unforeseen adverse event in a phase I clinical trial." Mol Ther **18**(4): 666-668.
- Brunstein, C. G., D. J. Weisdorf, et al. (2006). "Marked increased risk of Epstein-Barr virus-related complications with the addition of antithymocyte globulin to a nonmyeloablative conditioning prior to unrelated umbilical cord blood transplantation." Blood **108**(8): 2874-2880.
- Buchholz, V. R., M. Neuenhahn, et al. (2011). "CD8+ T cell differentiation in the aging immune system: until the last clone standing." Curr Opin Immunol **23**(4): 549-554.
- Bulek, A. M., D. K. Cole, et al. (2012). "Structural basis for the killing of human beta cells by CD8(+) T cells in type 1 diabetes." Nat Immunol **13**(3): 283-289.
- Burgert, H. G. and S. Kvist (1985). "An adenovirus type 2 glycoprotein blocks cell surface expression of human histocompatibility class I antigens." Cell **41**(3): 987-997.
- Burwitz, B. J., Z. Ende, et al. (2011). "Simian immunodeficiency virus SIVmac239Deltanef vaccination elicits different Tat28-35SL8-specific CD8+ T-cell clonotypes compared to a DNA prime/adenovirus type 5 boost regimen in rhesus macaques." J Virol **85**(7): 3683-3689.
- Busch, D. H. and E. G. Pamer (1999). "T cell affinity maturation by selective expansion during infection." J Exp Med **189**(4): 701-710.
- Busch, D. H., I. M. Pilip, et al. (1998). "Coordinate regulation of complex T cell populations responding to bacterial infection." Immunity **8**(3): 353-362.

- Butler, M. O., P. Friedlander, et al. (2011). "Establishment of antitumor memory in humans using in vitro-educated CD8+ T cells." Sci Transl Med **3**(80): 80ra34.
- Butler, N. S., J. Moebius, et al. (2012). "Therapeutic blockade of PD-L1 and LAG-3 rapidly clears established blood-stage Plasmodium infection." Nat Immunol **13**(2): 188-195.
- Chapuis, A. G., J. A. Thompson, et al. (2012). "Transferred melanoma-specific CD8+ T cells persist, mediate tumor regression, and acquire central memory phenotype." Proc Natl Acad Sci U S A **109**(12): 4592-4597.
- Chen, H. L., D. Gabilovich, et al. (1996). "A functionally defective allele of TAP1 results in loss of MHC class I antigen presentation in a human lung cancer." Nat Genet **13**(2): 210-213.
- Chen, J. L., P. R. Dunbar, et al. (2000). "Identification of NY-ESO-1 peptide analogues capable of improved stimulation of tumor-reactive CTL." J Immunol **165**(2): 948-955.
- Chinnasamy, N., J. A. Wargo, et al. (2011). "A TCR targeting the HLA-A*0201-restricted epitope of MAGE-A3 recognizes multiple epitopes of the MAGE-A antigen superfamily in several types of cancer." J Immunol **186**(2): 685-696.
- Cobbold, M., N. Khan, et al. (2005). "Adoptive transfer of cytomegalovirus-specific CTL to stem cell transplant patients after selection by HLA-peptide tetramers." J Exp Med **202**(3): 379-386.
- Cohen, C. J., Y. Zhao, et al. (2006). "Enhanced antitumor activity of murine-human hybrid T-cell receptor (TCR) in human lymphocytes is associated with improved pairing and TCR/CD3 stability." Cancer Res **66**(17): 8878-8886.
- Cohen, C. J., Z. Zheng, et al. (2005). "Recognition of fresh human tumor by human peripheral blood lymphocytes transduced with a bicistronic retroviral vector encoding a murine anti-p53 TCR." J Immunol **175**(9): 5799-5808.
- Cole, D. J., D. P. Weil, et al. (1994). "Identification of MART-1-specific T-cell receptors: T cells utilizing distinct T-cell receptor variable and joining regions recognize the same tumor epitope." Cancer Res **54**(20): 5265-5268.
- Cole, T. S. and A. J. Cant (2010). "Clinical experience in T cell deficient patients." Allergy Asthma Clin Immunol **6**(1): 9.
- Collins, K. L., B. K. Chen, et al. (1998). "HIV-1 Nef protein protects infected primary cells against killing by cytotoxic T lymphocytes." Nature **391**(6665): 397-401.
- Dash, P., J. L. McClaren, et al. (2011). "Paired analysis of TCRalpha and TCRbeta chains at the single-cell level in mice." J Clin Invest **121**(1): 288-295.
- Davis, J. L., M. R. Theoret, et al. (2010). "Development of human anti-murine T-cell receptor antibodies in both responding and nonresponding patients enrolled in TCR gene therapy trials." Clin Cancer Res **16**(23): 5852-5861.

- Davis, M. M. and P. J. Bjorkman (1988). "T-cell antigen receptor genes and T-cell recognition." Nature **334**(6181): 395-402.
- Day, C. L., D. E. Kaufmann, et al. (2006). "PD-1 expression on HIV-specific T cells is associated with T-cell exhaustion and disease progression." Nature **443**(7109): 350-354.
- Deacon, N. J., A. Tsykin, et al. (1995). "Genomic structure of an attenuated quasi species of HIV-1 from a blood transfusion donor and recipients." Science **270**(5238): 988-991.
- Dembic, Z., W. Haas, et al. (1986). "Transfer of specificity by murine alpha and beta T-cell receptor genes." Nature **320**(6059): 232-238.
- Demirer, T., L. Barkholt, et al. (2008). "Transplantation of allogeneic hematopoietic stem cells: an emerging treatment modality for solid tumors." Nat Clin Pract Oncol **5**(5): 256-267.
- Deus, H. F., D. F. Veiga, et al. (2010). "Exposing the cancer genome atlas as a SPARQL endpoint." J Biomed Inform **43**(6): 998-1008.
- Dietrich, P. Y., P. R. Walker, et al. (1997). "TCR analysis reveals significant repertoire selection during in vitro lymphocyte culture." Int Immunol **9**(8): 1073-1083.
- Dillman, R. O., R. K. Oldham, et al. (1991). "Continuous interleukin-2 and tumor-infiltrating lymphocytes as treatment of advanced melanoma. A national biotherapy study group trial." Cancer **68**(1): 1-8.
- Dong, H., S. E. Strome, et al. (2002). "Tumor-associated B7-H1 promotes T-cell apoptosis: a potential mechanism of immune evasion." Nat Med **8**(8): 793-800.
- Dudley, M. E., C. A. Gross, et al. (2010). "CD8+ enriched "young" tumor infiltrating lymphocytes can mediate regression of metastatic melanoma." Clin Cancer Res **16**(24): 6122-6131.
- Dudley, M. E., J. R. Wunderlich, et al. (2002). "Cancer regression and autoimmunity in patients after clonal repopulation with antitumor lymphocytes." Science **298**(5594): 850-854.
- Dudley, M. E., J. R. Wunderlich, et al. (2005). "Adoptive cell transfer therapy following non-myeloablative but lymphodepleting chemotherapy for the treatment of patients with refractory metastatic melanoma." J Clin Oncol **23**(10): 2346-2357.
- Dudley, M. E., J. C. Yang, et al. (2008). "Adoptive cell therapy for patients with metastatic melanoma: evaluation of intensive myeloablative chemoradiation preparative regimens." J Clin Oncol **26**(32): 5233-5239.
- Dunn, S. M., P. J. Rizkallah, et al. (2006). "Directed evolution of human T cell receptor CDR2 residues by phage display dramatically enhances affinity for cognate peptide-MHC without increasing apparent cross-reactivity." Protein Sci **15**(4): 710-721.

- Einsele, H., E. Roosnek, et al. (2002). "Infusion of cytomegalovirus (CMV)-specific T cells for the treatment of CMV infection not responding to antiviral chemotherapy." Blood **99**(11): 3916-3922.
- Ellebaek, E., T. Z. Iversen, et al. (2012). "Adoptive cell therapy with autologous tumor infiltrating lymphocytes and low-dose Interleukin-2 in metastatic melanoma patients." J Transl Med **10**(1): 169.
- Endharti, A. T., Y. Okuno, et al. (2011). "CD8+CD122+ regulatory T cells (Tregs) and CD4+ Tregs cooperatively prevent and cure CD4+ cell-induced colitis." J Immunol **186**(1): 41-52.
- Engels, B., H. Cam, et al. (2003). "Retroviral vectors for high-level transgene expression in T lymphocytes." Hum Gene Ther **14**(12): 1155-1168.
- Enouz, S., L. Carrie, et al. (2012). "Autoreactive T cells bypass negative selection and respond to self-antigen stimulation during infection." J Exp Med **209**(10): 1769-1779.
- Erickson, A. L., Y. Kimura, et al. (2001). "The outcome of hepatitis C virus infection is predicted by escape mutations in epitopes targeted by cytotoxic T lymphocytes." Immunity **15**(6): 883-895.
- Feuchtinger, T., S. Matthes-Martin, et al. (2006). "Safe adoptive transfer of virus-specific T-cell immunity for the treatment of systemic adenovirus infection after allogeneic stem cell transplantation." Br J Haematol **134**(1): 64-76.
- Feuchtinger, T., K. Opherk, et al. (2010). "Adoptive transfer of pp65-specific T cells for the treatment of chemorefractory cytomegalovirus disease or reactivation after haploidentical and matched unrelated stem cell transplantation." Blood **116**(20): 4360-4367.
- Figlin, R. A., J. A. Thompson, et al. (1999). "Multicenter, randomized, phase III trial of CD8(+) tumor-infiltrating lymphocytes in combination with recombinant interleukin-2 in metastatic renal cell carcinoma." J Clin Oncol **17**(8): 2521-2529.
- Fontenot, J. D., J. P. Rasmussen, et al. (2005). "Regulatory T cell lineage specification by the forkhead transcription factor foxp3." Immunity **22**(3): 329-341.
- Freeman, G. J., A. J. Long, et al. (2000). "Engagement of the PD-1 immunoinhibitory receptor by a novel B7 family member leads to negative regulation of lymphocyte activation." J Exp Med **192**(7): 1027-1034.
- Freeman, J. D., R. L. Warren, et al. (2009). "Profiling the T-cell receptor beta-chain repertoire by massively parallel sequencing." Genome Res **19**(10): 1817-1824.
- Fujita, K., H. Ikarashi, et al. (1995). "Prolonged disease-free period in patients with advanced epithelial ovarian cancer after adoptive transfer of tumor-infiltrating lymphocytes." Clin Cancer Res **1**(5): 501-507.
- Gao, L., I. Bellantuono, et al. (2000). "Selective elimination of leukemic CD34(+) progenitor cells by cytotoxic T lymphocytes specific for WT1." Blood **95**(7): 2198-2203.

- Gardini, A., G. Ercolani, et al. (2004). "Adjuvant, adoptive immunotherapy with tumor infiltrating lymphocytes plus interleukin-2 after radical hepatic resection for colorectal liver metastases: 5-year analysis." J Surg Oncol **87**(1): 46-52.
- Gattinoni, L., E. Lugli, et al. (2011). "A human memory T cell subset with stem cell-like properties." Nat Med **17**(10): 1290-1297.
- Goedegebuure, P. S., L. M. Douville, et al. (1995). "Adoptive immunotherapy with tumor-infiltrating lymphocytes and interleukin-2 in patients with metastatic malignant melanoma and renal cell carcinoma: a pilot study." J Clin Oncol **13**(8): 1939-1949.
- Gonzalez-Galarza, F. F., S. Christmas, et al. (2011). "Allele frequency net: a database and online repository for immune gene frequencies in worldwide populations." Nucleic Acids Res **39**(Database issue): D913-919.
- Gras, S., Z. Chen, et al. (2010). "Allelic polymorphism in the T cell receptor and its impact on immune responses." J Exp Med **207**(7): 1555-1567.
- Gronski, M. A., J. M. Boulter, et al. (2004). "TCR affinity and negative regulation limit autoimmunity." Nat Med **10**(11): 1234-1239.
- Guillonneau, C., M. Hill, et al. (2007). "CD40Ig treatment results in allograft acceptance mediated by CD8CD45RC T cells, IFN-gamma, and indoleamine 2,3-dioxygenase." J Clin Invest **117**(4): 1096-1106.
- Hammerman, P. S., D. N. Hayes, et al. (2012). "Comprehensive genomic characterization of squamous cell lung cancers." Nature **489**(7417): 519-525.
- Hanahan, D. and R. A. Weinberg (2011). "Hallmarks of cancer: the next generation." Cell **144**(5): 646-674.
- Haribhai, D., J. B. Williams, et al. (2011). "A requisite role for induced regulatory T cells in tolerance based on expanding antigen receptor diversity." Immunity **35**(1): 109-122.
- Hartmann, C. H. and C. A. Klein (2006). "Gene expression profiling of single cells on large-scale oligonucleotide arrays." Nucleic Acids Res **34**(21): e143.
- Hawiger, D., Y. Y. Wan, et al. (2010). "The transcription cofactor Hopx is required for regulatory T cell function in dendritic cell-mediated peripheral T cell unresponsiveness." Nat Immunol **11**(10): 962-968.
- Heslop, H. E., C. Y. Ng, et al. (1996). "Long-term restoration of immunity against Epstein-Barr virus infection by adoptive transfer of gene-modified virus-specific T lymphocytes." Nat Med **2**(5): 551-555.
- Hislop, A. D., M. E. Rensing, et al. (2007). "A CD8+ T cell immune evasion protein specific to Epstein-Barr virus and its close relatives in Old World primates." J Exp Med **204**(8): 1863-1873.

- Hodi, F. S., M. C. Mihm, et al. (2003). "Biologic activity of cytotoxic T lymphocyte-associated antigen 4 antibody blockade in previously vaccinated metastatic melanoma and ovarian carcinoma patients." Proc Natl Acad Sci U S A **100**(8): 4712-4717.
- Hodi, F. S., S. J. O'Day, et al. (2010). "Improved survival with ipilimumab in patients with metastatic melanoma." N Engl J Med **363**(8): 711-723.
- Holler, P. D. and D. M. Kranz (2003). "Quantitative analysis of the contribution of TCR/pepMHC affinity and CD8 to T cell activation." Immunity **18**(2): 255-264.
- Hunder, N. N., H. Wallen, et al. (2008). "Treatment of metastatic melanoma with autologous CD4+ T cells against NY-ESO-1." N Engl J Med **358**(25): 2698-2703.
- Jenkins, M. K., H. H. Chu, et al. (2010). "On the composition of the preimmune repertoire of T cells specific for Peptide-major histocompatibility complex ligands." Annu Rev Immunol **28**: 275-294.
- Jia, X., R. Singh, et al. (2012). "Structural basis of evasion of cellular adaptive immunity by HIV-1 Nef." Nat Struct Mol Biol **19**(7): 701-706.
- Jin, H. T., A. C. Anderson, et al. (2010). "Cooperation of Tim-3 and PD-1 in CD8 T-cell exhaustion during chronic viral infection." Proc Natl Acad Sci U S A **107**(33): 14733-14738.
- Johnson, L. A., R. A. Morgan, et al. (2009). "Gene therapy with human and mouse T-cell receptors mediates cancer regression and targets normal tissues expressing cognate antigen." Blood **114**(3): 535-546.
- Jones, T. R., E. J. Wiertz, et al. (1996). "Human cytomegalovirus US3 impairs transport and maturation of major histocompatibility complex class I heavy chains." Proc Natl Acad Sci U S A **93**(21): 11327-11333.
- Junker, A., J. Ivanidze, et al. (2007). "Multiple sclerosis: T-cell receptor expression in distinct brain regions." Brain **130**(Pt 11): 2789-2799.
- Kaech, S. M., E. J. Wherry, et al. (2002). "Effector and memory T-cell differentiation: implications for vaccine development." Nat Rev Immunol **2**(4): 251-262.
- Kessels, H. W., M. C. Wolkers, et al. (2001). "Immunotherapy through TCR gene transfer." Nat Immunol **2**(10): 957-961.
- Khammari, A., N. Labarriere, et al. (2009). "Treatment of metastatic melanoma with autologous Melan-A/MART-1-specific cytotoxic T lymphocyte clones." J Invest Dermatol **129**(12): 2835-2842.
- Khammari, A., J. M. Nguyen, et al. (2007). "Long-term follow-up of patients treated by adoptive transfer of melanoma tumor-infiltrating lymphocytes as adjuvant therapy for stage III melanoma." Cancer Immunol Immunother **56**(11): 1853-1860.
- Khan, N., M. Cobbold, et al. (2010). "Persistent viral infection in humans can drive high frequency low-affinity T-cell expansions." Immunology **131**(4): 537-548.

- Kim, S. M., L. Bhonsle, et al. (2012). "Analysis of the Paired TCR alpha- and beta-chains of Single Human T Cells." PLoS One **7**(5): e37338.
- Kirchhoff, F., T. C. Greenough, et al. (1995). "Brief report: absence of intact nef sequences in a long-term survivor with nonprogressive HIV-1 infection." N Engl J Med **332**(4): 228-232.
- Klarenbeek, P. L., E. B. Remmerswaal, et al. (2012). "Deep Sequencing of Antiviral T-Cell Responses to HCMV and EBV in Humans Reveals a Stable Repertoire That Is Maintained for Many Years." PLoS Pathog **8**(9): e1002889.
- Knabel, M., T. J. Franz, et al. (2002). "Reversible MHC multimer staining for functional isolation of T-cell populations and effective adoptive transfer." Nat Med **8**(6): 631-637.
- Koebel, C. M., W. Vermi, et al. (2007). "Adaptive immunity maintains occult cancer in an equilibrium state." Nature **450**(7171): 903-907.
- Kolb, H. J., J. Mittermuller, et al. (1990). "Donor leukocyte transfusions for treatment of recurrent chronic myelogenous leukemia in marrow transplant patients." Blood **76**(12): 2462-2465.
- Kradin, R. L., J. T. Kurnick, et al. (1989). "Tumour-infiltrating lymphocytes and interleukin-2 in treatment of advanced cancer." Lancet **1**(8638): 577-580.
- Kurimoto, K., Y. Yabuta, et al. (2007). "Global single-cell cDNA amplification to provide a template for representative high-density oligonucleotide microarray analysis." Nat Protoc **2**(3): 739-752.
- Lathrop, S. K., S. M. Bloom, et al. (2011). "Peripheral education of the immune system by colonic commensal microbiota." Nature **478**(7368): 250-254.
- Leen, A. M., A. Christin, et al. (2009). "Cytotoxic T lymphocyte therapy with donor T cells prevents and treats adenovirus and Epstein-Barr virus infections after haploidentical and matched unrelated stem cell transplantation." Blood **114**(19): 4283-4292.
- Leen, A. M., G. D. Myers, et al. (2006). "Monoculture-derived T lymphocytes specific for multiple viruses expand and produce clinically relevant effects in immunocompromised individuals." Nat Med **12**(10): 1160-1166.
- Leimgruber, A., M. Ferber, et al. (2011). "TCRRep 3D: an automated in silico approach to study the structural properties of TCR repertoires." PLoS One **6**(10): e26301.
- Levitskaya, J., A. Sharipo, et al. (1997). "Inhibition of ubiquitin/proteasome-dependent protein degradation by the Gly-Ala repeat domain of the Epstein-Barr virus nuclear antigen 1." Proc Natl Acad Sci U S A **94**(23): 12616-12621.
- Li, L., Y. Muzahim, et al. (2012). "Crystal structure of adenovirus E3-19K bound to HLA-A2 reveals mechanism for immunomodulation." Nat Struct Mol Biol.

- Li, Y., R. Moysey, et al. (2005). "Directed evolution of human T-cell receptors with picomolar affinities by phage display." Nat Biotechnol **23**(3): 349-354.
- Liu, X. and M. A. Gorovsky (1993). "Mapping the 5' and 3' ends of *Tetrahymena thermophila* mRNAs using RNA ligase mediated amplification of cDNA ends (RLM-RACE)." Nucleic Acids Res **21**(21): 4954-4960.
- Loh, E. Y., J. F. Elliott, et al. (1989). "Polymerase chain reaction with single-sided specificity: analysis of T cell receptor delta chain." Science **243**(4888): 217-220.
- Louis, C. U., K. Straathof, et al. (2010). "Adoptive transfer of EBV-specific T cells results in sustained clinical responses in patients with locoregional nasopharyngeal carcinoma." J Immunother **33**(9): 983-990.
- Lucas, K. G., D. Salzman, et al. (2004). "Adoptive immunotherapy with allogeneic Epstein-Barr virus (EBV)-specific cytotoxic T-lymphocytes for recurrent, EBV-positive Hodgkin disease." Cancer **100**(9): 1892-1901.
- Lyons, G. E., J. J. Roszkowski, et al. (2006). "T-cell receptor tetramer binding or the lack there of does not necessitate antigen reactivity in T-cell receptor transduced T cells." Cancer Immunol Immunother **55**(9): 1142-1150.
- Mackensen, A., N. Meidenbauer, et al. (2006). "Phase I study of adoptive T-cell therapy using antigen-specific CD8+ T cells for the treatment of patients with metastatic melanoma." J Clin Oncol **24**(31): 5060-5069.
- Marcen, R., J. Pascual, et al. (2003). "Influence of immunosuppression on the prevalence of cancer after kidney transplantation." Transplant Proc **35**(5): 1714-1716.
- Marmont, A. M., M. M. Horowitz, et al. (1991). "T-cell depletion of HLA-identical transplants in leukemia." Blood **78**(8): 2120-2130.
- Matsushita, H., M. D. Vesely, et al. (2012). "Cancer exome analysis reveals a T-cell-dependent mechanism of cancer immunoediting." Nature **482**(7385): 400-404.
- McHeyzer-Williams, M. G. and M. M. Davis (1995). "Antigen-specific development of primary and memory T cells in vivo." Science **268**(5207): 106-111.
- McKee, M. D., T. M. Clay, et al. (2000). "Quantitation of T-cell receptor frequencies by competitive polymerase chain reaction: dynamics of T-cell clonotype frequencies in an expanding tumor-infiltrating lymphocyte culture." J Immunother **23**(4): 419-429.
- Micklethwaite, K., A. Hansen, et al. (2007). "Ex vivo expansion and prophylactic infusion of CMV-pp65 peptide-specific cytotoxic T-lymphocytes following allogeneic hematopoietic stem cell transplantation." Biol Blood Marrow Transplant **13**(6): 707-714.
- Micklethwaite, K. P., L. Clancy, et al. (2008). "Prophylactic infusion of cytomegalovirus-specific cytotoxic T lymphocytes stimulated with Ad5f35pp65 gene-modified dendritic cells after allogeneic hemopoietic stem cell transplantation." Blood **112**(10): 3974-3981.

- Miles, J. J., A. M. Bulek, et al. (2010). "Genetic and structural basis for selection of a ubiquitous T cell receptor deployed in Epstein-Barr virus infection." PLoS Pathog **6**(11): e1001198.
- Monfregola, L., R. M. Vitale, et al. (2009). "A SPR strategy for high-throughput ligand screenings based on synthetic peptides mimicking a selected subdomain of the target protein: a proof of concept on HER2 receptor." Bioorg Med Chem **17**(19): 7015-7020.
- Moon, J. J., H. H. Chu, et al. (2007). "Naive CD4(+) T cell frequency varies for different epitopes and predicts repertoire diversity and response magnitude." Immunity **27**(2): 203-213.
- Moosmann, A., I. Bigalke, et al. (2010). "Effective and long-term control of EBV PTLD after transfer of peptide-selected T cells." Blood **115**(14): 2960-2970.
- Moretta, A., C. Bottino, et al. (1996). "Receptors for HLA class-I molecules in human natural killer cells." Annu Rev Immunol **14**: 619-648.
- Morgan, R. A., M. E. Dudley, et al. (2006). "Cancer regression in patients after transfer of genetically engineered lymphocytes." Science **314**(5796): 126-129.
- Morgan, R. A., J. C. Yang, et al. (2010). "Case report of a serious adverse event following the administration of T cells transduced with a chimeric antigen receptor recognizing ERBB2." Mol Ther **18**(4): 843-851.
- Moris, A., V. Teichgraber, et al. (2001). "Cutting edge: characterization of allorestricted and peptide-selective alloreactive T cells using HLA-tetramer selection." J Immunol **166**(8): 4818-4821.
- Mule, J. J., S. Shu, et al. (1984). "Adoptive immunotherapy of established pulmonary metastases with LAK cells and recombinant interleukin-2." Science **225**(4669): 1487-1489.
- Munz, C., R. Obst, et al. (1999). "Alloreactivity as a source of high avidity peptide-specific human CTL." J Immunol **162**(1): 25-34.
- Murphy, K. M., P. Travers, et al. (2011). Janeway's Immunobiology, Garland Science.
- Myers, G. D., R. A. Krance, et al. (2005). "Adenovirus infection rates in pediatric recipients of alternate donor allogeneic bone marrow transplants receiving either antithymocyte globulin (ATG) or alemtuzumab (Campath)." Bone Marrow Transplant **36**(11): 1001-1008.
- Nishimura, M. I., D. Avichezer, et al. (1999). "MHC class I-restricted recognition of a melanoma antigen by a human CD4+ tumor infiltrating lymphocyte." Cancer Res **59**(24): 6230-6238.
- Nishimura, M. I., M. C. Custer, et al. (1998). "T cell-receptor V gene use by CD4+ melanoma-reactive clonal and oligoclonal T-cell lines." J Immunother **21**(5): 352-362.

- Obar, J. J., K. M. Khanna, et al. (2008). "Endogenous naive CD8+ T cell precursor frequency regulates primary and memory responses to infection." Immunity **28**(6): 859-869.
- Obst, R., C. Munz, et al. (1998). "Allo- and self-restricted cytotoxic T lymphocytes against a peptide library: evidence for a functionally diverse allorestricted T cell repertoire." Eur J Immunol **28**(8): 2432-2443.
- Ozawa, T., K. Tajiri, et al. (2008). "Comprehensive analysis of the functional TCR repertoire at the single-cell level." Biochem Biophys Res Commun **367**(4): 820-825.
- Papatriantafyllou, M., G. Moldenhauer, et al. (2012). "Dickkopf-3, an immune modulator in peripheral CD8 T-cell tolerance." Proc Natl Acad Sci U S A **109**(5): 1631-1636.
- Parkhurst, M. R., J. Joo, et al. (2009). "Characterization of genetically modified T-cell receptors that recognize the CEA:691-699 peptide in the context of HLA-A2.1 on human colorectal cancer cells." Clin Cancer Res **15**(1): 169-180.
- Parkhurst, M. R., J. C. Yang, et al. (2011). "T cells targeting carcinoembryonic antigen can mediate regression of metastatic colorectal cancer but induce severe transient colitis." Mol Ther **19**(3): 620-626.
- Paust, S. and U. H. von Andrian (2011). "Natural killer cell memory." Nat Immunol **12**(6): 500-508.
- Peggs, K. S. and S. Mackinnon (2004). "Augmentation of virus-specific immunity after hematopoietic stem cell transplantation by adoptive T-cell therapy." Hum Immunol **65**(5): 550-557.
- Peggs, K. S., S. A. Quezada, et al. (2009). "Blockade of CTLA-4 on both effector and regulatory T cell compartments contributes to the antitumor activity of anti-CTLA-4 antibodies." J Exp Med **206**(8): 1717-1725.
- Phillips, R. E., S. Rowland-Jones, et al. (1991). "Human immunodeficiency virus genetic variation that can escape cytotoxic T cell recognition." Nature **354**(6353): 453-459.
- Pittet, M. J., V. Rubio-Godoy, et al. (2003). "Alpha 3 domain mutants of peptide/MHC class I multimers allow the selective isolation of high avidity tumor-reactive CD8 T cells." J Immunol **171**(4): 1844-1849.
- Price, M. R., P. D. Rye, et al. (1998). "Summary report on the ISOBM TD-4 Workshop: analysis of 56 monoclonal antibodies against the MUC1 mucin. San Diego, Calif., November 17-23, 1996." Tumour Biol **19 Suppl 1**: 1-20.
- Qasim, W., S. Derniame, et al. (2011). "Third-party virus-specific T cells eradicate adenoviraemia but trigger bystander graft-versus-host disease." Br J Haematol **154**(1): 150-153.
- Queirolo, P., M. Ponte, et al. (1999). "Adoptive immunotherapy with tumor-infiltrating lymphocytes and subcutaneous recombinant interleukin-2 plus interferon alfa-2a for melanoma patients with nonresectable distant disease: a phase I/II pilot trial. Melanoma Istituto Scientifico Tumori Group." Ann Surg Oncol **6**(3): 272-278.

- Radvanyi, L. G., C. Bernatchez, et al. (2012). "Specific lymphocyte subsets predict response to adoptive cell therapy using expanded autologous tumor-infiltrating lymphocytes in metastatic melanoma patients." Clin Cancer Res.
- Ratto, G. B., P. Zino, et al. (1996). "A randomized trial of adoptive immunotherapy with tumor-infiltrating lymphocytes and interleukin-2 versus standard therapy in the postoperative treatment of resected nonsmall cell lung carcinoma." Cancer **78**(2): 244-251.
- Ravaud, A., E. Legrand, et al. (1995). "A phase I trial of repeated tumour-infiltrating lymphocyte (TIL) infusion in metastatic melanoma." Br J Cancer **71**(2): 331-336.
- Restifo, N. P., F. Esquivel, et al. (1993). "Identification of human cancers deficient in antigen processing." J Exp Med **177**(2): 265-272.
- Ridolfi, L., R. Ridolfi, et al. (2003). "Adjuvant immunotherapy with tumor infiltrating lymphocytes and interleukin-2 in patients with resected stage III and IV melanoma." J Immunother **26**(2): 156-162.
- Robbins, P. F., Y. F. Li, et al. (2008). "Single and dual amino acid substitutions in TCR CDRs can enhance antigen-specific T cell functions." J Immunol **180**(9): 6116-6131.
- Robbins, P. F., R. A. Morgan, et al. (2011). "Tumor regression in patients with metastatic synovial cell sarcoma and melanoma using genetically engineered lymphocytes reactive with NY-ESO-1." J Clin Oncol **29**(7): 917-924.
- Robins, H. S., P. V. Campregher, et al. (2009). "Comprehensive assessment of T-cell receptor beta-chain diversity in alphabeta T cells." Blood **114**(19): 4099-4107.
- Rosenberg, S. A., M. T. Lotze, et al. (1987). "A progress report on the treatment of 157 patients with advanced cancer using lymphokine-activated killer cells and interleukin-2 or high-dose interleukin-2 alone." N Engl J Med **316**(15): 889-897.
- Rosenberg, S. A., M. T. Lotze, et al. (1985). "Observations on the systemic administration of autologous lymphokine-activated killer cells and recombinant interleukin-2 to patients with metastatic cancer." N Engl J Med **313**(23): 1485-1492.
- Rosenberg, S. A., M. T. Lotze, et al. (1993). "Prospective randomized trial of high-dose interleukin-2 alone or in conjunction with lymphokine-activated killer cells for the treatment of patients with advanced cancer." J Natl Cancer Inst **85**(8): 622-632.
- Rosenberg, S. A., B. S. Packard, et al. (1988). "Use of tumor-infiltrating lymphocytes and interleukin-2 in the immunotherapy of patients with metastatic melanoma. A preliminary report." N Engl J Med **319**(25): 1676-1680.
- Rosenberg, S. A., P. Spiess, et al. (1986). "A new approach to the adoptive immunotherapy of cancer with tumor-infiltrating lymphocytes." Science **233**(4770): 1318-1321.
- Rosenberg, S. A., J. C. Yang, et al. (2011). "Durable complete responses in heavily pretreated patients with metastatic melanoma using T-cell transfer immunotherapy." Clin Cancer Res **17**(13): 4550-4557.

- Rosenberg, S. A., J. R. Yannelli, et al. (1994). "Treatment of patients with metastatic melanoma with autologous tumor-infiltrating lymphocytes and interleukin 2." J Natl Cancer Inst **86**(15): 1159-1166.
- Sallusto, F., D. Lenig, et al. (1999). "Two subsets of memory T lymphocytes with distinct homing potentials and effector functions." Nature **401**(6754): 708-712.
- Sawamukai, N., A. Satake, et al. (2012). "Cell-autonomous role of TGFbeta and IL-2 receptors in CD4+ and CD8+ inducible regulatory T-cell generation during GVHD." Blood **119**(23): 5575-5583.
- Scaviner, D. and M. P. Lefranc (2000). "The human T cell receptor alpha variable (TRAV) genes." Exp Clin Immunogenet **17**(2): 83-96.
- Schietinger, A., J. J. Delrow, et al. (2012). "Rescued tolerant CD8 T cells are preprogrammed to reestablish the tolerant state." Science **335**(6069): 723-727.
- Schmitt, A., T. Tonn, et al. (2011). "Adoptive transfer and selective reconstitution of streptamer-selected cytomegalovirus-specific CD8+ T cells leads to virus clearance in patients after allogeneic peripheral blood stem cell transplantation." Transfusion **51**(3): 591-599.
- Schwartzentruber, D. J., S. S. Hom, et al. (1994). "In vitro predictors of therapeutic response in melanoma patients receiving tumor-infiltrating lymphocytes and interleukin-2." J Clin Oncol **12**(7): 1475-1483.
- Skerra, A. (1992). "Phosphorothioate primers improve the amplification of DNA sequences by DNA polymerases with proofreading activity." Nucleic Acids Res **20**(14): 3551-3554.
- Skerra, A. and T. G. Schmidt (1999). "Applications of a peptide ligand for streptavidin: the Strep-tag." Biomol Eng **16**(1-4): 79-86.
- Smith, C., J. Tsang, et al. (2012). "Effective treatment of metastatic forms of Epstein-Barr virus-associated nasopharyngeal carcinoma with a novel adenovirus-based adoptive immunotherapy." Cancer Res **72**(5): 1116-1125.
- Somerville, R. P., L. Devillier, et al. (2012). "Clinical scale rapid expansion of lymphocytes for adoptive cell transfer therapy in the WAVE(R) bioreactor." J Transl Med **10**: 69.
- Sommermeier, D., J. Neudorfer, et al. (2006). "Designer T cells by T cell receptor replacement." Eur J Immunol **36**(11): 3052-3059.
- Stemberger, C., K. M. Huster, et al. (2007). "A single naive CD8+ T cell precursor can develop into diverse effector and memory subsets." Immunity **27**(6): 985-997.
- Sun, X., M. Saito, et al. (2012). "Unbiased Analysis of TCRalpha/beta Chains at the Single-Cell Level in Human CD8(+) T-Cell Subsets." PLoS One **7**(7): e40386.
- Takayama, T., T. Sekine, et al. (2000). "Adoptive immunotherapy to lower postsurgical recurrence rates of hepatocellular carcinoma: a randomised trial." Lancet **356**(9232): 802-807.

- Therasse, P., S. G. Arbuck, et al. (2000). "New guidelines to evaluate the response to treatment in solid tumors. European Organization for Research and Treatment of Cancer, National Cancer Institute of the United States, National Cancer Institute of Canada." J Natl Cancer Inst **92**(3): 205-216.
- Thomas, E. D., H. L. Lochte, Jr., et al. (1959). "Supralethal whole body irradiation and isologous marrow transplantation in man." J Clin Invest **38**: 1709-1716.
- Thornton, A. M., P. E. Kory, et al. (2010). "Expression of Helios, an Ikaros transcription factor family member, differentiates thymic-derived from peripherally induced Foxp3+ T regulatory cells." J Immunol **184**(7): 3433-3441.
- Tomazin, R., J. Boname, et al. (1999). "Cytomegalovirus US2 destroys two components of the MHC class II pathway, preventing recognition by CD4+ T cells." Nat Med **5**(9): 1039-1043.
- Topalian, S. L., F. S. Hodi, et al. (2012). "Safety, activity, and immune correlates of anti-PD-1 antibody in cancer." N Engl J Med **366**(26): 2443-2454.
- Topalian, S. L., D. Solomon, et al. (1988). "Immunotherapy of patients with advanced cancer using tumor-infiltrating lymphocytes and recombinant interleukin-2: a pilot study." J Clin Oncol **6**(5): 839-853.
- Trautmann, L., M. Rimbert, et al. (2005). "Selection of T cell clones expressing high-affinity public TCRs within Human cytomegalovirus-specific CD8 T cell responses." J Immunol **175**(9): 6123-6132.
- Uhlin, M., J. Gertow, et al. (2012). "Rapid salvage treatment with virus-specific T cells for therapy-resistant disease." Clin Infect Dis **55**(8): 1064-1073.
- Uhlin, M., M. Okas, et al. (2010). "A novel haplo-identical adoptive CTL therapy as a treatment for EBV-associated lymphoma after stem cell transplantation." Cancer Immunol Immunother **59**(3): 473-477.
- van der Merwe, P. A. and S. J. Davis (2003). "Molecular interactions mediating T cell antigen recognition." Annu Rev Immunol **21**: 659-684.
- van Loenen, M. M., R. de Boer, et al. (2011). "Optimization of the HA-1-specific T-cell receptor for gene therapy of hematologic malignancies." Haematologica **96**(3): 477-481.
- Venturi, V., M. F. Quigley, et al. (2011). "A mechanism for TCR sharing between T cell subsets and individuals revealed by pyrosequencing." J Immunol **186**(7): 4285-4294.
- Verdegaal, E. M., M. Visser, et al. (2011). "Successful treatment of metastatic melanoma by adoptive transfer of blood-derived polyclonal tumor-specific CD4+ and CD8+ T cells in combination with low-dose interferon-alpha." Cancer Immunol Immunother **60**(7): 953-963.
- Vita, R., L. Zarebski, et al. (2010). "The immune epitope database 2.0." Nucleic Acids Res **38**(Database issue): D854-862.

- Wallen, H., J. A. Thompson, et al. (2009). "Fludarabine modulates immune response and extends in vivo survival of adoptively transferred CD8 T cells in patients with metastatic melanoma." PLoS One **4**(3): e4749.
- Walter, E. A., P. D. Greenberg, et al. (1995). "Reconstitution of cellular immunity against cytomegalovirus in recipients of allogeneic bone marrow by transfer of T-cell clones from the donor." N Engl J Med **333**(16): 1038-1044.
- Wang, C., C. M. Sanders, et al. (2010). "High throughput sequencing reveals a complex pattern of dynamic interrelationships among human T cell subsets." Proc Natl Acad Sci U S A **107**(4): 1518-1523.
- Wang, G. C., P. Dash, et al. (2012). "T cell receptor alphabeta diversity inversely correlates with pathogen-specific antibody levels in human cytomegalovirus infection." Sci Transl Med **4**(128): 128ra142.
- Wang, Q. J., K. Hanada, et al. (2011). "Development of a genetically-modified novel T-cell receptor for adoptive cell transfer against renal cell carcinoma." J Immunol Methods **366**(1-2): 43-51.
- Warren, R. L., J. D. Freeman, et al. (2011). "Exhaustive T-cell repertoire sequencing of human peripheral blood samples reveals signatures of antigen selection and a directly measured repertoire size of at least 1 million clonotypes." Genome Res **21**(5): 790-797.
- Weekes, M. P., M. R. Wills, et al. (1999). "The memory cytotoxic T-lymphocyte (CTL) response to human cytomegalovirus infection contains individual peptide-specific CTL clones that have undergone extensive expansion in vivo." J Virol **73**(3): 2099-2108.
- Wehler, T. C., M. Karg, et al. (2008). "Rapid identification and sorting of viable virus-reactive CD4(+) and CD8(+) T cells based on antigen-triggered CD137 expression." J Immunol Methods **339**(1): 23-37.
- Wehler, T. C., M. Nonn, et al. (2007). "Targeting the activation-induced antigen CD137 can selectively deplete alloreactive T cells from antileukemic and antitumor donor T-cell lines." Blood **109**(1): 365-373.
- Weiden, P. L., N. Flournoy, et al. (1979). "Antileukemic effect of graft-versus-host disease in human recipients of allogeneic-marrow grafts." N Engl J Med **300**(19): 1068-1073.
- Weiden, P. L., K. M. Sullivan, et al. (1981). "Antileukemic effect of chronic graft-versus-host disease: contribution to improved survival after allogeneic marrow transplantation." N Engl J Med **304**(25): 1529-1533.
- Weng, N. P., Y. Araki, et al. (2012). "The molecular basis of the memory T cell response: differential gene expression and its epigenetic regulation." Nat Rev Immunol **12**(4): 306-315.

- Wiertz, E. J., T. R. Jones, et al. (1996). "The human cytomegalovirus US11 gene product dislocates MHC class I heavy chains from the endoplasmic reticulum to the cytosol." Cell **84**(5): 769-779.
- Wiertz, E. J., D. Tortorella, et al. (1996). "Sec61-mediated transfer of a membrane protein from the endoplasmic reticulum to the proteasome for destruction." Nature **384**(6608): 432-438.
- Wing, K., Y. Onishi, et al. (2008). "CTLA-4 control over Foxp3+ regulatory T cell function." Science **322**(5899): 271-275.
- Woo, S. R., M. E. Turnis, et al. (2012). "Immune inhibitory molecules LAG-3 and PD-1 synergistically regulate T-cell function to promote tumoral immune escape." Cancer Res **72**(4): 917-927.
- Xystrakis, E., A. S. Dejean, et al. (2004). "Identification of a novel natural regulatory CD8 T-cell subset and analysis of its mechanism of regulation." Blood **104**(10): 3294-3301.
- Yamane, H. and W. E. Paul (2012). "Cytokines of the gamma(c) family control CD4(+) T cell differentiation and function." Nat Immunol **13**(11): 1037-1044.
- Yee, C., J. A. Thompson, et al. (2002). "Adoptive T cell therapy using antigen-specific CD8+ T cell clones for the treatment of patients with metastatic melanoma: in vivo persistence, migration, and antitumor effect of transferred T cells." Proc Natl Acad Sci U S A **99**(25): 16168-16173.
- Yin, Y., B. Manoury, et al. (2003). "Self-inhibition of synthesis and antigen presentation by Epstein-Barr virus-encoded EBNA1." Science **301**(5638): 1371-1374.
- York, I. A., C. Roop, et al. (1994). "A cytosolic herpes simplex virus protein inhibits antigen presentation to CD8+ T lymphocytes." Cell **77**(4): 525-535.
- Yron, I., T. A. Wood, Jr., et al. (1980). "In vitro growth of murine T cells. V. The isolation and growth of lymphoid cells infiltrating syngeneic solid tumors." J Immunol **125**(1): 238-245.
- Zhao, Y., A. D. Bennett, et al. (2007). "High-affinity TCRs generated by phage display provide CD4+ T cells with the ability to recognize and kill tumor cell lines." J Immunol **179**(9): 5845-5854.
- Zhou, D., R. Srivastava, et al. (2006). "High throughput analysis of TCR-beta rearrangement and gene expression in single T cells." Lab Invest **86**(3): 314-321.
- Zhou, Q., M. E. Munger, et al. (2011). "Coexpression of Tim-3 and PD-1 identifies a CD8+ T-cell exhaustion phenotype in mice with disseminated acute myelogenous leukemia." Blood **117**(17): 4501-4510.
- Zhu, C., A. C. Anderson, et al. (2005). "The Tim-3 ligand galectin-9 negatively regulates T helper type 1 immunity." Nat Immunol **6**(12): 1245-1252.